Preparation of a set of rotavirus SA 11 transcription plasmids for T7- transcript based reverse genetics

JJ van der Merwe

orcid.org/0000-0002-3930-5528

Dissertation submitted in *partial* fulfilment of the requirements for the *Masters* degree in *Biochemistry* at the North-West University

Supervisor:	Prof AA van Dijk
Co-supervisor:	Dr HG O'Neill
Co-supervisor:	Prof AC Potgieter

Graduation May 2018

22822224

ACKNOWLEDGEMENTS

I would like to express my sincerest appreciation and gratitude to the following people and organisations for their support and contributions towards the completion of this dissertation:

Professor A.A. van Dijk, first and foremost many thanks to her for the opportunity she gave me to conduct my Masters degree under her supervision and for all the time and effort she put into this study. Without her dedication and support this dissertation would not have taken shape as it did.

Professor A.C. Potgieter, for always being prepared to help with any obstacle in the way and the countless helpful suggestions he offered when I needed direction. Without his expertise in virology and reverse genetics this dissertation would not have been possible.

Professor H.G. O'Neill, for her continuous support throughout this study.

Deltamune, to all the members of the Research and Development department who was always willing to lend a hand and share their expertise. Also for all the material provided during our visits.

My family, special thanks in particular to my mom and dad who made this opportunity possible. My brother and two aunts for their continued love and support throughout the course of this study. I love you all very much.

The Poliomyelitis Research foundation and the North-West University for their financial assistance.

Finally, my Heavenly Father who has blessed my life with so many wonderful opportunities and who gave me the strength and persistence during this study.

TABLE OF CONTENTS

SUMMARY

Rotaviruses belong to the *Reoviridae* family, and rotavirus infection is the biggest contributor to diarrhoea-related death in the world for children under the age of five years. The rotavirus genome consists of 11 double-stranded RNA segments and is build into a triple-layer particle. The 11 genome segments encode six structural proteins VP1, VP2, VP3, VP4, VP6 and VP7 together with six non-structural proteins NSP1, NSP2, NSP3, NSP4 and NSP5/6. Reverse genetics are biological methods that are used to generate insights into the workings and characteristics of pathogenesis and the replication cycle of viruses. Reverse genetics systems have been established for several dsRNA viruses such as Bluetongue virus (BTV) and African horsesickness virus (AHSV) and is used to develop better vaccines for these viruses. It was not until early 2017 when a plasmid-based reverse genetics system for rotavirus was developed (Kanai et al., 2017), and there is currently still no rotavirus transcript-based reverse genetics system. This project aimed to develop such a transcript-based reverse genetics system for rotavirus by incorporating different aspects of reverse genetics systems of BTV, AHSV and the plasmid-based system of rotavirus.

To achieve this a design flaw in four rotavirus multiple genome segment plasmids from a previous study had to be corrected. This design flaw had three additional guanines at the 5' terminal ends of all 11 genome segments which led to the (+)ssRNAs to not be packaged. The design was corrected through In-Fusion HD cloning which is a state-of-the-art cloning method that allows cloning of one or multiple DNA fragments into any vector of choice at any position, provided there is a 15-base pair overlap on both ends of the vector and DNA fragment. The 15-base overlap was generated with PCR with specifically designed primers, and the 5' and 3' terminal ends were joined with the In-Fusion enzyme creating 10 rotavirus transcription plasmids pSMART-GS1/2/4/5/6/7/8/9/10/11. After multiple failed attempts to clone genome segment 3 into pSMART, it was decided to correct the design flaw for this genome segment with PCR and use the amplicon to synthesise (+)ssRNAs.

To determine if the initial design flaw of three extra guanine nucleotides were successfully removed and that the respective 5' and 3' ends annealed correctly, the transcription plasmids were sent for Sanger sequencing. In addition, the transcription plasmids underwent next-generation sequencing to determine if any nucleotide

changes had occurred in the sequences of the transcription plasmids. The results of the Ion-Torrent S5 sequencing showed a nucleotide change from a thymine to a cytosine in genome segment 11 at position 289. This change in sequence would invoke a change in amino acid from a cysteine to an arginine (C289R). However, due to time limitations, we had to proceed with this error. The transcription plasmids were used to synthesise (+)ssRNAs through *in vitro* transcription. The identity of the (+)ssRNAs was confirmed with agarose gel electrophoresis.

Finally, the 11 newly synthesised (+)ssRNAs together with the fusogenic orthoreovirus FAST plasmid, two vaccinia virus capping enzyme plasmids (D1R and D12L) and seven rotavirus expression plasmids encoding the replication complex and viroplasm (VP1, VP2, VP3, VP6, NSP1, NSP2 and NSP5) was transfected into BHK-T7 cells with Lipofectamine® 2000. After 22 hours the BHK-T7 cells were co-seeded with MA104 cells, and after 7 days of incubation, no cytopathic effect (CPE) was observed. An immunofluorescence monolayer assay (IMFA) was conducted on the co-seeded cell monolayer to determine if any rotavirus was rescued. However, no fluorescence was observed. The lack of rescue was attributed to the nucleotide change in genome segment 11 and the overuse of the FAST plasmid during transfection. Thus, this attempt to establish a rotavirus transcript-based reverse genetics system was unsuccessful, but the transcription plasmids should be useful for future experiments.

OPSOMMING

Rotavirusse behoort aan die *Reoviridae* familie en rotavirus infeksie is die grootste bydraer tot diarree-verwante sterftes in die wêreld vir kinders onder die ouderdom van vyf jaar. Die rotavirusgenoom bestaan uit 11 dubbelstring RNA segmente en word in 'n trippellaag kapsied ingebou. Die 11 genoom segmente kodeer vir ses strukturele proteïene VP1, VP2, VP3, VP4, VP6 en VP7 saam met ses nie-strukturele proteïene NSP1, NSP2, NSP3, NSP4 en NSP5/6. Tru-genetika is biologiese metodes wat gebruik word om insig te verkry in die werking en eienskappe van patogenese en die repliseringsiklus van virusse. Tru-genetika stelsels is al ontdek vir verskeie dsRNA virusse soos Bloutong virus (BTV) en Afrika perdesiekte virus (APSV) en word gebruik vir die ontwikkeling van nuwe generasie entstowwe vir hierdie virusse. Eers in vroeg 2017 is 'n plasmied-gebaseerde tru-genetika-stelsel vir rotavirus ontwikkel (Kanai et al., 2017). Daar is tans nog geen transkrip-gebaseerde tru-genetika-stelsel vir rotavirus nie. Hierdie projek het beoog om so 'n transkrip-gebaseerde tru-genetika stelsel vir rotavirus te ontwikkel deur verskillende aspekte van tru-genetika stelsels van BTV, APSV en die plasmied-gebaseerde stelsel van rotavirus te inkorporeer.

Om dit te bereik, moes 'n ontwerpsfout in vier rotavirus meervoudige genoom segment plasmiede van 'n vorige studie reggestel word. Hierdie ontwerpsfout het drie addisionele guaniene by die 5' terminale ente van al 11 genoom segmente tot gevolg gehad en het veroorsaak dat die (+)esRNAs nie verpak sou word nie. Die ontwerp is gekorrigeer deur In-Fusion HD klonering te gebruik, wat 'n moderne kloneringsmetode is wat die kloning van een of meer DNA fragmente in enige vektor van keuse in enige posisie toelaat, mits daar 'n oorvleueling van 15 basispare op albei ente van die vektor en DNA-fragment is. Die 15 basispare oorvleueling is gegenereer met PKR met spesiaal ontwerpte primers, en die 5'- en 3'- eindpunte is aan mekaar geheg met die In-Fusion ensiem. Dit het 10 rotavirus transkripsie plasmiede pSMART-GS1/2/4/5/6/7/8/9/10/11 geskep. Na verskeie mislukte pogings om genoom segment 3 in pSMART te kloneer, is daar besluit om die ontwerpsfout vir hierdie genoom segment met PKR te korrigeer en die amplikon te gebruik om (+)esRNAs te sintetiseer.

Om vas te stel of die aanvanklike ontwerpsfout van drie ekstra guanien nukleotiede suksesvol verwyder is en dat die onderskeie 5'- en 3'- termini korrek geheg het, is die transkripsie-plasmiede vir Sanger-volgordebepaling gestuur. Die transkripsie

plasmiede het ook volgende generasie volgordebepaling ondergaan om te bepaal of enige nukleotied veranderinge plaasgevind het. Die resultate van die Ion-Torrent S5-volgordebepaling het 'n nukleotied verandering van 'n timien na 'n sitosien in genoom-segment 11by posisie 289 getoon. Hierdie verandering in volgorde sou 'n verandering in aminosuur van 'n sustien na 'n arginien oproep (C289R). As gevolg van tydsbeperkings, moes ons egter met hierdie fout voortgaan. Die transkripsie plasmiede is gebruik om (+)esRNAs te sintetiseer deur *in vitro* transkripsie. Die identiteit van die (+)esRNAs is bevestig met agarose gelelektroforese.

Ten slotte is die 11 nuut-gesintetiseerde (+)esRNAs tesame met die fusogene orthoreovirus FAST plasmid, twee vaccinia virus plasmiede (D1R en D12L) en sewe rotavirus ekspressie plasmiede wat die repliseringskompleks en viroplasma (VP1, VP2, VP3, VP6, NSP1, NSP2 en NSP5) koördineer, getransfekteer in BHK-T7-selle met Lipofektamine® 2000. Na 22ure is die BHK-T7 selle saamgesaai met MA104 selle. Na 7 dae van inkubasie is geen sitopatiese effekte waargeneem nie. 'n immunofluoreseerende monolaag evaluering (IMFA) is op die gesamentlike sel monolaag uitgevoer om te bepaal of enige rotavirus gered is. Geen fluoresensie is egter waargeneem nie. Die onvermoë om virus te red is toegeskryf aan die nukleotied verandering in genoom segment 11 en die oorgebruik van die FAST plasmied tydens transfeksie. Dus was hierdie poging om 'n rotavirus transkrip-gebaseerde tru-genetika stelsel op die been te bring, onsuksesvol maar die stel transkripsie plasmiede wat gegenereer was sal hulpvaardig wees in toekomstige eksperimente.

ABBREVIATIONS

AHSV	African horsesickness virus
ATP	adenosine tri-phosphate
BHK-T7	Baby hamster kidney-T7 cells
bp	base pair
BTV	Bluetongue virus
Ca^{2+}	calcium
CAF	Central Analytical Facility
cDNA	circular DNA
CO_2	Carbon dioxide
CPE	cytopathic effect
DLP	double-layered particle
DMEM	Dulbecco's modified Eagle's medium
DNA	deoxyribonucleic acid
dNTPs	deoxyribonucleotide triphosphate
ds	double-stranded
dsRNA	double-stranded ribonucleic acid
EDTA	ethylene diamine tetra acetic acid
EtBr	ethidium bromide
FBS	foetal bovine serum
GS	genome segment
IFMA	immunofluorescent monolayer assay
IFN	Interferons
IRFs	interferon-regulating factors
ISGs	interferon-stimulated genes
LB	Luria broth
MA104	African green monkey kidney cells
MDA5	melanoma differentiation associated gene 5
Mg^{2+}	magnesium
$MgCl_2$	magnesium chloride
ml	milliliter
mM	millimol
mRNA	messenger RNA
MRV	mammalian orthoreovirus
NaOH	sodium hydroxide
NICD	National Institute for Communal Diseases
ng	nanogram
NGS	Next generation sequencing
nm	nanometer
NSP	non-structural viral proteins
NWU	North-West University
ORF	open reading frame
PAGE	Polyacrylamide gel electrophoresis

PBS	Phosphate-buffered saline
PCR	polymerase chain reaction
PCs	polymerase complexes
PRR	pattern recognition receptors
RIG-I	RNA sensitive retinoic acid-induced gene
RNA	ribonucleic acid
Rpm	revolutions per minute
RV	rotavirus
SA11	simian agent 11
SOC	super optimal broth with catabolite repression
ss	single-stranded
TAE	tris-acetate EDTA
TLP	triple-layered particle
VP	viral protein
µg	microgram
µl	microliter
°C	degrees Celsius
(+)ssRNAs	positive sense single stranded ribonucleic acid
(-)ssRNAs	negative sense single stranded ribonucleic acid

KEYWORDS:

Rotavirus, simian agent 11, reverse genetics, *in vitro* transcription, transcript-based reverse genetics system, In-Fusion cloning.

LIST OF FIGURES:

LIST OF TABLES:

Chapter 1: Introduction

1.1. Background and problem statement

In an ever-developing world and advancements in technology made every day the limit of what can be achieved is constantly shifting. This is especially true in the field of science as questions that were impossible to answer yesterday may be investigated today with new technology. The statement is echoed when we take a look at the "birth" of virology where Louis Pasteur and Charles Chamberland invented the Pasteur-Chamberland filter. This filter was unique in that it had pores smaller than bacteria which allowed a solution to be purified from any bacteria and so shifting the focus of research to a field which will be later on be termed virology. This shows that basic scientific research is paramount to understand the world we live in and how we can ultimately make it better.

Rotaviruses belong to the *Reoviridae* family, and rotavirus infection is the biggest contributor to diarrhoea-related death in the world for children under the age of five years (Madhi et al., 2010). Simian agent 11 (SA11) is a strain of rotavirus that was isolated from the rectum of a healthy vervet monkey in South-Africa by Dr. Malherbe in 1958 (Malherbe and Harwin, 1963). It was only in 1973 when Ruth Bishop and collaborators found a link between severe gastroenteritis in infants and young children and rotavirus. Because the SA11 strain is asymptomatic and the fact that it propagates well in cell cultures, it became the model strain for rotavirus studies such as the determination of protein functions and investigations into the replication cycle (Mlera et al., 2013). The infectious rotavirus particle has three layers and is also termed a triple-layered particle. The rotavirus genome consists of 11 genome dsRNA segments which encode six structural proteins (VP1-6) and six non-structural proteins (NSP1-7) (Estes and Greenberg, 2013). Currently, there are two vaccines commercially available against rotavirus diarrhoea, RotaTeq and Rotarix that elicit broad immunity against different strains of the virus (Glass et al., 2014). The current vaccines were derived from strains prevalent in the USA and Europe and are more effective against these specific strains of rotavirus than strains found in Asia and Africa (Clarke and Desselberger, 2015).

Reverse genetics is a molecular biology approach which enables the alteration of viral cDNA to generate a mutant/altered virus. The effect on gene functions are then observed to get a better understanding of the intricate workings of viruses such as its replication cycle and pathogenesis. Reverse genetics systems are already established for various viruses of the *Reoviridae* family such as African horsesickness virus (AHSV), orthoreovirus and bluetongue virus (BTV). These reverse genetics systems have led to valuable knowledge regarding each virus. The development of influenza vaccines was spearheaded by reverse genetics and is an outstanding example of the usefulness of such a system (Subbarao and Katz, 2004). In the influenza system, a recombinant virus was created after cDNAs and ribonucleo-proteins were both transfected into cells together with a helper Influenza A virus to help incorporate the cDNAs (Neumann et al., 2012). The extrapolation of the reverse genetics systems for the viruses of *Reoviridae* to rotavirus was unsuccessful and only strong selection, and helper virus-dependent systems were described (Komoto et al., 2006, Trask et al., 2010, Troupin et al., 2010). However, in early 2017 a fully plasmid-based rotavirus reverse genetics system was created by Kanai and collaborators where 11 viral plasmids, each containing one genome segment, were co-transfected with two capping plasmids and a plasmid encoding fusogenic orthoreovirus proteins (Kanai et al., 2017).

For more than a decade now, the rotavirus group here at the North-West University have strived to establish a reverse genetics system for rotavirus. Unfortunately, in two previous studies conducted at this university, no reverse genetics system was established. One studies' approach, led by Dr L. Mlera, sought to establish a transcript-based reverse genetics system by transfecting transcripts derived from the DS-1 and SA11 strains into different mammalian cells. This system was not successful due to the strong innate immune response it elicited which caused the cells to die before any virus was recovered. In the other study, led by Dr. J.F. Wentzel, two approaches were followed: (1) the transfection of transcripts derived from codon-optimised transcription plasmids and (2) a hybrid system where the same transcripts were co-transfected with rotavirus expression plasmids that expressed the replication complex of rotavirus. In both cases, the system yielded no viable rotavirus because of a vital design flaw that compromised the 5' terminal of the *in vitro*-transcribed transcripts.

When this study started in 2015, there was no reverse genetics system devoid of all selection that allowed manipulation of the rotavirus viral genome and that was the problem that needed a solution. But, as mentioned above, in early 2017 Kanai and collaborators succeeded in a plasmid-based rotavirus reverse genetics system. However, there is still no transcript-based rotavirus reverse genetics system based on those of BTV and AHVS.

1.2. Aims and objectives

1.2.1. Aim of study

The long-term aim of the rotavirus vaccine initiative at the NWU-Potchefstroom campus includes the development of rationally designed, safely attenuated rotavirus vaccine strains, engineered to match the G/P type antigens of specific South African strains.

1.2.2. Objectives of the study

1. To correct a design error on a set of SA11 multi-genome segment expression plasmids by using PCR to prepare a full set of SA11 rotavirus individual genome segment transcription plasmids (Chapter 3).
2. To create *in vitro*-transcribed (+)ssRNAs to use in transfections (Chapter 3).
3. To verify expression of SA11 proteins in tissue culture after transfection of i*n vitro* transcribed (+)ssRNAs (Chapter 4).

1.3. Structure of dissertation

This dissertation will be comprised of five chapters, of which two will be experimental in nature. Each of the experimental chapters will be provided with a short introduction to the chapter followed by materials and methods, results and discussion and will be concluded with a summary.

Chapter 1: Introduction

- Background of the study together with a problem statement, aims and objectives and the structural outline of the dissertation will be provided.

Chapter 2: Literature review

- An in-depth review of all the relevant literature regarding rotavirus and reverse genetics.

Chapter 3: The construction of a full set of SA11 rotavirus transcription plasmids and the synthesis of *in vitro*-transcribed (+)ssRNAs

- The construction of 11 rotavirus transcription plasmids through In-Fusion cloning and the implementation of these plasmids to synthesise (+)ssRNAs through *in vitro* transcription.

Chapter 4: Transfection of *in vitro* transcribed rotavirus (+)ssRNAs

- Transfection of the 11 *in vitro*-transcribed rotavirus transcripts in mammalian cells and the evaluation of their expression.

Chapter 5: Conclusion and future prospects

- The study will be summarised. Concluding remarks will be presented, and recommendations will be made for any future studies.

Chapter 2: Literature Review

2.1 Introduction

The single most important cause of gastroenteritis in infants and young children in the world is rotavirus (RV). The worldwide mortality rate due to this disease is still estimated at 250 000 deaths per annum in 2017 (Crawford et al., 2017). Approximately 44% of these deaths occur in sub-Sahara Africa. Furthermore, of the top seven countries with the highest rotavirus diarrhoea mortality rate, six are in Africa. Irrespective of the cause of the disease, diarrhoeal diseases are one of the six leading causes of death in children younger than 5 years of age per annum, which are altogether 10.6 million deaths. It is also one of the most common illnesses for children younger than 5 years and accounts for approximately 18% of deaths in this age group (Estes and Greenberg, 2013).

In the 1970s viruses were discovered to be a notable cause of diarrhoea-related illnesses. Norwalk virus was the first agent to be discovered in 1972 (Kapikian et al., 2005). In 1973 human rotavirus was discovered by Bishop and collaborators, when they visualised particles of duodenal mucosa from an infant with acute gastroenteritis in electron micrographs, and later it was also seen in the faeces (Bishop et al., 1973). The SA11 rotavirus strain was already discovered in 1958 (Malherbe and Harwin, 1963). In the ten years prior to the discovery of human rotavirus, several animal viruses were described that was later found to be rotavirus. These animal agents were the EDIM virus in mice (Adams and Kraft, 1963), the simian agent 11 (SA11) in vervet monkey kidney cells (Malherbe and Harwin, 1963) and diarrhoea of cattle and termed NCDV (Mebus et al., 1969).

The mature rotavirus particle itself is approximately 70 nm in diameter, and with the VP4 spike, it reaches 100 nm and has a wheel-like appearance when observed through an electron microscope. Thus, it was named rotavirus because “rota” means wheel in Latin (Flewett et al., 1974). Rotaviruses are part of the *Reoviridae* family. Rotaviruses are non-enveloped particles which contain 11 double-stranded RNA (dsRNA) genome segments. These genome segments encode 12 different proteins,

six structural (VP1-4, VP6 and VP7) and six non-structural proteins (NSP1-4, NSP5 and NSP6) **Figure 2.1** (Desselberger, 2014).

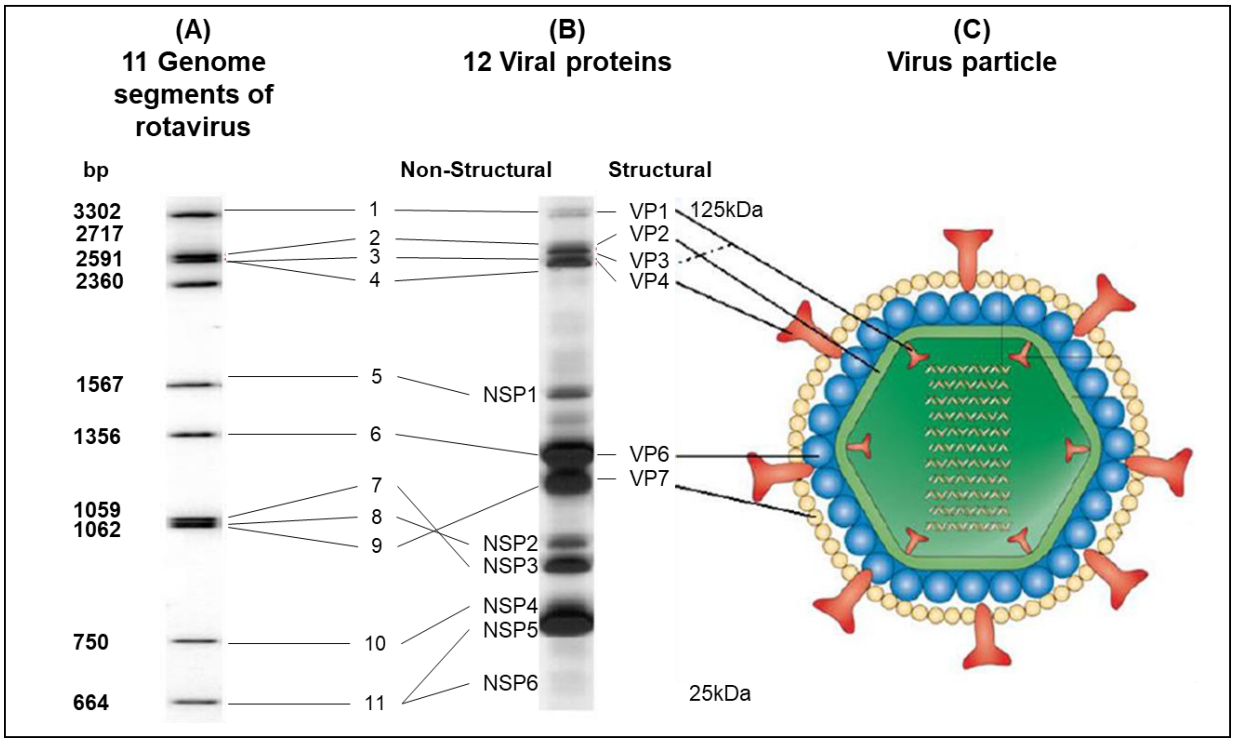

Figure 2.1: Illustration of rotavirus SA11 genome and protein organisation.
(A) The migration of all 11 genome segments of rotavirus through a polyacrylamide gel. (B) The structural and non-structural proteins visualised by SDS-PAGE. (C) The structural proteins and the rotavirus particle. Adapted from Robert F. Ramig, PhD. (2004).

Reverse genetics is a molecular biology method that enables one to alter and manipulate specific viral genomes at cDNA-level to generate mutants and artificial viruses. The advances in technology in the field of virology has led to the development of reverse genetic systems for almost all major groups of RNA- and DNA-containing viruses (Kobayashi et al., 2010). Thanks to these reverse genetic systems, valuable information regarding the replication and pathogenesis of these viruses were discovered.

There are still many questions regarding rotavirus, its replication cycle and innate immune response to it that need to be answered. A reverse genetic system may lead to answers of these questions.

2.2 Classification of rotavirus

Rotaviruses are members of the *Reoviridae* family and cause severe diarrhoea disease in animals and humans. The family *Reoviridae* is subdivided into two sub-families named *Sedoreovirinae* and *Spinareovirinae* that have six and nine genera respectively. Altogether these 15 genera have 87 species of different viruses. Rotavirus belongs to the *Sedoreovirinae* sub-family and the genus *Rotavirus.* Rotavirus is divided into eight groups based on the serological reactivity and genetic variability of the VP6 protein **Table 2.1**. These groups are termed species and are designated RVA-RVH (Matthijnssens et al., 2012) (Taxonomy, 2017).The species of rotavirus that infect humans, as well as animals, are RVA, RVB and RVC, whereas RVD, RVE, RVF and RVG infect animals only.

Table 2.1: Classification of the *Reoviridae* family (Taxonomy, 2017)

Sub-family	Genera	Number of species
Sedoreovirinae	*Cardoreovirus*	1
	Mimoreovirus	1
	Orbivirus	22
	Phytoreovirus	3
	Rotavirus	8
	Seadornavirus	3
Spinareovirinae	*Aquareovirus*	7
	Coltivirus	2
	Cypovirus	16
	Dinovernavirus	1
	Fijivirus	9
	Idnoreovirus	5
	Mycoreovirus	3
	Orthoreovirus	6
	Oryzavirus	2

The most prevalent of all these species for human infection and disease is rotavirus A (RVA). RVA has been further classified into a binary system of G- and P-types. These classifications are defined by the reactivity in plaque reduction neutralisation assays in which distinct types of VP7 and VP4 are recognised. The neutralisation assays

measure the reactivity of antibodies against the two outer capsid neutralising antigens VP7 and VP4. Currently, there are 27 G-types which refers to the glycoprotein, VP7, and 37 protease-sensitive VP4, P-types (Matthijnssens et al., 2011) (Estes and Greenberg, 2013).

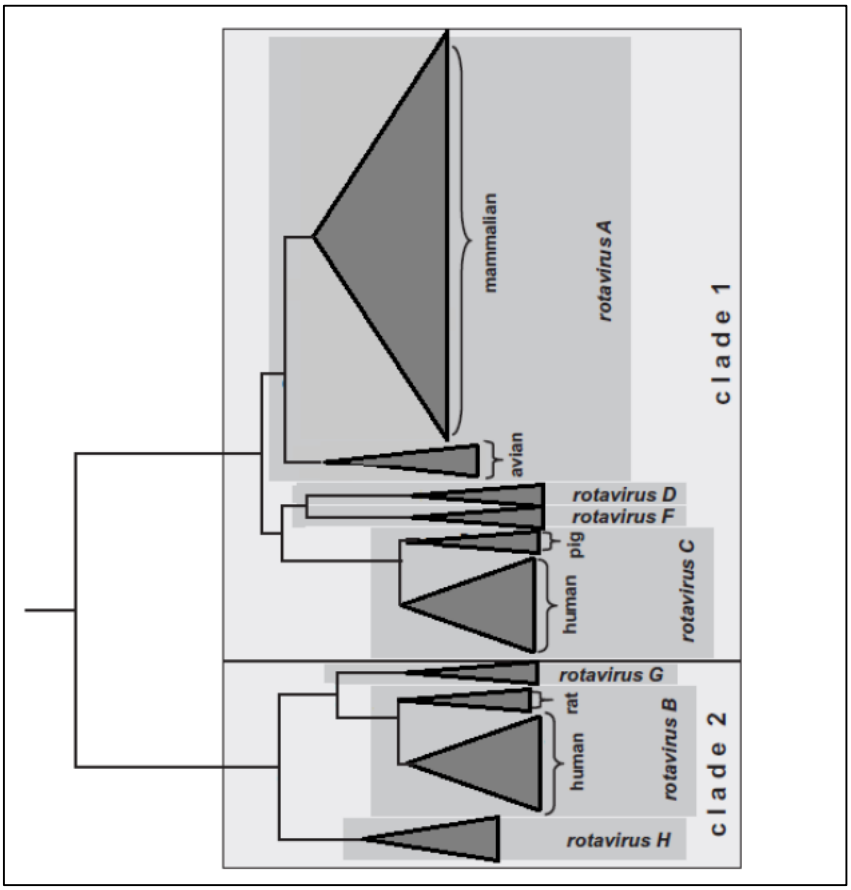

Figure 2.2: ***Phylogenetic relationship of rotavirus serogroups A – H based on all 11 genome segments (Wentzel, 2014).***

Due to the fact that antigenic characterisation is a considerable time-consuming process and the lack of proper immunological reagents in many laboratories together with the increasing ease of sequencing, the antigenic classification is slowly being replaced by sequence analysis to determine VP4 and VP7 (Matthijnssens et al., 2008b).

For VP7, encoded by genome segment 9, the correlation for the serotypes and genotypes are synonymous, for example, G1, G2 etc. For VP4 it is not as clear, because there are a lot more genotypes than P-serotypes and therefore a double nomenclature system was implemented. For example, a P1A[8], the P serotype is

designated 1A and the P genotype 8 (Estes and Greenberg, 2013). In humans, the most prevalent strains are genotypes G1, G2, G3, G4, G9 and G12, in association with P[4], P[6] and P[8] (Heiman et al., 2008) (Matthijnssens et al., 2010).

The genetic relatedness among homologous genome segments have been studied by RNA-RNA hybridisation, as well as direct sequence comparisons. This provided evidence of close interspecies relationships amongst human and animal strains which proves the natural occurrence of rotavirus strain reassortment (Matthijnssens et al., 2008b). Some of these human strains such as the DS-1-like genogroup show a common origin with a bovine rotavirus strain, while the human strain belonging to the Wa-like genogroup has a common origin with porcine rotaviruses (Matthijnssens et al., 2008a). With these naturally occurring strain reassortments, it is imperative to have a universal classification system. In 2008 Matthijnssens and co-workers suggested a classification system based on the sequence of all 11 rotavirus genome segments to ascertain a more definitive overview of rotavirus strain diversity. In 2009, a classification system to simplify the identification of all 11 genome segments of rotavirus serotype A was proposed (Maes et al., 2009). An easy to use, web-based tool, RotaC (http://rotac.regatools.be) was developed. This system assigns a specific genotype to each of the 11 rotavirus genome segments according to an established nucleotide percent cut-off value. Simian agent 11 (SA11) rotavirus is given the designation RVA/Simian-tc/ZAF/SA11-H96/1958/G3P5B[2] and with the new proposed method, it is indicated as G3-P[2]-I2-R2-C5-M5-A5-N5-T5-E2-H5 (Estes and Greenberg, 2013).

Table 2.2: The whole-genome genotype constellation of selected prototype rotavirus strains. Reassortants are visualised by a non-homogenous constellation colour.

Strain	Species	Genotype*									
		VP[7]	VP4	VP6	VP1	VP2	VP3	NSP1	NSP2	NSP3	NSP4	NSP5
Wa	Hu	G1	P[8]	I1	R1	C1	M1	A1	N1	T1	E1	H1
DS-1	Hu	G2	P[4]	I2	R2	C2	M2	A1	N2	T2	E2	H2
Au-1	Hu	G3	P[9]	I3	R3	C3	M3	A3	N3	T3	E3	H3
OSU	Po	G5	P[7]	I5	R1	C1	M1	A1	N1	T1	E1	H1
PO-13	Av	G18	P[17]	I4	R4	C4	M4	A4	N4	T4	E4	H4
SA11-H96	Si	G3	P[2]	I2	R2	C5	M5	A5	N5	T5	E2	H5

*The colour scheme is used to enhance the visualisation of certain patterns or genome segment constellations. Green, red and orange depict the human strains (Hu) Wa-like, DS-1-like, and AU-like genome segments, respectively. Yellow, blue and purple, respectively, indicate the avian (Av) PO-13-like rotavirus genome segments; some typical porcine (Po) VP4, VP7, and VP6 genotypes; and the SA-11-like genome segments. Table adapted from Matthijnssens *et al.*, 2008b by Dr. L. Mlera (2012).

2.3 Rotavirus particle structure

The fully infectious rotavirus particle or as it is known, virion, is build up of 3 layers of protein and is also known as a triple-layered particle (TLP), see **Figure 2.3**. The outer-most layer of the TLP consists of the glycoprotein VP7 and the protease-sensitive spike protein VP4 and is approximately 100nm in diameter. This outer layer is responsible for host-cell binding and penetration during infection (Estes and Greenberg, 2013) (Settembre et al., 2011). VP4 forms spike-like projections that extend outward from the outer protein shell which is formed by VP7. VP4 is cleaved into two subunits VP8* and VP5*. This cleavage divides the VP4 protein into the “head” (N-terminal fragment) VP8* which attaches itself onto the cell membrane during infection. Furthermore, it forms the VP5* subunit or “body” (C-terminal fragment) which is rooted in VP6 and protrudes outward through VP7 (Crawford et al., 2001, McClain et al., 2010, Settembre et al., 2011). The intermediate layer of the rotavirus particle consists of VP6, and it surrounds the core particle’s shell VP2. There are channels that pierce both the intermediate VP6 layer and the thin VP2 core-shell that cations and nucleotides can utilise to access the core (McDonald and Patton, 2011, Estes and Greenberg, 2013). VP6 interacts with both the outer and inner layer of protein capsids. It acts as the scaffold for the VP4 spike proteins, as well as stabilising the core particle (VP1-VP3) (Trask et al., 2012, Charpilienne et al., 2002, Mathieu et al., 2001).

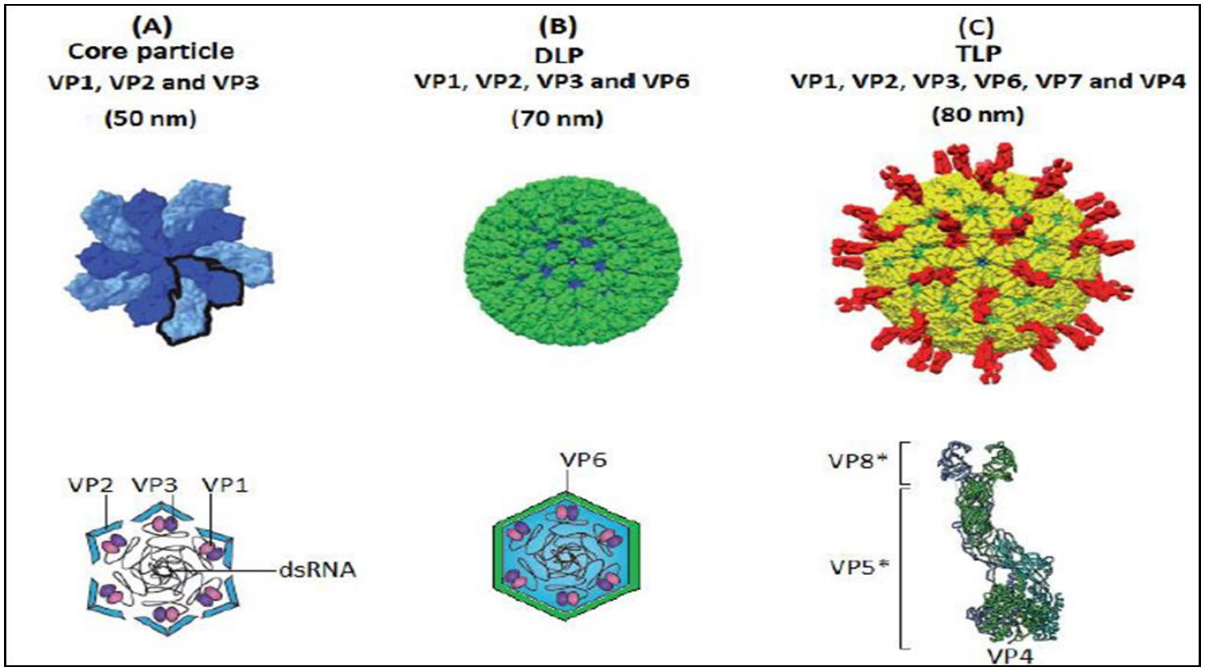

Figure 2.3: The structural layers of rotavirus. (A) The core particle constructed from VP1, VP2 and VP3. (B) The double-layered particle (DLP) where VP6 is shown in green. (C) The triple-layered particle (TLP) with the VP7 coat in yellow and VP4 spikes in red. In addition, VP4 is shown when cleaved into VP5* and VP8* subunits. Adapted from Trask et al. 2012 by Jaco Wentzel PhD (2014).

The complex containing the four structural proteins VP1, VP2, VP3, and VP6, is known as the double-layered particle or DLP. The innermost rotavirus particle is comprised of three structural proteins: VP1, VP2 and VP3. The RNA-dependent RNA polymerase, VP1, and the RNA capping enzyme, VP3, form the viral polymerase complex. The polymerase complex and the genomic dsRNA are all encapsulated by the VP2 core protein shell (McDonald and Patton, 2011).

2.4 Rotavirus genome structure

The rotavirus genome is made up of 11 dsRNA segments and is packed into a triple-layer particle (TLP). The 11 genome segments encode 12 proteins in total, six structural proteins (VP1-4, VP6 and VP7), together with the six non-structural proteins (NSP1-4 and NSP5/6) which make up rotavirus genome. The functions of these structural and non-structural proteins are summarised in **Table 2.3.** Ten of the rotavirus genome segments are monocistronic. The exception is genome

Table 2.3: A summary of the 11 genome segments of rotavirus, encoded viral proteins and their function (Attoui et al., 2011)(Mlera,2012)

Genome segment	Size (bp)	Protein	Size (kDa)	Location	Genotype	Protein function
1	3302	VP1	125	Core	R	RNA-dependent RNA polymerase; 3'-mRNA binding; forms transcription complex with VP3
2	2690	VP2	102	Inner capsid	C	Inner capsid structural protein; non-specific ssRNA and dsRNA binding; myristoylated; required for replicase activity of VP1
3	2594	VP3	95	Core	M	Guanylyltransferase and methyltransferase; non-specific ssRNA binding; part of transcription complex with VP1
4	2362	VP4	VP4: 88 VP5*: 60 VP8*: 28	Outer capsid	P	Outer capsid spike protein; P-type neutralization antigen; virulence determinant; cell attachment protein; trypsin cleavage into VP5* and VP8* enhances infectivity; VP5* permeabilises membranes; VP8* contains the heamagglutinin domain
5	1611	NSP1	59	Cytoplasm	A	Associates with cytoskeleton; high degree of sequence variation; role in suppression of host interferon response
6	1356	VP6	48	Middle capsid	I	Major virion protein; middle capsid structural protein; homotrimeric structure; groups and subgroup-specific antigen
7	1105	NSP3	35	Cytoplasm	T	Homodimer; virus-specific 3'-mRNA binding; binds elongation factor eIF4G1 and circularises mRNA on translation initiation complex; involved in translational regulation and host shut-off
8	1059	NSP2	37	Cytoplasm	N	NTPase and helicase activity; non-specific ssRNA binding; major component of the viroplasm; binds NSP5 and VP1; essential for dsRNA synthesis and formation of infectious viral progeny
9	1059	VP7	37	Outer capsid	G	Outer capsid structural glycoprotein; G-type neutralization antigen; N-linked high mannose glycosylation and trimming; RER transmembrane calcium-binding
10	751	NSP4	20	Cytoplasm	E	Viral enterotoxin; receptor for double-layer particle budding through ER membrane; N-linked high mannose glycosylation; modulates intracellular calcium levels essential for viral RNA replication and formation of infectious viral progeny
11	667	NSP5/6	NSP5: 22 NSP6: 11	Cytoplasm	H	NSP5: viroplasm formation; multimerizes; O-linked glycosylation; hyper-phosphorylated; autokinase activity; enhanced by NSP2 interaction; binds ssRNA; component of viroplasms NSP6: interacts with NSP5 and localises to viroplasms

segment 11 which is polycistronic and encodes two proteins, NSP5 and NSP6 (Estes and Greenberg, 2013).The size of the genome segments vary from approximately 667-3302 base pairs, and the entire genome is about 18 500 base pairs. Each of the genome segments starts with a 5'-GGC… sequence followed by a highly conserved region, ranging from 9-48 nucleotides, making up the 5' non-coding region, see **Figure 2.4**. The open reading frame (ORF), which encodes the viral proteins, follows and ends in a stop codon. The ORF is followed by another highly conserved region that ranges from 17-182 nucleotides and makes up the 3' non-coding region with most genome segments ending with the consensus sequence …UGUGACC-3' (Desselberger, 2014). This consensus sequence contains various signals that regulate genome replication and gene expression, while the …GACC-3' nucleotides act as a translation enhancer. It is thought that the highly conserved non-coding regions on either side of the ORF contain signals for genome segment-specific packaging. The (+)ssRNA strand of rotavirus folds into a panhandle structure with the 5' and 3' terminal ends annealing through base pairing. The panhandle structure is maintained through interactions of NSP3 with the 3' terminal end and association of the eukaryotic initiation factor (eIF4G) with NSP3, see **Figure 2.5**. (Li et al., 2010), (McDonald and Patton, 2011), (Tortorici et al., 2006).

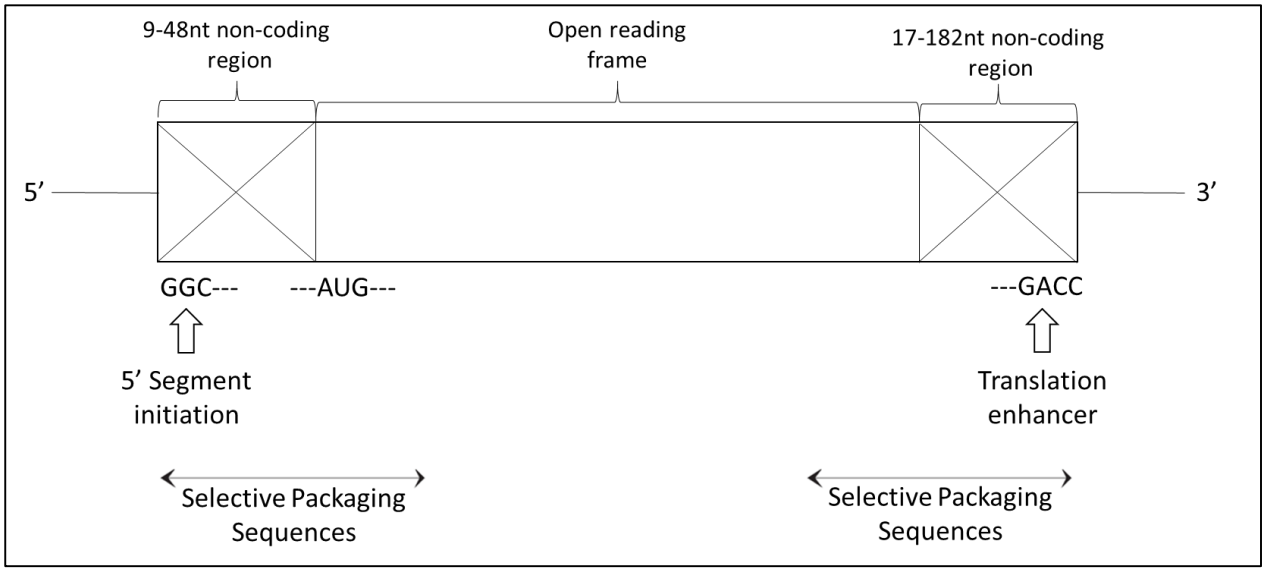

Figure 2.4: Genome structure of rotavirus. This picture illustrates the major features of the rotavirus genome structure with the ORF flanked by two conserved non-coding regions, the 5' GCC segment initiation and the 3' GACC translation enhancer (Estes and Greenberg, 2013).

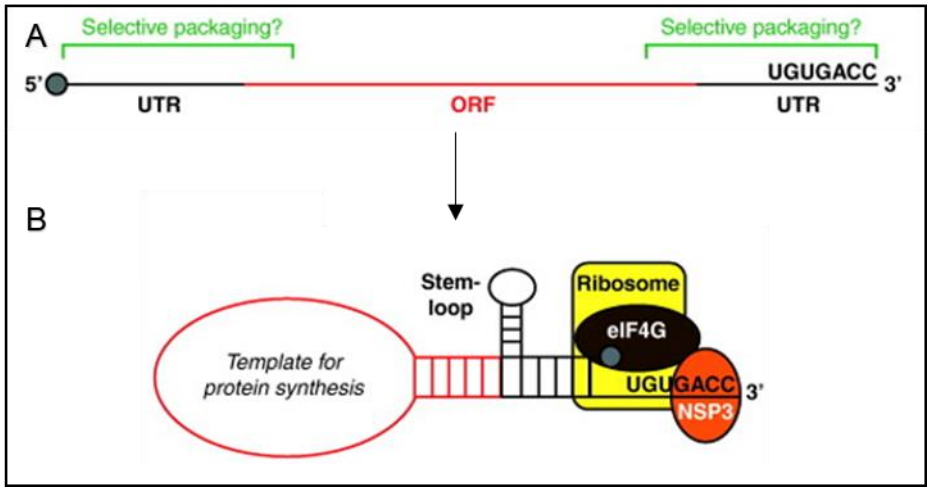

Figure 2.5: Panhandle structure of (+)ssRNA strand. (A) Representation of a linear rotavirus (+)ssRNA strand. The central ORF is shown in red, and the 5′ and 3′ non-coding regions are shown in black. (B) Proposed folding of the (+)ssRNA into a panhandle structure with association of eIF4G and NSP3 (McDonald and Patton, 2011).

2.5 Replication cycle

The replication cycle of rotavirus is a complex set of steps, see **Figure 2.6** (Desselberger, 2014). There is a general expectation that a robust rotavirus reverse genetics system would give answers to various questions regarding the replication cycle. The replication cycle of rotavirus is primarily conducted in the cytoplasm of mature enterocytes of the villi in the small intestine. This suggests that these cells express the specific receptors for viral attachment and penetration (Estes and Greenberg, 2013). The replication cycle consists of the following steps: virus attachment, penetration and uncoating, transcription and translation of viral mRNA, RNA replication and packaging, and virus particle maturation and release (Desselberger, 2014). In the discussion that follows, these steps will be examined based on published literature.

2.5.1 Virus attachment

Rotavirus cell attachment, penetration and uncoating are very complex and not completely understood, and the precise cellular receptors enabling binding to cells differ from strain to strain (Estes and Greenberg, 2013). For example, animal rotavirus strains (e.g. SA11) binds to receptors on the terminal or sub-terminal positions of the cell that contain sialic acid (SA) to infect polarised cultured cells (Fiore et al., 1991). This is in contrast with human rotavirus, which initiates infection of cells by sialic acid-independent mechanisms (Ciarlet and Estes, 1999).

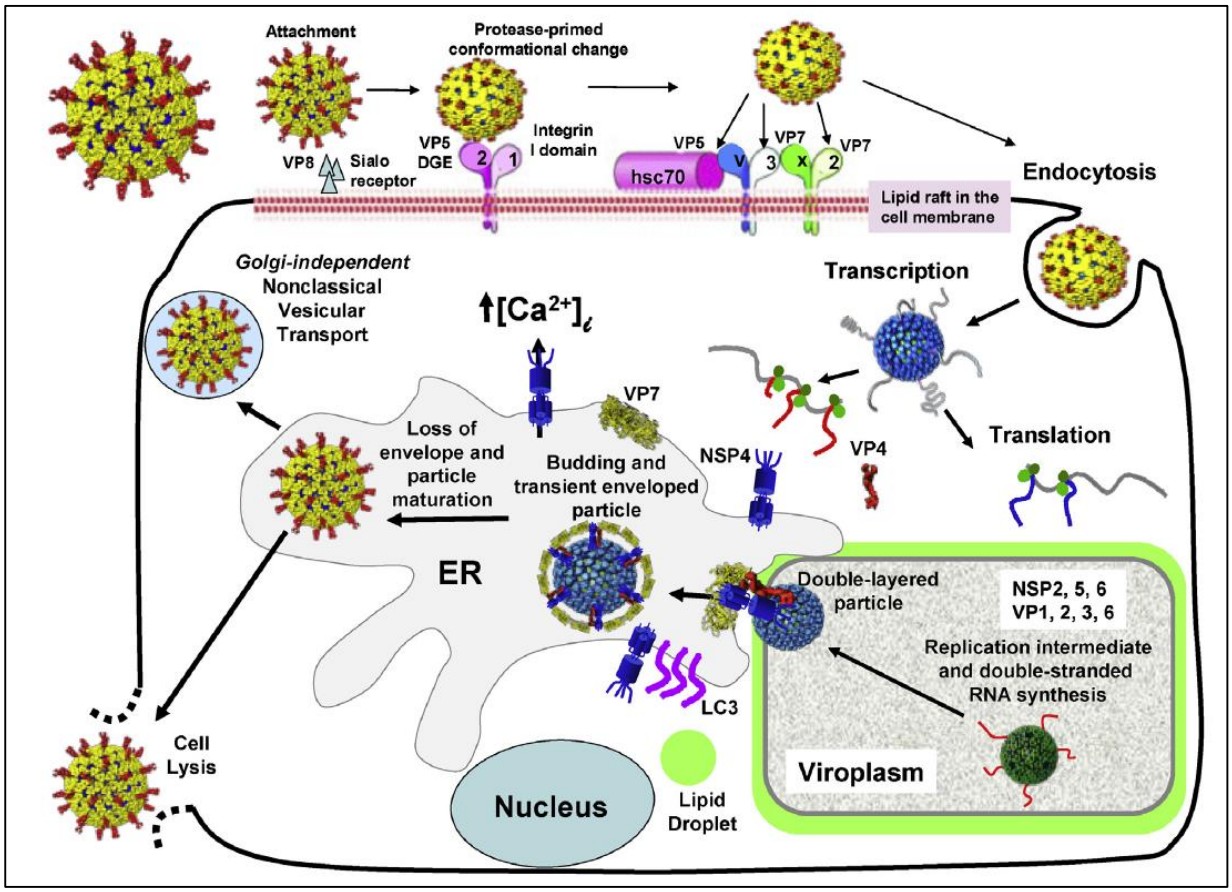

Figure 2.6: The rotavirus replication cycle. The rotavirus replication cycle. The rotavirus triple-layered particles (TLPs) first attach to sialo-glycans (or histo-blood group antigens) on the host cell surface, followed by interactions with other cellular receptors, including integrins and Hsc70. Virus is then internalized by receptor-mediated endocytosis. Removal of the outer layer, triggered by the low calcium of the endosome, results in the release of transcriptionally active double-layered particles (DLPs) into the cytoplasm. The DLPs start rounds of mRNA transcription, and these mRNAs are used to translate viral proteins. Once enough viral proteins are made, the RNA genome is replicated and packaged into newly made DLPs in specialized structures called viroplasms, which interact with lipid droplets. The newly made DLPs bind to NSP4, which serves as an endoplasmic reticulum (ER) receptor, and bud into the ER. NSP4 also acts as a viroporin to release Ca^{2+} from intracellular stores. Transiently enveloped particles are seen in the ER. The transient membranes are removed as the outer capsid proteins VP4 and VP7 assemble, resulting in the maturation of the TLPs. The progeny virions are released through cell lysis. In polarized epithelial cells, particles are released by a non-classical vesicular transport mechanism (Estes and Greenberg, 2013).

The actual attachments to cells are mediated by the two outer-most proteins of the TLP, the spike VP4 and the outer shell VP7. The precise attachment method is unknown, but there is strong evidence of the following factors that play a vital role in attachment. First, the VP4 spike, *in vitro*, is cleaved by an exogenous proteases such as trypsin to yield two subunits VP5* and VP8*, which in turn mediates attachment and subsequent penetration of the cell, see **Figure 2.7**. A shallow groove on the VP8* surface interacts with a sialic acid-containing receptor and thus completes attachment (Estes and Greenberg, 2013). However, it is also shown that certain strains of rotavirus bind to non-sialic acid-containing histo-blood group antigens, e.g. G10P[11] (Dormitzer et al., 2002a, Dormitzer et al., 2002b). After this first step of attachment, a second slower binding step exists where multiple cellular surfaces molecules can

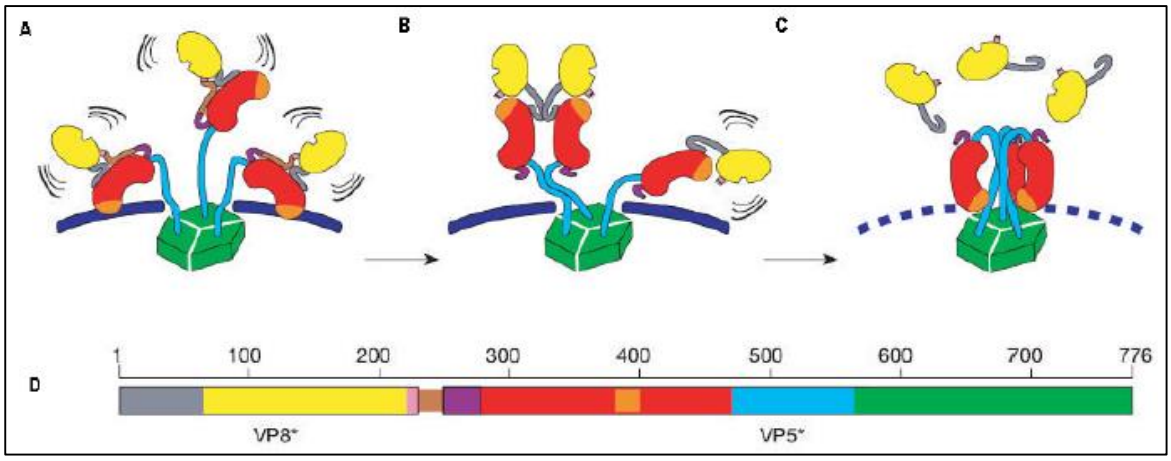

Figure 2.7: The cleavage of VP4 during attachment. Non-cleaved state with possible, flexible, free play indicated by wavy lines. The brown line attached to the purple line represents the non-cleaved trypsin cleavage site. **B**, Trypsin cleaved state. **C**, Folded-back state which exposes the hydrophobic regions during membrane penetration. **D**, Colour coded, linear VP4 indicating the location of amino acid regions in VP5* and VP8*. The head region is coloured in yellow (the VP8* core), notched at the sialoside-binding cleft. The body includes the red domain (VP5* antigenic region) and the orange cap (the potential membrane interaction loop), the purple appendage, and part of the grey and cyan tubes. The stalk is the lower part of the cyan tubes and the foot is shown in green (Dormitzer *et al.*, 2004).

act as co-receptors. Surfaces molecules including multiple integrins, α2β1, αvβ3, αxβ2 and α4β1, which associate with integrin ligand motifs on VP5* or VP7, as well as association of the VP5* to heat shock cognate protein 70 (Hsc70) (Coulson et al., 1997, Guerrero et al., 2002).

2.5.2 Rotavirus penetration and uncoating

As previously stated, the VP4 spike and VP7 outer shell interactions with host cells initiate binding to the targeted cell. However, the exact process of penetration and uncoating (where the TLP or outer capsid is shed, and then delivers the DLP into the cytoplasm of the host cell) are still not entirely clear (Desselberger, 2014). There is evidence suggesting it may be achieved through receptor-mediated endocytosis or direct membrane penetration (Ludert et al., 1987). The uncoating of the outer protein capsid VP4 and VP7 is due to low Ca^{2+} concentration in the endocytic vesicle that removes the TLP and delivers the DLP into the cytoplasm (Ruiz et al., 1997).

2.5.3 Rotavirus transcription

The DLP of rotavirus is transcriptionally active, which means it possess all the enzymes it needs to successfully mediate transcription and replication of all 11 rotavirus genome segments. It is speculated that the low Ca^{2+} concentration in the endocytic vesicles are responsible for the loss of the outermost layer of the virion (Ruiz et al., 1997), (Pesavento et al., 2006). This is thought to trigger the viral polymerase complexes (PCs) to initiate transcription which generates numerous copies of full length, capped, non-poly A tail plus sense ssRNAs [(+)ssRNA] (Patton et al., 2004). These transcripts are made from the minus sense strand [(-)ssRNA] as its template. The polymerase complexes consist of a single viral RNA-dependent RNA polymerase VP1, as well as RNA capping enzyme VP3. These polymerase complexes are attached to the inner surface of the DLPs VP2 shell (McDonald and Patton, 2011). These polymerase complexes constructed from these three structural proteins (VP1, VP2 and VP3) and each individual complex is responsible for transcribing a single genome segment; although still in symmetry with the other polymerase complexes to simultaneously create 11 (+)ssRNA transcripts. Transcription does not occur in equimolar fashion, because the polymerase complexes operate independently from each other and it seems it is also size dependent as smaller transcripts are transcribed more rapidly and in a greater amount than the larger counterparts (Ayala-Breton et al., 2009). The cell's immune response is suppressed by NSP1 which has the ability to degrade several interferon factors. This is done by the down-regulation of the RNA sensitive retinoic acid-induced gene or RIG-I (Barro and Patton, 2007). The newly

synthesised (+)ssRNA are capped by VP3 in the polymerase complex prior to their exit from the DLP. This is made possible by type I channels in the VP2 inner capsid where mRNA can move through after transcription (McDonald and Patton, 2011).

2.5.4 Rotavirus translation and viroplasm formation

The newly synthesised (+)ssRNAs accumulate in the cytosol of the host cells where it uses cellular systems to serve a dual role. Firstly, they can serve as mRNA for the synthesis of new proteins or secondly as a template strand for the replication of the genome. Most of the viral proteins are synthesised on free ribosomes in the cytosol, except for VP7 and NSP4 which are synthesised on ribosomes associated with the endoplasmic reticulum (Estes and Greenberg, 2013). For this to occur efficiently NSP3 plays an important role in that the …ACC-3' terminal end of the viral (+)ssRNAs associates with the N-terminal of NSP3 along with the association of the C-terminal of NSP3 with the translation factor elF4G. This association circularises NSP3 and lets it function like the PolyA binding protein (PABP) of cellular mRNAs thus suppressing the translation of cellular mRNAs expeditiously (Piron et al., 1998, Piron et al., 1999, Vende et al., 2000).

Rotavirus formation occurs when nascent (+)ssRNAs and rotavirus proteins interact with each other in a particular way inside cytoplasmic inclusion bodies termed "viroplasms". These inclusion bodies or viroplasms form approximately 3-4 hours after infection and are constructed by several viral proteins, including VP1, VP2, VP3, VP6, NSP2, and NSP5. The two non-structural proteins NSP2 and NSP5 are the most important components as the co-expression of these proteins are responsible for the formation of empty viroplasms, even in the absence of any other viral proteins (Criglar et al., 2014) (Fabbretti et al., 1999). If the expression of these two proteins are silenced by the use of intrabodies or RNA interference technologies (RNAi), the construction of the viroplasms does not occur (Criglar et al., 2014), and this shows that these two proteins are essential in the formation of viroplasms.

The multifunctional protein NSP2 has core functions in the genome replication period, including the following: it binds to ssRNA, which helps with the unwinding of the ATP-dependent helix and it exhibits kinase activity in nucleoside diphosphate (NDP) and nucleoside triphosphatase (NTPase) (Estes and Greenberg, 2013). Several ligand interactions have been observed in addition to the enzymatic functions of NSP2

(Criglar et al., 2014). Cryo-electron microscopy structural pictures indicate grooves in the structure of NSP2, and it serves as a binding site for ssRNAs, NSP5 and tubulin. The competitive binding nature of these ligands may help regulate the balance between genome replication and the assembly of the virus (Criglar et al., 2014), (Martin et al., 2010) (Jiang et al., 2006).

The exact role and functions of NSP5 are not completely known. Research has shown that NSP5 is involved in multiple processes, such as viroplasm formation and regulation (Criglar et al., 2014). NSP5 is found in various complexes with different proteins such as NSP2, NSP6, VP1, VP2, VP3 and VP6. The down-regulation of NSP2 results in a loss in the formation of the viroplasms, as mentioned previously.

2.5.5 RNA replication, packaging and assembly

The atomic resolution structural detail of TLPs and DLPs are well known, thus giving us insight into the protein organisation of the capsids (Settembre et al., 2011). However, the structures of early replication intermediates of rotavirus are not so well known. There are various reasons for this such as the fact that they are encapsulated in viroplasms which are too electron dense to get a high-resolution image through electron microscopy and these intermediates are too small for conventional light microscopy (Long and McDonald, 2017). This all contributes to the fact that the exact mechanism for replication, packaging and assembly are not very well understood. The RNA replication and packaging of nascent core particles simultaneously takes place in the viroplasms, and it is believed that dsRNA synthesis occurs in a specific replication complex constructed of VP1, VP2 and VP3 with NSP1, NSP2, NSP3 and NSP5 that also may play a part in this process (Gallegos and Patton, 1989). In contrast to transcription and despite the variation in the size of the different genome segments replication, occurs in equimolar amounts, indicating this is a highly regulated process (Patton et al., 2004). If this process was not highly regulated the dsRNA might not be packaged.

Several models for RNA packaging have been hypothesised. The two most widely accepted ones will be highlighted, see **Figure 2.8**. The first model is based on the collection of functional complexes. Each of these complexes contains an RNA dependent RNA polymerase (VP1) and a capping enzyme (VP3) (Trask et al., 2012). The packaging in this model runs in synchrony with capsid assembly when the

association of the VP1/VP3 complex with a specific mRNA occurs and causes the attraction of a core VP2 protein, thus completing the complex. It is assumed that the association with VP2 causes a conformational change in VP1 and thus activates the minus-strand synthesis and completing the dsRNA (Estes and Greenberg, 2013). The second model is based on the suggestion that cores are formed first without any mRNAs inside, which then presumably associate with the core later on (Estes and Greenberg, 2013). The core VP2 is formed with the VP1 polymerase and VP3 capping complex inside. Only after it has formed are the 11 (+)ssRNAs inserted into the core, presumably with the help of NSP2/NSP5, and then the minus-strand RNA is synthesised, completing the dsRNA (McDonald and Patton, 2011). With further research, the exact model will be identified.

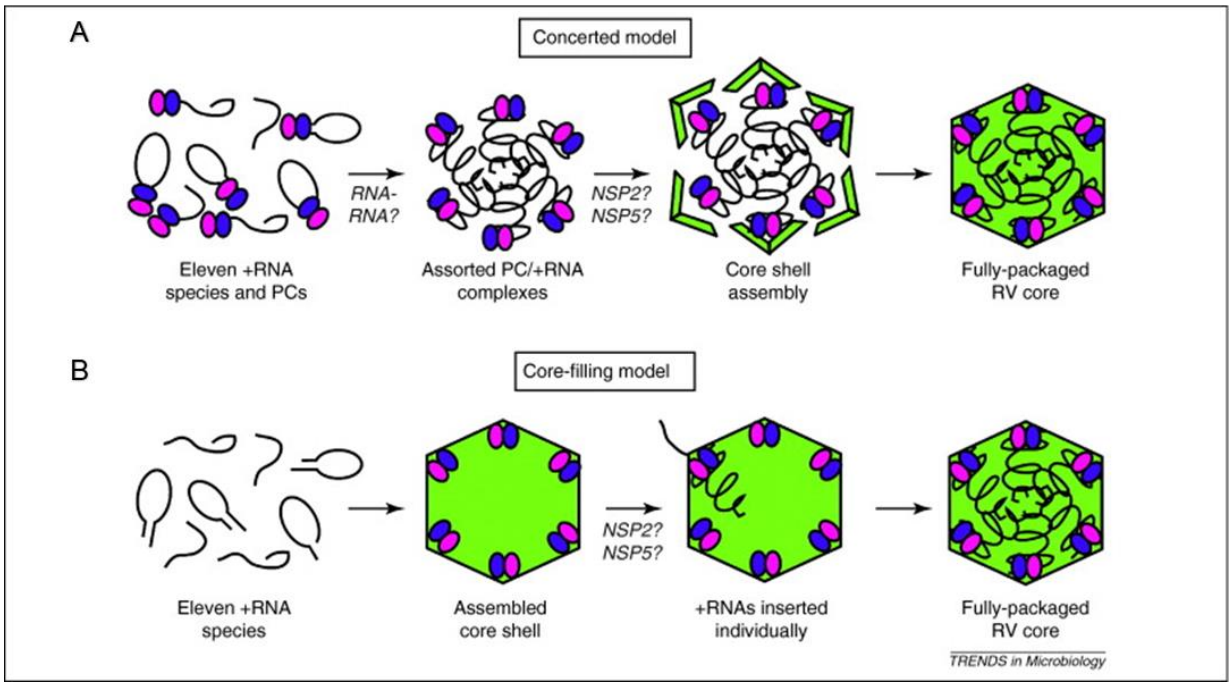

Figure 2.8: Proposed RNA packaging models. (A) VP1/VP3 complexes associate with (+)ssRNAs and attracts a VP2 core. Once the DLP is formed the synthesis of the (-)ssRNAs occurs. (B) DLPs containing VP1/VP2 complexes and a VP2 shell form first. The (+)ssRNAs are transported into the DLP with the help of NSP2/NSP5 and synthesis of the (-)ssRNAs occurs (McDonald and Patton, 2011).

A clear-cut feature of the morphogenesis of rotavirus is that the DLPs which are formed in the viroplasms bud through the endoplasmic reticulum's (ER) membrane, which is different than any other genera of the *Reoviridae* family (Estes and Greenberg, 2013). Through this procedure, the DLPs acquire an envelope of transient lipids that is later

lost and replaced by a thin layer of protein which ultimately builds up the outer layer of the TLP with VP4 and VP7 to form fully mature virions (Lopez et al., 2005). The viral protein responsible for budding through the ER and the rest of the morphogenesis is NSP4 and is the key regulator for the assembly of the outer capsid (Trask et al., 2012). NSP4 is also known to be a calcium agonist and uses intracellular calcium to help support effective budding (Estes and Greenberg, 2013). NSP4 has three distinct domains, each with their respective functions. Firstly, we have the H1 domain which function is to form intra-molecular disulphide bonds. Secondly, the H2 transmembrane domain which anchors NSP4 into the ER's lipid bi-layer. The C-terminal cytoplasmic domain which binds to the DLPs and this interaction drives the transmembrane "budding" of these DLP across the membrane and into the lumen of the ER (Estes and Greenberg, 2013, Lopez et al., 2005).

The current working model of TLP assembly suggests that NSP4 recruits VP4 from the cytosolic surface of the ER, as well as DLP from the viroplasms and the subsequent association of these elements trigger the budding of the DLP/VP4/NSP4 complex into the ER (Trask et al., 2012). The lipid envelope is lost during this process, and after entry into the ER, VP7 assembles onto the DLP locking the VP4 into place and completing the TLP structure of the virion (Trask et al., 2012).

2.5.6. Virus release

The permeability of the plasma membranes late during infection is altered by drastic cytolysis that results in the release of viral and cellular proteins. Electron microscopy studies have shown newly synthesised rotavirus virions in nonpolarized cells are released from the host cell by cell lysis (Estes and Greenberg, 2013). This suggests that the bulk of rotaviruses are released in this manner. Contrary to this, it has been shown that epithelial cells' membranes can be destabilised and allow rotavirus exit that does not immediately cause cell death. This is done by using VP4 as a remodelling agent (Gardet et al., 2006).

A reoccurring theme throughout the replication cycle of rotavirus is that the exact mechanisms for various parts of it are still not known or that there are multiple theories for a single aspect of the cycle. Some examples are the unknown mechanism for DLP extraction from viroplasms (Trask et al., 2012), transport mechanism for ssRNA to the

viroplasms etc. This reconfirms the need for a comprehensive rotavirus reverse genetics system to aid in the further study of the replication cycle of rotavirus.

2.6. Rotavirus immune responses

As for many subjects surrounding rotavirus, the exact mechanisms that correlate with protection against rotavirus is not clear. It is established that rotavirus infection prompts three types of responses: Non-specific or innate immune responses, virus-specific humoral (acquired) immune responses and cellular immune responses (Desselberger and Huppertz, 2011).

2.6.1. Humoral and cellular immunity

After rotavirus infection, the host's humoral immune responses are triggered, subsequently activating B cells to produce specific antibodies against the viral proteins and T cells that have the ability to recognise T cell-specific rotavirus epitopes on the infected cells surfaces (Desselberger, 2014). These antibodies are primarily directed against the epitopes on the surface of the VP4 and VP7. The T cells specific to rotavirus are responsible for eliminating rotavirus in the primary infection stage, while B cells are responsible for long-term protection against subsequent infections (Franco et al., 2006). The first rotavirus infection usually results in acute gastroenteritis because of the lack of antibodies against the virus, but for subsequent rotavirus infections, the effects are far less severe due to the increase in protection from humoral immunity (Desselberger and Huppertz, 2011). In children, the degree of protection against severe diarrhoea was 87% after the first natural infection and 100% protection after the second natural infection, and the evidence suggests that both primary symptomatic and asymptomatic infection leads to the same degree of protection (Velazquez, 2009). Also, after the primary infection, homotypic and heterotypic neutralising antibodies have been reported, suggesting that neutralising epitopes on VP4 and VP7 molecules of different strains of rotavirus can cross-react with each other (Chiba et al., 1986). The protection against rotavirus infection is not just from neutralising antibodies generated against VP4 and VP7. Upon infection, whether from natural exposure or vaccination, antibodies against other structural proteins (VP2 and VP6) and non-structural protein (NSP4) are formed. These antibodies are, however, non-neutralizing *in vitro* but show protection against infection *in vivo* (Burns et al., 1996). In the case of VP6, antibodies specific against this protein are taken up and

bind to newly developed DLPs, thus preventing them to mature to fully developed TLPs (Burns et al., 1996, Desselberger, 2014). The $CD8^+$ cells can secrete certain cytokines that can help against rotavirus infection. However, infection of rotavirus is an inefficient inducer of these cells. When dendritic cells are infected with rotavirus *in vitro* they are able to activate rotavirus-specific T cells that can secrete Th1 cytokine. Dendritic cells are also necessary to trigger B cell activation after rotavirus infection (Jaimes et al., 2002) (Desselberger and Huppertz, 2011).

2.6.2. Innate immune response

When host cells are infected by pathogens, they trigger numerous responses that can rapidly mount an efficient defence against intruders. The innate immunity is the host's first response to infection **Figure 2.9**. However, it only grants short time protection and mounts a defence against viruses by suppressing the mechanisms of viral replication through various cell signalling pathways. Interferons (IFN) are a family of inducible cytokines that have antiviral activity. These cytokines are primarily type I and III interferon and their secretion is mediated by the expression of interferon-stimulated genes (ISGs) (Samuel, 2001). The release of the cytokines from IFN aids in the defence of viral infection by inhibiting viral replication through various means (Edinger and Thompson, 2004). Recent studies have shown the adaptive ability of rotavirus to evade or neutralise the innate immune responses to aid in their replication. Rotavirus especially inhibits the IFN responses with the help of NSP1 that degrades various interferon-regulating factors (IRFs) (Angel et al., 2012).

IFN type I (IFN-α/ IFN-β) and type III (IFN-λ) is critical for early defence against viral infection and has been shown to decrease rotavirus infection *in vitro,* and the secretion of it can be elicited in a number of different ways. Rotaviruses are recognised through their viral genome segments or proteins by pattern recognition receptors (PRRs) (Villena et al., 2016). There are three different pattern recognition receptors. Two cytoplasmic detectors namely, RNA retinoic acid-induced gene-I or RIG-I and the melanoma differentiation associated gene 5 (MDA5), and the transmembrane toll-like receptor (TLR). After the genomic material of viral infection is recognised, an intricate series of cellular events follow that leads to the establishment of an antiviral state (Angel et al., 2012). Thus, after the detection of viral genomic material by the cytoplasmic detector PRRs, a signal is transmitted to the mitochondrial antiviral

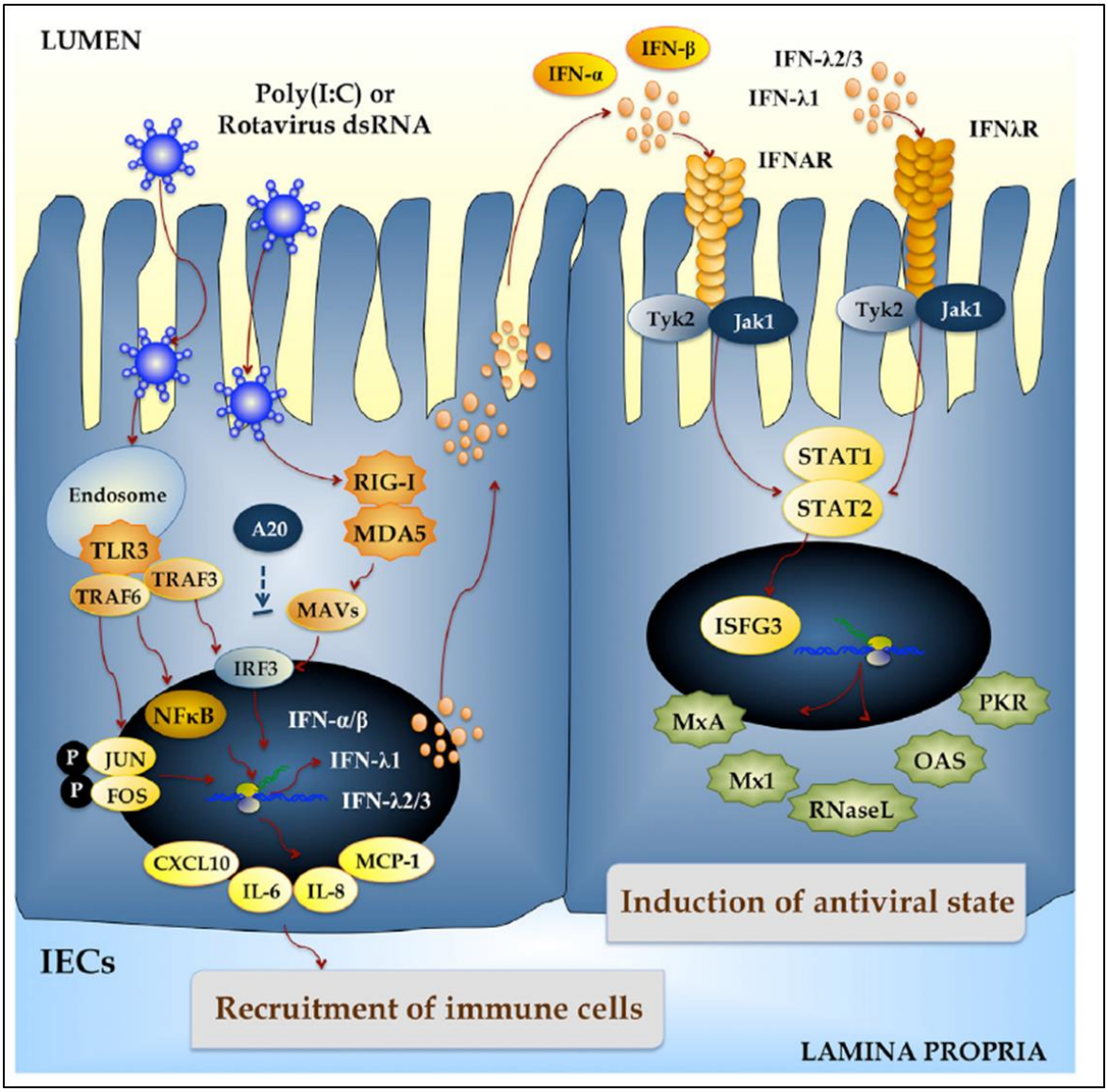

Figure 2.9: Innate immune response against rotavirus in intestinal epithelial cells (IECs). The Rotavirus double-strand genomic RNA activates toll-like receptor 3 (TLR3), retinoic acid-inducible gene-I (RIG-I), and melanoma differentiation-associated gene-5 (MDA-5), which are pattern recognition receptors (PRRs) expressed in IECs. Cellular signaling cascades are activated and converge at the level of interferon (IFN) regulatory factor-3 (IRF3) that upregulate the expression of type I (IFN-α, IFN-β) and type III (IFNλ1, IFNλ2/3) IFN, which in turn induces the synthesis of IFN-stimulated genes with antiviral activities (MxA, Mx1, RNase L, OAS, PKR). Antiviral PRRs also activate nuclear factor κB (NF-κB) pathway and induce the secretion of proinflammatory cytokines and chemokines (IL-6, IL-8, MCP-1, CXCL10). Those effects could be imitated *in vitro* and *in vivo* by administration of the dsRNA synthetic analog poly(I:C) (Villena et al., 2016).

signalling protein (MAVS) which in turn activates IRF3/ IRF7 together with nuclear factor-κB (NF- κB). The IRF3/IRF7 and NF- κB subsequently migrate into the nucleus where they up-regulate the expression of both type I and type III IFN, which afterwards generates the transcription of IFN-stimulated genes and IFN (Desselberger, 2014) (Villena et al., 2016).

In addition to the cytoplasmic detectors, viral genomic material which is enveloped by endosomes are detected by TLRs. TLR3 utilises signals to the TIR-domain-containing adaptor-inducing IFNβ (TRIF) to activate IRF3/IRF7, both of which are present in inactive forms in the cytoplasm and are activated when the C-terminal region is phosphorylated (Arnold and Patton, 2011). The TLR7/TLR8 incorporate the myeloid differentiation primary response 88 to activate these IRFs (Honda and Taniguchi, 2006). From the point where IRF3/IRF7 are activated both the PRR pathways converge and assist in the transcription of ISGs. It has been found that IRF7 has a stronger effect in activating type I and III IFN than IRF3; although for optimal expression of IFNs both IRF3/IRF7 is needed (Arnold and Patton, 2011, Villena et al., 2016). After the production of IFN is elicited through PRRs in an infected cell, type I and Type III IFN are secreted from that cell. The goal of this is that the secreted IFNs bind to a specific receptor on uninfected cells so that the production of IFNs are upregulated to help fight against infection. The secreted type I IFNs binds to IFN-α/IFN-β specific receptors which are generally expressed on most cell surfaces, while type III IFN binds to IFN-λ specific receptors which are exclusively found on epithelial cell surfaces (Donnelly and Kotenko, 2010). These binding signals initiate the formation of interferon-stimulated gene factor 3 (ISGF3) which is a complex of 3 proteins, comprised of signal transducers and activators of transcription 1 (STAT1), STAT2 as well as IRF9. Once ISGF3 is assembled, it is translocated into the nucleus of the cell where it binds to ISGs and aids in the production of an antiviral state in the cell (Donnelly and Kotenko, 2010, Estes and Greenberg, 2013)

A number of studies determined that rotaviruses have the capacity to evade host cell's innate immune responses. It has the ability to circumvent type I IFN responses thanks to the viral proteins NSP1. Rotavirus NSP1 has been shown to interact with several cellular protein such as IRF3 and β-transducin repeat-containing protein (β-TrCP) and

results in the proteasomal degradation of these proteins, thus inhibiting or down-regulating an early IFN response (Barro and Patton, 2005, Estes and Greenberg, 2013). Further evidence also shows down-regulation of IRF5 and IRF7 attributed to NSP1, indicating the broad antagonistic nature of this protein (Barro and Patton, 2007, Arnold et al., 2013a). As mentioned, the translocation of IRF3 is essential for the innate immune response to effectively create an antiviral state to fend off infection, and by the down-regulation of it, it helps to create a favourable environment for viral replication. NSP1 has an affinity for IRF3 and binds to the dimerization domain of the protein (Arnold et al., 2013b). The phosphorylation of STAT1 is also inhibited by NSP1 and thus effectively impedes the translocation of the ISGF3 protein complex (Sen et al., 2014). The proteasomal degradation of β-TrCP blocks the activation of NF- κB which is ever-present in the cytoplasm in an inactive form. The β-TrCP activates NF-κB by phosphorylating the κB-inhibitors and subsequently leads to the translocation of NF- κB into the nucleus to co-activate IFN-β (Graff et al., 2007). NSP1 lastly induces the proteasomal degradation of the pro-apoptotic cellular protein p53, thus delaying the time of cell apoptosis in early stages of rotavirus replication (Bhowmick et al., 2013).

A previous study conducted in our laboratory sought to investigate the innate immune responses elicited from rotavirus transcripts. This study determined that the transfection of *in vitro*-transcribed (+)ssRNAs derived from rotavirus DS-1 and SA11 strains in HEK 293H cells elicited a strong innate immune response. Western blot analysis in this study concluded that the (+)ssRNAs were sensed by the RIG-I pattern recognition receptor. In addition, it was found that the inhibition of protein kinase R (PKR) lowered the expression of IFN-β, IFN-λ, TNF-α and CXCL10 cytokines. The study suggested that in order to increase the chances of rescuing virus the transfection of (+)ssRNAs should be in cells where the RIG-I was deficient or inhibited (Mlera, 2012). Another study done in our laboratory investigated ways to suppress the innate immune response of rotavirus transcripts. This study found that the expression of certain viral proteins reduced the expression of some cytokines. In particular, it was determined that the transfection of cells with plasmids encoding NSP1 and NSP2 or with NSP2 and NSP5/6 24h prior to the transfection of rotavirus transcripts, mass cell death was substantially reduced. The results of qRT-PCRs showed that cells transfected with NSP1 and NSP2 lowered the expression of IFN-α, IFN-β and CXCL10

cytokines, while the transfection of NSP2 and NSP5/6 suppressed both type I and III interferon responses (Wentzel, 2014). These findings were incorporated into the approach taken in this study.

2.7. Rotavirus vaccines

Before the advent of rotavirus vaccines, rotavirus in developing countries accounted for 25% of severe cases of gastroenteritis in children younger than 5 years of age and out of diarrhoea-associated death rate of 3.2 million per annum, 873 000 were attributed to rotavirus. Due to this high mortality rate, it was imperative to develop a vaccine to counteract the virus (Parashar et al., 2009).

In 1998, after extensive safety and efficacy trails, RotaShield®, the first rotavirus vaccine, was introduced and made available to the public (Estes and Greenberg, 2013). The results of trials done in Finland, United States of America, Native Americans and Venezuela showed that the efficacy of the vaccine varied from 48% to 68% against diarrhoea caused by rotavirus and protection against severe diarrhoea varied from 91% in Finland to 88% and 69% in Venezuela and Native Americans, respectively (Santosham et al., 1991). RotaShield® was a quadrivalent vaccine that included specificity of VP7 for four human G serotypes together with the attenuation phenotype of rhesus rotavirus (RRV) and was administrated to children at 2, 4 and 6 months of age (Kapikian et al., 1996). Only a year after its release, 15 cases of intussusception were reported that caused the suspension of the use of this vaccine. After an investigation that found that 1 in 600 children got intussusception after the use of the vaccine, it was discontinued for good (Estes and Greenberg, 2013).

After the discontinuation of RotaShield®, it was of the utmost importance to find a replacement vaccine for rotavirus. Two separate approaches were followed, and today there are two different licenced vaccines available for rotavirus. The first is a live-attenuated monovalent vaccine produced by GlaxoSmithKline called Rotarix™. Rotarix™ is constructed out of a virulent human strain 89-12 together with G1:P1A[8] serotype specificity and is administered at 2 and 4 months to young children (Ruiz-Palacios et al., 2006, Bernstein et al., 1999). The results of efficacy studies showed that Rotarix™ gave 85% protection against severe gastroenteritis, was released in 2005 and is now licenced in more than 110 countries worldwide. The second vaccine readily available today is the pentavalent human-bovine reassortant Rotateq®

manufactured by Merck (Estes and Greenberg, 2013). This pentavalent vaccine is constructed out of five human-bovine reassortant strains, each encoding 10 genome segments of the bovine strains G6P[5] together with one human genome segment that encodes for one outer protein of the following serotypes: G1, G2, G3, G4 and P1 (Heaton et al., 2005). These 4 serotypes are the most prevalent in causing gastroenteritis worldwide. Safety and efficacy studies revealed that Rotateq® is highly effective in preventing severe gastroenteritis with a protection rate of 98% (Vesikari et al., 2006). This vaccine is administered at 2, 4 and 6 months of age and was first licenced in early 2006 and is available in over 100 countries (Estes and Greenberg, 2013).

However, the protection granted from these vaccines varies tremendously from region to region (Clarke and Desselberger, 2015). Efficacy studies conducted in high-medium- and low-income settings were performed for both Rotarix™ and Rotateq®, and the results show that the lower income groups tend to have less protection against severe gastroenteritis (Estes and Greenberg, 2013). For Rotarix™ the studies were conducted in high-income settings that included Hong Kong, Japan and European countries, a middle-income group consisting of Latin America and Finland and a low-income group, made up by South-Africa and Malawi. The studies show that the vaccine provided greater than 95% of protection for high-income groups and between 80 and 85% in middle-income groups. However, in the low-income groups, the efficacy of the vaccine was considerably lower with South Africa having less than 75% protection and Malawi lower than 50%. Similar studies done on the Rotateq® vaccine have come to the same conclusion that countries in Europe and North America have much higher protection rates than developing countries such as Bangladesh, Ghana, Kenya and Mali (Clarke and Desselberger, 2015). This may be attributed to the fact that the current two vaccines are manufactured with strains more prevalent to regions in North America and Europe. Although the efficacy of these vaccines is lower in regions in Asia and sub-Sahara Africa, it is important to note that the burden of disease is still lowered by these vaccines (Madhi et al., 2016). It is, however, imperative to create vaccines that are manufactured with strains specific to these lower rate of protection regions to ensure maximum protection against rotavirus.

2.8 Reverse genetic systems

A reverse genetic system is a biological tool used to artificially induce manipulations such as site-directed mutagenesis, rearrangements and insertion/deletion at cDNA level to generate insight into the workings of biological characteristics, pathogenesis and the replication cycles of various virus families and genera (Komoto et al., 2006). The knowledge gained from this can be used to create targeted vaccines that can provide longer and more effective protection against disease. Currently, there are reverse genetics systems for several dsRNA viruses in the *Reoviridae* family, including African horsesickness virus (AHSV), bluetongue virus and mammalian orthoreovirus (MRV), see **Figure 2.10** (Trask et al., 2013, van Rijn et al., 2016). Unfortunately, the extrapolation of these known systems directly to rotavirus was unsuccessful. However, in early 2017 a reverse genetics system for rotavirus comprised entirely from plasmids was accomplished and will be discussed later (Kanai et al., 2017).

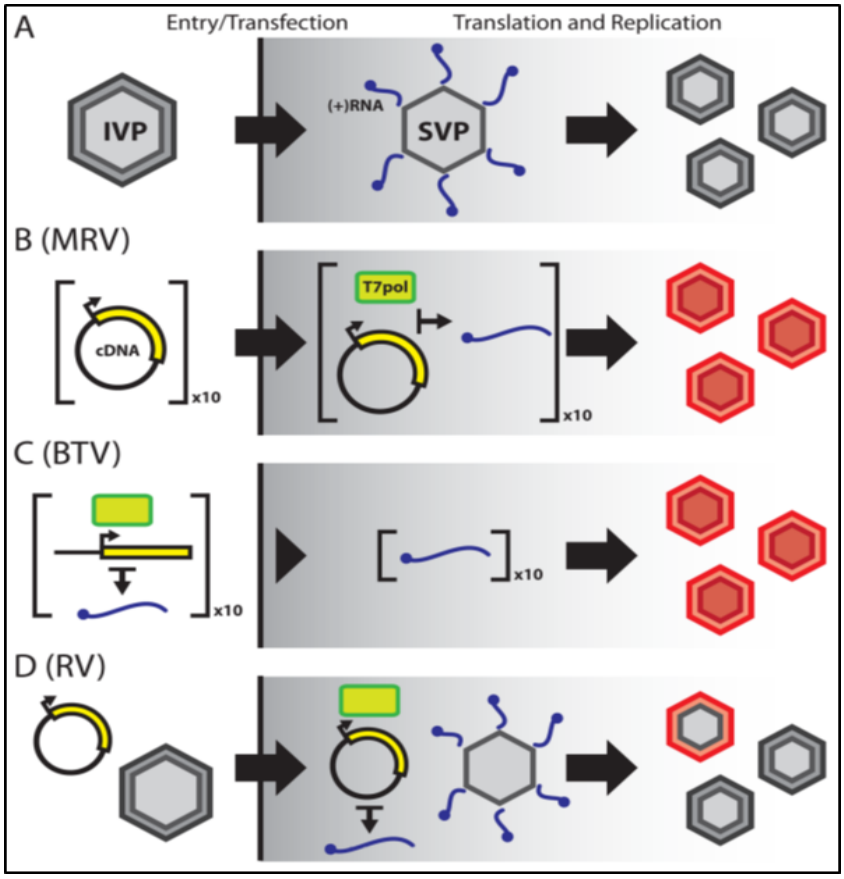

Figure 2.10: Comparison of *Reoviridae* reverse genetics methods with authentic virus replication. (A) Schematic of *Reoviridae* virus replication. A multilayered, icosahedral infectious virus particle (IVP) binds and enters a target cell, prompting loss of the outer capsid. Once in the cytosol, the resulting subviral particle (SVP) becomes transcriptionally active and extrudes capped, [+]RNAs that serve as templates for viral protein synthesis and dsRNA genome replication. Viral inclusions are the sites of genome replication and nascent IVP assembly. (B) MRV reverse genetics. Ten plasmid cDNAs (corresponding to the ten MRV genome segments) are transfected into cells expressing T7 RNA polymerase (T7pol, green brick), wherein the cDNAs are transcribed into MRV [+]RNAs (blue squiggle). As with authentic virus, these [+]RNAs serve as templates for viral protein expression and dsRNA genome replication, resulting in formation of entirely recombinant IVPs (red). (C) BTV reverse genetics. Linearized plasmid cDNAs are transcribed *in vitro* using T7pol to generate a complement of the ten BTV [+]RNAs. The [+]RNAs are transfected into cells and are used for viral protein expression and virus replication to generate recombinant IVPs. (D) RV single-segment replacement. A plasmid cDNA encoding a single RV genome segment is transfected into cells expressing T7pol, followed by infection with a helper RV. Few helper virus particles incorporate the recombinant [+]RNA into their genome during replication, in place of the native species. This results in a virus population that is largely unmodified helper RV, but also contains a small population of single-segment recombinant RV (indicated by the red and grey IVP). Several selection strategies have been devised to isolate the single-segment recombinant RV from the helper virus (Trask et al., 2013).

Primarily, reverse genetics systems follow one of two strategies, either a transcript-based reverse genetics system or a plasmid-based reverse genetics system. For a transcript-based reverse genetics approach to be implemented successfully a couple of factors should be taken into account. It is absolutely essential to generate (+)ssRNAs of all 11 genome segments that have precise 5' and 3' termini. This is accomplished when all viral genome segments are *in vitro*-transcribed into active (+)ssRNAs that has a promoter sequence upstream at their 5' end and a restriction enzyme site at their 3' end. All the transcripts for all the genome segments are then transfected into mammalian cells for the rescue of the viruses. In the plasmid-based system, all genome segments of the virus are individually cloned into their own suitable transcription vectors flanked upstream (5' end) with a promoter sequence and a ribozyme sequence downstream (3' end). All the plasmids are then transfected into mammalian cells which are suitable for the propagation of rotavirus (Wentzel, 2014). **Figure 2.11** illustrates the different reverse genetics approaches.

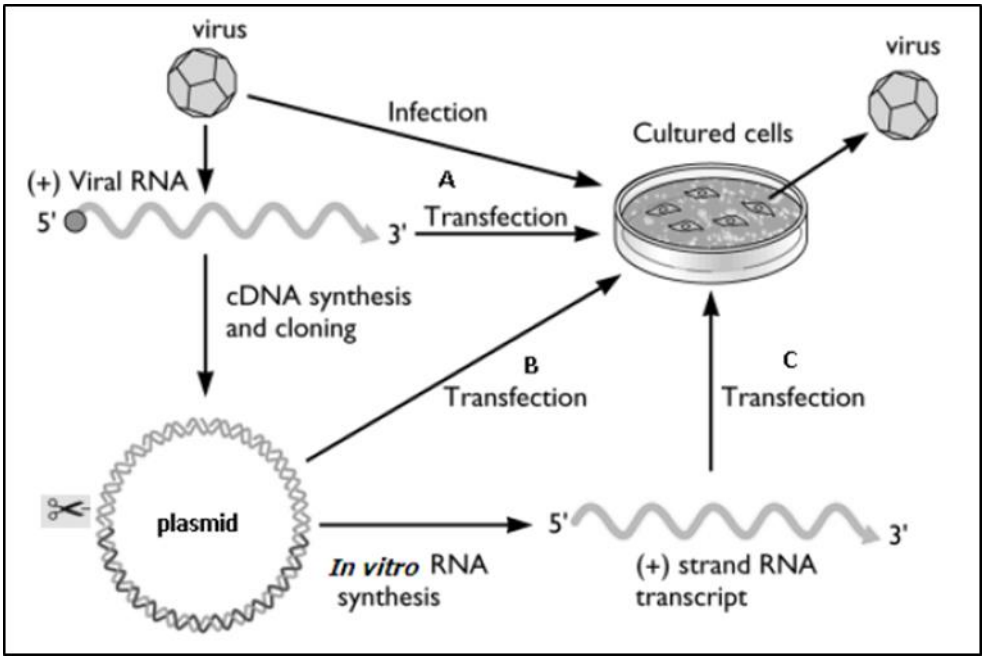

Figure 2.11: Illustration of reverse genetics strategies for (+) ssRNA viruses.
(A) Wild-type viral transcripts can be transfected into cells. (B) The viral transcripts can be reverse transcribed and cloned into plasmids. These plasmids are then transfected into cells. (C) The plasmids can be linearised and be used as templates for *in vitro* transcription and the transcripts can then be transfected (Mlera, 2012).

2.8.1. Rotavirus reverse genetics systems

Several rotavirus reverse genetics systems have been reported. However, all of these systems are dependent on the presence of a helper virus and are subject to strong selection conditions (Desselberger, 2014). Furthermore, all of these systems only allow the manipulation of a single genome segment. The first reverse genetics system for rotavirus was developed in 2006. The full sequence of genome segment 4 (VP4) cDNA was cloned into a vector and was flanked by a T7 promoter region on the 5' end and a hepatitis delta virus (HDV) ribozyme at the 3' end, followed by a T7 terminator region. This plasmid was then transfected into cultured cells infected with a recombinant vaccinia virus, which provided the T7 RNA polymerase, and incubated for approximately 20 hours. The cultured cells were then infected with a helper virus, human rotavirus strain KU (G1P[8]), and incubated for 24 hours after which the recombinant virus with the VP4 gene was rescued using P[8] specific neutralising antibodies (Komoto et al., 2006).

In 2010, a reverse genetics system that relies on a temperature sensitive (ts) rotavirus mutant as a helper virus was developed. A plasmid with the cDNA of genome segment 8 (NSP2) flanked by a T7 promoter region at the 5' end and an HDV ribozyme and T7 terminator region at the 3' end was transfected into cells infected with rDIs-T7pol, followed by the transfection of the ts mutant and incubated at 30°C. The virus contained inside the cell lysates was further passaged in cultured cells at 39°C to select for the recombinant virus (Trask et al., 2010). The biggest limitation of this system is the lack of known temperature sensitive rotaviruses with only 4 SA11 rotaviruses being mapped (Criglar et al., 2011).

Lastly, Troupin and collaborators used the cDNA of an *in vitro* manipulated genome segment 7 (NSP3) that encodes a modified NSP3 protein. The altered plasmid was transfected into COS-7 cells also infected with rDIs-T7pol to provide the T7 RNA polymerase together with the helper virus, bovine rotavirus RF, and no additional selection pressure (Troupin et al., 2010) (Taniguchi and Komoto, 2012). Because of no selection pressure being used the need arose for the cells to undergo multiple serial passages to remove the helper bovine rotavirus. The preferential packaging of these rearranged genome segments held no growth advantaged and thus this reverse genetics system is limited to to rearranged genome segments.

In early 2017 the first reverse genetics system for rotavirus comprised of only plasmids was described. In this system, all 11 genome segments were cloned into individual plasmids with a T7 promoter region on the 5' end of the insert and an HDV ribozyme on the 3' end. In addition to these 11 plasmids containing the cDNA of all the genome segments of the SA11 rotavirus, three more plasmids were added. The first plasmid encodes fusogenic orthoreovirus (FAST) protein that aids viral replication and pathogenesis *in vivo*. These proteins are the smallest nonenveloped viral fusogenic proteins, and it was assumed that they could accelerate the replication cycle of other *Reoviridae* viruses (Kanai et al., 2017). The second (D1R) and third (D12L) plasmids encode two subunits of the VV capping enzyme. This capping enzyme effectively caps the 5' end of viral mRNAs in the cytoplasm resulting in more efficient translation of viral proteins. The 14 plasmids were co-transfected into BHK-T7 cells, and after 3-5 days of incubation the cells underwent three cycles of freezing and thawing, and afterwards, the lysates were seeded onto MA104 cells. After a couple of days since the first passage, a notable amount of cytopathic effect (CPE) was noticed which indicated a recombinant strain of rotavirus was present (Kanai et al., 2017).

Before the major accomplishment from Kanai and collaborators of establishing a helpe-independent rotavirus reverse genetics system, all other systems lacked the means of manipulating all the different genome segments of rotavirus at the same time. With this newly established system, it opens the door for numerous new studies that can help answer a lot of the questions surrounding the replication cycle and pathogenesis of rotavirus. Ulrich Desselberger has comprised a list of topics about rotavirus that will require in-depth research. The list is as follows: the 3D structure of the dsRNA segments packaged in the RV core and their potential interaction with the core-shell VP2; the different receptor specificities of different RV strains; details of the interaction of viroplasms with lipid droplets; the mechanisms controlling assortment/reassortment of 11 RNA segments in replication complexes (i.e. RNA/RNA interactions); the mechanisms controlling RV RNA packaging; the formation and loss of temporary enveloped RV particles in the ER during the viral maturation process; the potential of intestinal organoid cell cultures for the study of RV replication; the factors (mutations) determining RV pathogenicity and virulence; the molecular basis for host range and organ/cell-specific viral replication; the significance of the different arms of the immune response in establishing protection against RV disease;

the full identification of the correlates of protection against RV disease; the factors determining RV spread; the reasons for decreased efficacy of RV vaccines in reserve-strapped settings and areas of low socioeconomic conditions; the further evolution of human RVs under the condition of universal mass vaccination against RV disease; the development of alternative (non-live attenuated) RV vaccine candidates; the development of RV antivirals (Desselberger, 2014).

The valuable information that could be gained from a reverse genetics system will undoubtedly shape the future for more effective and strain-specific vaccine development.

Chapter 3: The construction of a full set of SA11 rotavirus transcription plasmids and the synthesis of *in vitro*-transcribed (+)ssRNAs

3.1. Introduction

In a previous study conducted in our laboratory for the development of a plasmid-based reverse genetics system, all eleven SA11 consensus sequence rotavirus genome segments were cloned into one of four pUC57-based plasmids (pAlpha, pBeta, pGamma and pDelta) by GenScript (**Figure 3.1**). Each of the constructs, was designed with a T7 promoter region at the 5' end of the viral genome segment followed by a HDV-ribozyme and a T7 terminator region at the 3' end. However, in the process, a design flaw at the 5' end of the viral genome segments was made. Three additional guanine nucleotides were inserted between the T7 promoter region and the viral genome segment insert. In every instance, the sequences were substituted with the following sequence, 5-TAATACGACTCACTATAGGG-3', instead of 5-TAATACGACTCACTATA-3'. It was speculated that due to this error the mRNA derived from this design would not be packaged and no rescue of rotavirus will be possible (Wentzel, 2014).

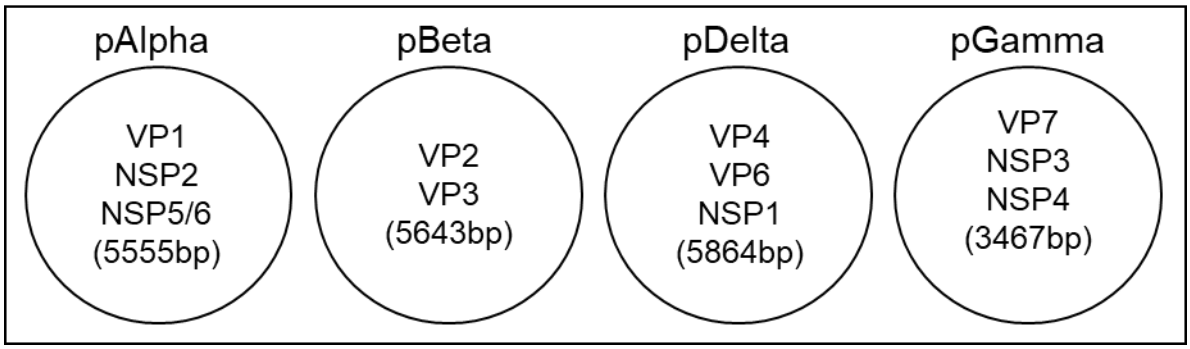

Figure 3.1: Four SA11 rotavirus multiple genome segment plasmids from Dr.J.F. Wentzel. pAlpha contains GS1 (VP1), GS8 (NSP2) and GS11 (NSP5/6). pBeta contains GS2 (VP2) and GS3 (VP3). pGamma contains GS4 (VP4), GS5 (VP6) and GS6 (NSP1). pDelta contains GS7 (VP7), GS9 (NSP3) and GS10 (NSP4).

For a reliable reverse genetics system to function the viral genome segments must have exact 5' and 3' ends. Thus, this flaw needed to be corrected. The experimental approach for this study was to individually clone all 11 genome segments into pSMART through In-Fusion® HD cloning. In-Fusion® HD cloning is a commercial state-of-the-art seamless cloning method that allows the cloning of one or multiple DNA fragments into any vector of choice at any position, provided there is a 15-base pair overlap on both ends of the vector and DNA fragment. These overlaps can be generated by PCR with specifically designed primers (**Figure 3.2**). The In-Fusion® HD cloning method is independent of any ligation due to the unique proofreading properties of poxvirus DNA polymerase's 3'-5' exonuclease activity (Zhu et al., 2007). When the linearised DNA from both the vector and insert with homologous ends are incubated with dNTPs, the poxvirus's DNA polymerase proofreading activity slowly removes nucleotides from the 3' end and by doing this exposes the complementary DNAs, allowing it to anneal by spontaneous base pairing.

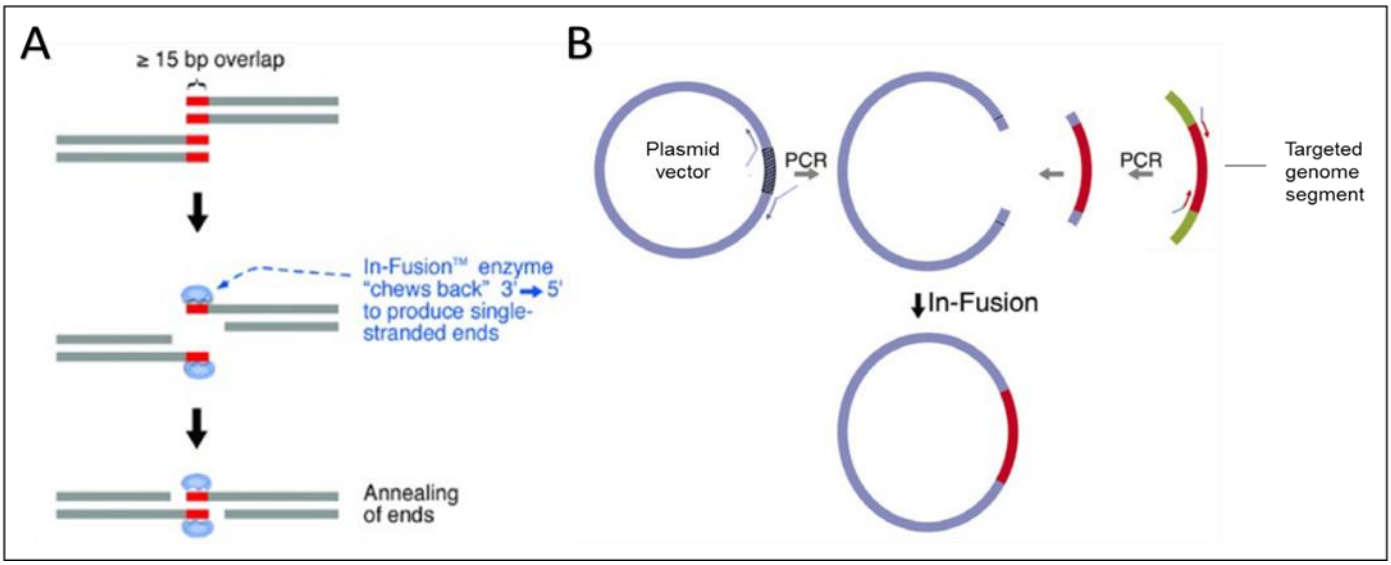

Figure 3.2: Schematic representation of In-Fusion cloning. (A) The In-Fusion enzyme removes nucleotides in a 3'-5' direction to expose complementary base pair DNA. B) DNA in In-Fusion cloning can be used to clone any fragment of DNA into any vector.

The aim of the work described in this chapter was to utilise In-Fusion HD cloning to correct the initial design flaw of three extra guanine nucleotides on the 5' ends of all eleven viral genome segments of rotavirus and subsequently clone these corrected genome segments into individually pSMART and finally to use these plasmids to generate authentic (+)ssRNAs through *in vitro* transcription to use in a transcript-based reverse genetics system.

3.2. Materials and Methods

3.2.1 Transformation of chemically competent bacterial cells

To generate bacterial grown multiple genome segment plasmids, the original sample DNA was diluted to a concentration of 0.2ng/µl and subsequently transformed into E. cloni® 5-alpha chemically competent cells. Before the start of the protocol, six 15ml Falcon tubes (one for each four of the plasmids and one for the positive control and one for the negative control) were pre-chilled on ice. The E. cloni® 5-alpha chemically competent cells were removed from the -80°C freezer and thawed on wet ice for 20 minutes. Once completely thawed, 50µl of the competent cells were added to each Falcon tube, followed by the addition of 0.2ng of the various plasmids. 10pg pUC19 DNA was added as a positive control while no DNA was added for negative control. The mixture was mixed by gently swirling the tube and then it was incubated on ice for 30 minutes. After this incubation, the cells were heat shocked for 30 seconds at 42°C in a pre-heated heat bath and then placed on ice for another 2 minutes. Next 950µl of room temperature super optimal broth with catabolite repression (**SOC**) or recovery medium, were then added to the cells and the Falcon tubes were placed in a shaking incubator for 1 hour at 37°C. Lastly, 100µl of the transformation mixtures were plated on fresh pre-heated agar plates containing 100µg/ml ampicillin and incubated at 37°C overnight.

The following day the colonies that were present on the plates were picked with a pipette tip and incubated in a Falcon tube with 15ml Luria broth (LB) media in a shaking incubator for 14 hours at 37°C. The plasmids were then extracted with QIAGEN's QIAprep® Spin Miniprep Kit, see **Section 3.2.2**. for details.

The principle of heat shock transformation is that the cells are made competent by treating it with calcium (Ca^{2+}). The positive charge of Ca^{2+} neutralises the charges of the cells and plasmids, thus eliminating electrostatic repulsion. When plasmids and the cells (which are incubated on ice) are exposed to a dramatic increase in temperature, a pressure difference is created between the inside and the outside of the cells. This causes the formation of pores in the cell membranes, thus allowing the plasmids to enter the cells. When the temperature is lowered, the cells' membranes will reform (Sambrook and Russell, 2001).

To generate bacterial clones for the pSMART plasmid, it had to be transformed into SURE competent cells. These cells are specifically for DNA segments that are not cloneable in conventional competent cells. The pSMART high copy plasmid that was kindly provided by Professor Christiaan Potgieter from Deltamune had a virulent segment 2 of African horse sickness virus already cloned in it. Due to this genome segment, the plasmid was not stable in other competent cells. The standard heat shock method as described above was followed, with one additional step. After the plasmids and competent cells were added together, 1.7µl of β-mercaptoethanol was added which helps to increase the transformation efficiency. The cells containing the pSMART were then plated onto agar plates containing ampicillin, kanamycin and tetracycline as the SURE cells have resistance to kanamycin and tetracycline and the pSMART has resistance to ampicillin.

Zymo 5α cells were used to transform the In-Fusion reaction that is described in **Section 3.2.8**. The Zymo 5α cells were used because of their high transformation efficiency, and it eliminates the need to heat shock cells and recovery procedures, thus saving a considerable amount of time. In this transformation procedure, the Zyme 5α cells were thawed on ice and 50µl transferred to a 15ml sterile Falcon tube. Next, 2.5µl of the In-Fusion reaction was added to cells, and the mixture was incubated on ice for 2 minutes and then immediately after the entire reaction was spread on pre-heated 37°C agar plate containing 100µg/ml ampicillin and incubated overnight at 37ºC. The next day all the colonies were picked and grown further in 15ml LB media with 100µg/ml ampicillin for 14 hours. The plasmid DNA was extracted and purified with the sample method as described in **Section 3.2.2**. and the concentrations were determined by using a Nanodrop spectrophotometer.

For genome segments that were too unstable in Zymo5α cells, Epicentre's CopyCutter™ cells were used. This transformation protocol is the same as the E. cloni® 5-alpha cells' described above.

3.2.2 Plasmid extraction from bacteria

To extract plasmid DNA from bacteria, the QIAGEN QIAprep spin miniprep kit was used. This scientific principle the kit is based on is the alkaline lysis method of plasmid extraction first described by Birnboim and Doly in 1979. Before the first use of the kit LyseBlue reagent was added to Buffer P1 along with RNase A solution, and then it was stored at 4°C. LyseBlue is a colour indicator which provides a colour change when optimum buffer mixing is achieved. Furthermore, 220µl of 100% ethanol was added to Buffer PE, and the protocol was followed.

Overnight bacterial cultures (5ml) were pelleted at room temperature by centrifugation at 8000 rpm (6800 x g) for 3 minutes. The supernatant was discarded, and the pellet was dried for 10 minutes by leaving the tubes upside down on paper towels. The pellet was then resuspended in P1 buffer containing EDTA, Tris, RNase A and glucose. The EDTA chelates cations such as magnesium (Mg^{2+}) and calcium (Ca^{2+}), preventing damage to plasmids from DNases and helps to destabilise the cell wall. The RNase A helps to degrade any RNA when the cells are lysed while the glucose's function is to maintain osmotic pressure. The pellet was vortexed to ensure that the whole pellet dissolved and that there were no clumps left in the solution. The resuspension was transferred into a 1.5ml sterile microcentrifuge tube, and 250µl of buffer P2 was added. This lysis buffer (P2) contains sodium hydroxide (NaOH) and sodium dodecyl sulfate (SDS). The SDS will solubilise the cell membrane while the NaOH breaks the cell wall and denatures the plasmid and genomic DNA thus converting dsDNA into ssDNA. It also denatures the proteins in cells. The solution was mixed thoroughly, and due to the LyseBlue reagent, the solution will turn blue. The change in colour indicates that the pH of the solution is optimal for the DNA to denature. If the solution does not turn blue more NaOH can be added until the solution turns blue. This lysis reaction should not exceed 5 minutes. Next 350µl, of Buffer N3 was added and thoroughly mixed by inverting solution six times, and the solution turned colourless. The neutralisation buffer (N3) contains potassium acetate which decreases the alkalinity of the solution. This is the critical selection part of the method because the decrease in alkalinity

causes the DNA to re-nature. Thus, the ssDNA returns to dsDNA form. For small circular DNA such as plasmid DNA, it is much easier to re-nature fully than genomic DNA which is much larger making it impossible to fully re-nature. The solution was then centrifuged at 13 000 rpm (17 900 x g) for 10 minutes, and a white pellet will form in the bottom of the tube. The supernatant was carefully transferred into a QIAprep 2.0 spin column by pipetting. These spin columns have unique silica membranes that have selective adsorption for cDNA in the presence of a high salt buffer and elutes cDNA in the presence of a low-salt buffer. This ensures that all other proteins, RNA and cell debris are not retained with the cDNA in the silica membrane but flows through. The solution was centrifuged at 13 000 rpm for 60 seconds, and the flow-through was discarded. The column was then washed twice, first by adding 500µl of Buffer PB and centrifuged at 13 000rpm for 60 seconds and after discarding the flow-through by adding 750µl of Buffer PE followed by a second centrifuge step at 13 000 rpm for 60 seconds. After discarding the flow-through from the previous step, the column was centrifuged for 60 seconds to get rid of the excess wash buffer still present. The column was then transferred into a clean 1.5ml microcentrifuge tube, and cDNA was eluted by adding 30µl of nuclease-free water to the column and letting it stand for 60 seconds, followed by centrifugation at 13 000 rpm for 1 minute. The cDNA of all four multiple genome plasmids and pSMART were then analysed by restriction enzyme digestion (see **Section 3.2.3.**).

3.2.3. Restriction enzyme digestion

The restriction enzyme analyses were done to determine the extracted plasmid DNAs' length and identity. All the plasmids were linearised with a single cut enzyme as well as cut with a multiple cutter enzyme. For the digestion of plasmid DNA, the reactions were set up as follows: approximately 300ng of plasmid DNA was added together with 3µl of the appropriate 10x reaction buffer as was recommended by the manufacturer and 1 unit of the appropriate enzyme (kept on ice) in a sterile PCR tube. The sample mixture was brought up to a final volume of 30µl with nuclease-free water. The samples were incubated at 37°C for a minimum of 4 hours. Samples used for *in vitro* transcription, which needed to be linearised, were incubated overnight in a PCR thermocycler. The plasmid DNA samples were then loaded on an agarose gel for gel electrophoresis analyses, see **Section 3.2.4**.

3.2.4 Agarose gel electrophoresis

To visualise plasmid DNA and to determine the length of the plasmid DNA, gel electrophoresis was utilised. The agarose gels used in the experiments were made by adding the appropriate amount (w/v) of agar powder to 100ml of 1X working solution Tris-acetate and EDTA (TAE) buffer. For the purpose of this study, 1% agarose gels were used as it is the optimal concentration to study DNA fragments varying in size from 250bps to 12000bp (Sambrook and Russell, 2001). The solution was boiled in a microwave until all the powder dissolved, and after the solution cooled to approximately 60°C, ethidium bromide was added. The ethidium bromide is an intercalating agent and helps to detect nucleic acids including double stranded DNA or single single-stranded RNA, and has a final concentration of 0.5µg/ml per gel. The solution was then poured into the casting tray with a comb with 12 wells, yielding the standard gel size of 8cm x 12cm x 0.7cm. The gels were cooled for about an hour to let the gel set properly.

The gel was put into the tank containing enough 1x TAE buffer to completely cover the gel. Approximately 500ng of plasmid DNA was loaded with a drop (~1µl) of loading dye. A 1kb Generuler DNA ladder from Thermo Fisher Scientific was used as a marker. The samples were electrophoresed at 90 volts for 1 hour, after which the gels were visualised under fluorescent light in a ChemiDoc™ MP Imaging System from Bio-Rad laboratories.

3.2.5. Polymerase chain reaction

3.2.5.1. Primer design

The primers for the PCR reactions were carefully designed using CLC genomic workbench software to include the complementary 15 base-pair overlap on both inserts and vector, required for In-Fusion cloning (see **Section 3.2.8.**). The primers were ordered from TIB MOLBIOL. Upon arrival, the primer salts were briefly centrifuged at 10 000rpm to minimise loss of content. All primers were then resuspended as a 100mM stock solution in nuclease free water, and working stocks of 10mM were made. The stock solutions were stored at -20°C while working solutions were kept at 4°C.

3.2.5.2 Temperature gradient PCR

A temperature gradient PCR is where multiple PCR reactions are run simultaneously at the same experimental parameters, except for their annealing temperature. Each reaction was set up with a different annealing temperature to ascertain at what temperature optimal annealing of primers and DNA take place. Three temperature gradient PCRs were performed for each genome segment and pSMART. The first annealing temperature selected was 6°C less than the average melting temperatures of each forward and reverse primer set. The second and third annealing temperature was 4°C higher and lower than the first annealing temperature, respectively.

The PCRs were set up as follows: 5x High-Fidelity (HF) buffer was added to have a final concentration of 1x for the reaction volume, followed by the addition of 200uM deoxynucleotides (dNTPs), 0.5uM of both forward and reverse primers, 50-100ng of plasmid DNA and 1 unit of the Phusion DNA polymerase per 50µl PCR reaction. The reactions were brought to a final volume of 50µl with nuclease-free water. The thermocycling conditions were set up as follows: initial denaturation was set at 98°C for 30 seconds, followed by 25 cycles of an extended denaturing phase of 98°C for 10 seconds, an annealing phase with temperatures varying from between 45-60°C for 30 seconds, an extension phase at 72°C for 30 seconds per kilo base pair (thus every genome segment's conditions would differ). The repeated cycles were followed by a final extension phase of 10 minutes at 72°C, and lastly, the reaction was held at 4°C until samples were analysed by agarose gel electrophoresis (**Section 3.2.4**.). After optimal annealing temperatures were determined with temperature gradient PCRs, all the samples underwent another PCR reaction but set at their own optimal annealing temperatures.

3.2.6. Gel extraction purification of PCR amplicons

To purify a new PCR amplicon, Qiagen's MinElute PCR and gel extraction kit was used. This kit is ideal to purify PCR products ranging from 70bp to 4kbp, from polymerase, nucleotides and primers. When a new MinElute kit was used for the first time, 24ml of 100% ethanol was added to Buffer PE.

When non-specific background was observed on the gel, the desired fragment visible on the gel was first excised from the gel and then purified. The amount of gel that did

not contain any DNA was kept as small as possible. The protocol was performed as follows: first, the weight of the gel was determined by weighing a clean microcentrifuge tube before and after the excised gel fragment is added to the tube. This is done to determine the appropriate amount of QG buffer to be added. After the weight of the gel was determined three volumes of QG buffer to one volume of the gel was added to the tube where a 100mg gel equals 100µl of buffer. The QG buffer contains a pH indicator that will turn orange/violet if the pH is too high. For the DNA to bind to the Qiagen spin columns an optimal pH of 7.5 is recommended by the manufacturer. Thus, if the solution is orange/violet of colour, the pH can be adjusted until the solution turns yellow which indicates the optimal pH for adsorption of DNA. Next, the tube was incubated at 50°C for 10 minutes and vortexed every 2 minutes to help the gel dissolve completely. Next one volume of pre-heated isopropanol was added and mixed by inverting the tube five times, and the solution was transferred into a MinElute column that was placed in a 2ml collection tube. All the centrifugation steps were performed at 13 000rpm for 1 minute. The solution was centrifuged so that the DNA could bind to the silica membrane and the flow-through was discarded. Next two wash steps were performed. The first one was performed with 500µl of QG buffer then the second with 750µl of PE buffer, and after centrifugation of each wash step, the flow-through was discarded. After the second wash step, the small droplets of PE buffer present on the top of the silica membrane was removed by pipetting. Next, the spin column was centrifuged for 1 minute to dry the silica membrane from any residual wash buffer. The spin column was placed in a clean, sterile tube, and the DNA was eluted by adding 10-25µl of nuclease-free water exactly in the middle of the spin column and letting it stand at room temperature for 1 minute followed by a centrifugation step. The concentrations of all the amplicons were measured and recorded on a NanoDrop™ One Microvolume UV-Vis Spectrophotometers from Thermo-Scientific.

3.2.7. PCR clean-up

To purify PCR products where a single clear band was visible on gels, the protocol was done as follows. First the PCR reaction volume was brought up to 100µl with nuclease-free water, and three volumes of QG buffer relative to the final volume of the PCR reactions was added to the PCR product and mixed thoroughly by inverting tube 5-7 times. The rest of the protocol is the same as the gel extraction purification as described in **Section 3.2.6**.

3.2.8. In-Fusion cloning

After the eleven viral genome segments and pSMART backbone were amplified by PCR with specific primers to insert a 15 base-pair complementary region at their respective ends, they were fused together to create eleven rotavirus transcription plasmids. Standard In-Fusion reactions were set up in sterile PCR tubes by adding 200ng of the linearised pSMART DNA with 200ng of the purified individual genome segment DNA, together with 2µl of the 5x In-Fusion HD enzyme premix. The reactions were brought to a final volume of 10µl with deionised water and the reaction was mixed by pipetting up and down a couple of times. Next, the reaction was incubated at 50°C for 15 minutes in a thermocycler and placed on ice, or alternatively, the reaction can be stored at -20°C. A positive control reaction was done in parallel with my own reactions. The control reaction was set up by adding 2µl of the 2kbp control insert, and 1µl of a linearised pUC19 vector to a PCR tube, together with 2µl 5x In-Fusion HD enzyme premix. Lastly, the reaction was brought to a final volume of 10µl, mixed and incubated at 50°C for 15 minutes.

3.2.9. Sanger and Next Generation Sequencing

To determine if the initial design flaw of three extra guanine nucleotides were successfully removed and that the respective 5' and 3' ends correctly annealed with the In-Fusion cloning, all eleven samples were sent for Sanger sequencing at the Central Analytical Facility in Stellenbosch (CAF). Specific primers were designed to anneal 150bp upstream of the T7 promoter region at the 5' end and downstream of the SapI restriction enzyme site at the 3' end, respectively. The primers were sent with the samples and were analysed at CAF.

After the 5' and 3' ends were verified with Sanger sequencing, all the plasmids were sent for Next Generation Sequencing (NGS) to ascertain if any mutations occurred in any of the eleven genome segments. Illumina NGS was performed by Dr Arshad Ismail at the National Institute for Communal Diseases (NICD), and a round of Ion Torrent S5 NGS was done at the North-West University.

The NGS sequencing was done twice to see if the results could be reproduced at the NWU. Only the Ion Torrent S5 NGS data is shown because it had better forward and reverse coverage in all the rotavirus genome segments than that of Illumina NGS.

3.2.10. *In vitro* transcription of rotavirus (+)ssRNAs

After the successful cloning of individual rotavirus genome segments into pSMART, these plasmids were used to create (+)ssRNAs, to be used in the transfection of mammalian cells. These (+)ssRNAs were synthesised through *in vitro* transcription with an Ambion MEGAscript® Kit.

3.2.10.1. Linearization of SA11 rotavirus transcription plasmids

Before the *in vitro* transcription was performed the plasmids first had to be linearised with SapI. The reactions for all 11 plasmids were set up as follows: 2µl of enzyme buffer was added, followed by the addition of 3µg of plasmid DNA and 3 units of SapI (kept on ice). The reaction volumes were adjusted to a final volume of 30µl with PCR-grade water. The reactions were incubated at 37°C overnight to ensure complete digestion of plasmid DNA. The following day the DNA was analysed on an agarose gel to determine if complete digestion was achieved, as described in **Section 3.2.4**. The samples were also purified as described in **Section 3.2.6.**

3.2.10.2. Synthesis of rotavirus (+)ssRNAs

Once the plasmids were linearised the *in vitro* transcription was performed. All the reagents, the 10x reaction buffer and four ribonucleotides, were vortexed until they were completely thawed and the ribonucleotides were placed on ice. The 10x reaction buffer contains spermidine that could co-precipitate the DNA if it was put on ice or if the reaction was assembled on ice, thus care was taken when the reaction was assembled. Before the reagents were opened after thawing, they were briefly centrifuged to minimise the loss of any reagent.

Next, the reaction was assembled at room temperature by adding 2µl of all four the ribonucleotides (ATP; GTP; CTP; UTP) into a sterile PCR tube, followed by the addition of 2µl of the 10x reaction buffer, 8µl of the linearised DNA and 2µl of the enzyme mix. The reaction was mixed thoroughly by pipetting and incubated at 37°C for 2 hours. After the incubation period was over 1µl of the reaction mix was loaded on a 1% agarose gel and analysed as described in **Section 3.2.4.** to determine if synthesis of (+)ssRNAs were achieved.

3.2.10.3 Purification of *in vitro* transcribed (+)ssRNAs

After the successful generation of the (+)ssRNAs, they have to be purified before it can be used in the transfection of mammalian cell cultures. The purification of ssRNAs was performed with an Ambion® MEGAclear™ kit. Before purification, 1µl of TURBO DNase enzyme was added to the *in vitro* transcription reaction and incubated at 37ºC for 15 minutes to digest any remaining DNA template. Before the first use of the MEGAclear™ kit, 20ml of 100% ethanol was added to the wash solution. The standard protocol was followed by first bringing the samples' volume to 100µl with the provided elution solution, followed by the addition of 350µl binding solution concentrate and 250µl of 100% ethanol. After each addition, the reaction mix was thoroughly mixed by pipetting. Next, a filter cartridge was added to a collection tube, and the reaction mix was transferred into the filter cartridge, followed by centrifugation to bind the RNAs to the membrane and the flow through was discarded. Two wash steps followed by adding 500µl of wash solution to the filter cartridge and centrifuging it, and discarding the flow through. The membrane was dried by removing any buffer droplets on the membrane surface with a pipet followed by a centrifugation step. The RNA was eluted by the following method: first PCR-grade water was boiled in a microwave and once boiled 100µl of it was added to the filter cartridge that was placed in a clean collection tube. Next, the filter cartridge in the collection tube was placed in a heat block set at 60°C for 1 minute, followed by centrifugation of the filter cartridge. Lastly, the samples were analysed on an agarose gel as described in **Section 3.2.4.** and the concentration determined on a Nanodrop spectrophotometer. All centrifugation steps were performed at 13 000rpm for 1 minute.

3.3. Results and Discussion

3.3.1. Design of eleven rotavirus transcription plasmids

Exact terminal ends are necessary to ensure packaging of the rotavirus (+)ssRNAs derived from plasmid constructs, as is shown in **Figure 3.3**. To remove the additional guanine residues from the sequences of all eleven genome segments and clone them into pSMART-AHSV-VP2 HC, the genome segments were redesigned to be flanked with a T7 promoter region at their 5' end and a non-palindromic restriction enzyme site SapI at the 3' end. The T7 promoter will ensure an exact 5' end, while digestion with the SapI restriction enzyme site will do the same at the 3' end.

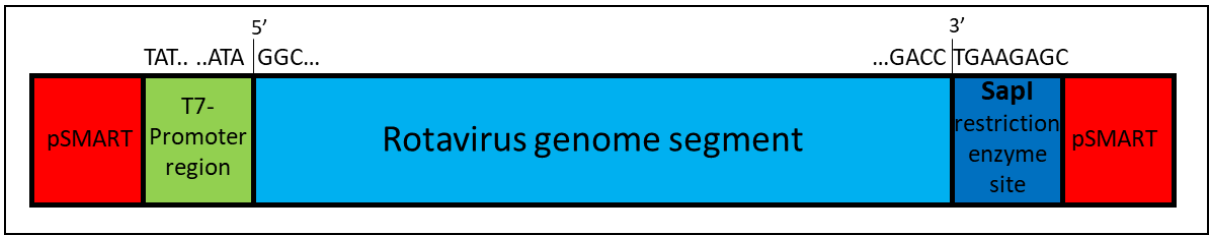

Figure 3.3: General overview of insert design cloned into plasmids. All of the plasmid inserts had a T7 promoter region upstream and a SapI restriction enzyme site downstream to ensure exact terminal ends.

3.3.2. Bacterial propagation of four multiple SA11 genome segment plasmids and pSMART

To individually clone all eleven rotavirus genome segments into pSMART, I transformed an aliquot of each of the original four multiple genome segment plasmids created by GenScript for previous studies in our laboratory. The four plasmids were transformed into E.coli 5α chemical competent cells and pSMART into SURE competent cells, as described in **Section 3.2.1.** The number of colonies on agar plates varied between 90-130 colonies per plate and 10 colonies of each plate was screened.

Plasmid DNA was extracted from the colonies and was analysed with restriction enzyme digestion as described in **Section 3.2.2. and 3.2.3,** respectively.

Each plasmid was digested with two different enzymes, one to linearise the plasmid so its length could be determined and the other one a multiple digestion to determine the identity of the plasmid. **Table 3.1** depicts the expected base pair lengths of each of the fragments after digestion.

Table 3.1: The expected lengths of fragments after restriction enzyme analyses

	Linearization enzyme	Double/triple digestion ensyme	Linearization length (bp)	Double digestion lengths (bp)	Triple digestion lengths (bp)
pAlpha	NcoI	XbaI	7580	4859	N/A
				2721	
pBeta	SalI	EcoRI	7671	N/A	4777
					2013
					881
pGamma	NcoI	HindIII	7950	4410	N/A
				3540	
pDelta	NcoI	EcoRI	5492	3479	N/A
				2013	
pSMART	ApaI	EcoRI	1975	1213	N/A
				762	

The restriction enzyme analyses of pAlpha (lanes 1-3) together with pBeta (lanes 5-7) can be seen in **Figure 3.4A**. The undigested plasmids (lane 1, 5) has two distinct bands. The thicker band that travelled further through the gel is the supercoiled DNA which is tightly wound and thus travels further through the gel. The smaller band above is the nicked circular DNA. This nicked DNA travels more slowly through gels, because during replication one of the strands of the double helix was cut to allow access to the polymerase and thereby unwinding the DNA causing more resistance when travelling through gels. pAlpha was linearised with NcoI (lane 2), and one band of approximately 7600bp is visible which was the expected size. The double digestion was performed with XbaI (lane3), and the two band visible seems to correlate with the expected fragment sizes of 4800bp and 2700bp. The smear (lane 3) may have been caused by damage to the gel. pBeta was linearised with SalI (lane 6), and one band of approximately 7600bp is visible. The triple digestion was performed with EcoRI (lane7)

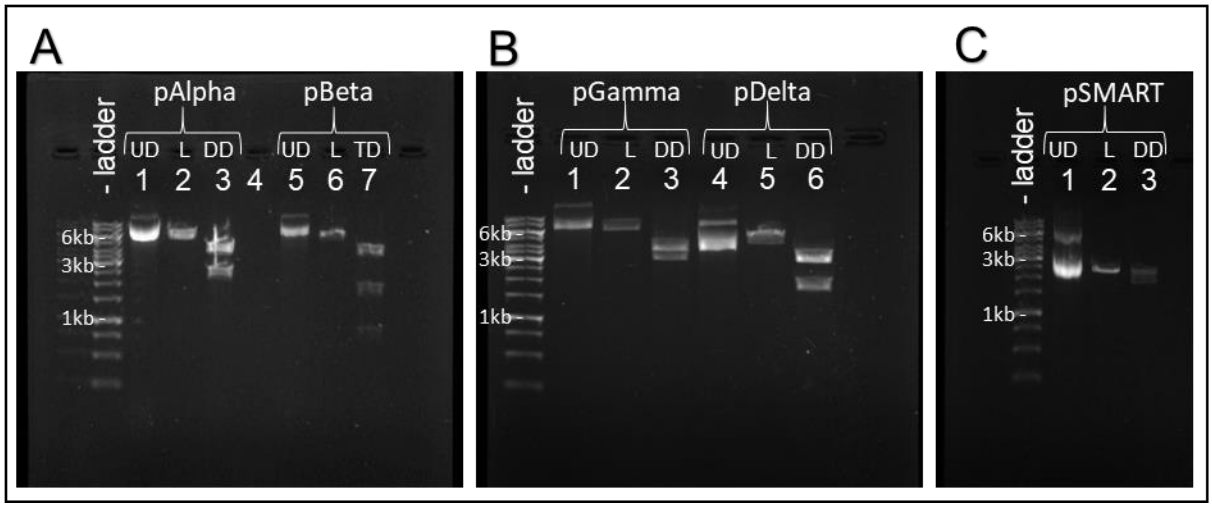

Figure 3.4: Agarose gel electrophoresis of restriction enzyme analysis of the four multiple genome segment plasmids and pSMART. (A) The restriction enzyme digestion of pAlpha (lanes 1-3) and pBeta (lanes 5-7). The undigested plasmids (lane 1, 5) depicts two respective bands, the supercoiled and nicked circular bands. pAlpha was linearised with NcoI (lane 2) and cut twice with XbaI (lane 3). pBeta was linearised with SalI (lane 6) and cut twice with EcoRI (lane 7). (B) The restriction enzyme digestion of pGamma (lanes 1-3) and pDelta (lanes 4-6). The undigested plasmids (lane 1, 4) depicts two respective bands, the supercoiled and nicked circular bands. pGamma was linearised with NcoI (lane 2) and cut twice with HindIII (lane 3). pDelta was linearised with NcoI (lane 5) and cut twice with EcoRI (lane 7). (C) The restriction digest of pSMART (lanes 1-3). The undigested plasmids (lane 1) can be seen. pSMART was linearised with ApaI (lane 2) and cut twice with EcoRI (lane 3).

and yielded three bands of approximately 4700bp, 2000bp and 900bp. All the bands were of expected size. Resolution for the larger fragments could have been better if the electrophoresis' time were extended to create more separation of larger fragments.

The restriction enzyme analyses of pGamma (lane 1-3) and pDelta (lane 4-6) can be seen in **Figure3.4B**. The respective undigested plasmids (lane 1, 4) yielded two bands. One the supercoiled DNA and the other the nicked circular DNA. pGamma was linearised with NcoI (lane 2) and yielded one band of approximately 7900bp. The double digestion performed with HindIII (lane 3) yielded two bands. The separation of these fragments was very slight, but the seemed to be the expected lengths of 4400bp and 3500bp, respectively. pDelta was linearised with NcoI (lane 5) and yielded one band of approximately 5500bp. The double digestion was conducted with EcoRI (lane 6) and two bands of approximately 3500bp and 2000bp was yielded. All of the bands were of expected size.

The restriction enzyme analyses of pSMART (lane 1-3) can be seen in **Figure 3.4C**. The undigested plasmid (lane 1) yielded two bands. pSMART was linearised with ApaI (lane 2) and yielded one band of approximately 2400bp. Although the plasmid was

linearized, the DNA fragment was larger than the expected result. The double digestion was conducted with EcoRI (lane 3). It yielded a smeared band and it was difficult to determine what the size was. The length discrepancy of the expected and the actual results were attributed to a mix-up of plasmids samples. It was decided to insert the SapI restriction enzyme site into another pSMART plasmid with PCR and continue in that way to save time. Thus, considering the expected and the actual results of the restriction enzyme analyses, the conclusion was made that the DNA extracted from transformed cells was that of pAlpha, pBeta, pGamma and pDelta

3.3.3. PCR of eleven rotavirus genome segments and pSMART

To perform the In-Fusion HD cloning, all eleven rotavirus genome segments and pSMART vector had to undergo PCR to linearise each of them and to add the 15 complementary base pair overlap on each end. The standard protocol for the PCR reactions was followed as described in **Section 3.2.5**. The optimal annealing temperatures of each genome segment were determined by a temperature gradient PCR, and the results of that can be seen in **Figures 3.5 – 3.6**

When determining the optimal annealing temperature, a couple of factors were taken into consideration with the temperature gradient PCR results. First, the amplified band must be clear and of sufficient concentration, second no non-specific background must be present in the agarose gel, and the amplicon must be the correct size.

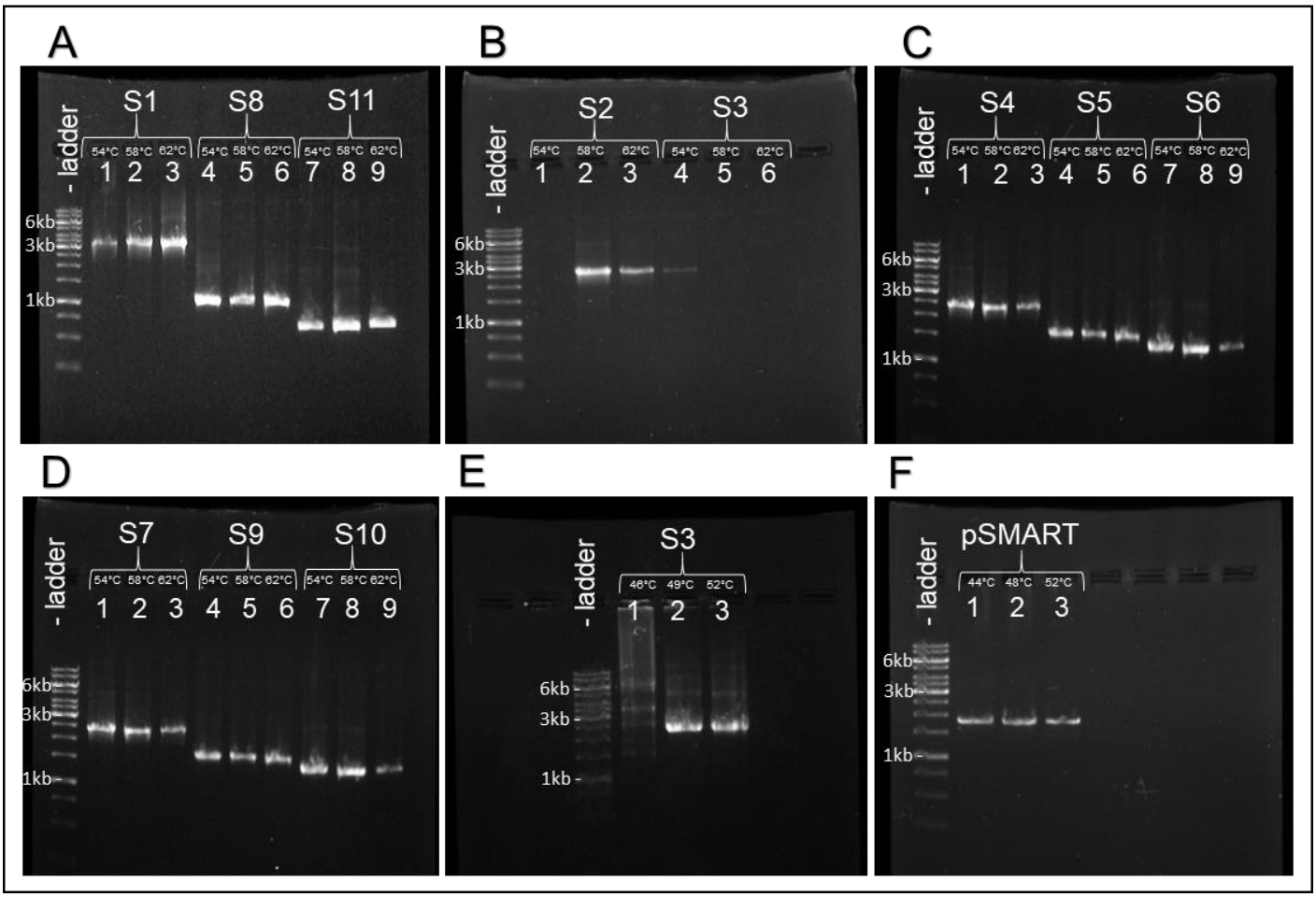

Figure 3.5: Temperature gradient PCR of eleven rotavirus genome segments. (A) The temperature gradient of genome segment 1 (lanes 1-3), genome segment 8 (lanes 4-6) and genome segment 11 (lanes 7-9). The temperatures gradients of all the rotavirus genome segments were conducted at 54°C, 58°C and 62°C. (B) The temperature gradient of genome segments 2 (lanes 1-3) and genome segment 3 (lanes 4-6). (C) The temperature gradient of genome segments 4 (lanes 1-3), genome segment 5 (lanes 4-6) and genome segment 6 (lanes 7-9). (D) The temperature gradient of genome segments 7 (lanes 1-3), genome segment 9 (lanes 4-6) and genome segment 10 (lanes 7-9). (E) The second temperature gradient of genome segment 3 (lanes 1-3). The second temperature gradient of genome segment 3 was conducted at 46°C, 49°C and 52°. (F) The temperature gradient of pSMART (lanes 1-3). The temperature gradients were conducted at 44°C, 48°C and 52°C.

Good amplification of amplicons of the desired length was generated at all three temperatures, see **Figure 3.5A**. For genome segment 1 (lanes 1-3) slight non-specific amplification was observed at 62°C (lane 3). There was no non-specific amplification for the amplicon at 58°C (lane 2). Thus, 58°C was used as annealing temperature for genome segment 1. For the genome segment 8 temperature gradient **Figure 3.5A** (lanes 4-6), good amplification of the desired length was obtained, but there was slight non-specific amplification (lane 4). At 58°C, there was sufficient amplification and no non-specific background (lane 5). Thus, 58°C was chosen as the annealing temperature. The temperature gradient of genome segment 11 all showed good

amplification of desired length **Figure 3.5A** (lanes 7-9). However, non-specific background was visible at 54°C and 58°C. Thus, 62°C was used as the annealing temperature for genome segment 11 (lane 9).

The temperature gradient of genome segment 2 **Figure 3.5B** (lanes 1-3) showed mixed results. No amplification was visible at 54°C (lane 1), although the most probable explanation is that a pipetting error was made and no sample was loaded. Good amplification was observed at 58°C and 62°C (lanes 2-3), however, non-specific amplification was visible at 58°C. Thus, 62°C was used as the annealing temperature for genome segment 2. The first temperature gradient for genome segment 3 **Figure 3.5B** (lanes 4-6) showed very little amplification at 54°C (lane 4) and no amplification at 58°C and 62°C (lanes 4-6). This suggested that the optimal annealing temperature was at a temperature lower than 54°C and thus a second temperature gradient PCR was conducted for genome segment 3.

The second temperature gradient conducted for genome segment 3 **Figure 3.5E** (lanes 1-3) showed significant non-specific amplification took place at 46°C and no amplicon of the desired length was produced (lane 1). The amplicons produced at 49°C and 52°C was sufficient, and of the desired length (lanes 2-3). However, significant non-specific amplification also took place in at these temperatures and was attributed to the low annealing temperatures. The difficulty of finding an optimal annealing temperature for genome segment 3 could be attributed to poor primer design. The forward and reverse primer set I had inherited for genome segment 3 had a 14°C difference in melting temperatures as indicated by the manufacturers' primer data sheet. The correct length DNA fragment was purified as described in **Section 3.2.6**.

The temperature gradient for genome segment 4 **Figure 3.5C** (lanes 1-3) yielded good amplification of the desired length. Slight non-specific background was visible at 54°C and 58°C (lanes 1-2). Thus, 62°C was used as annealing temperature for genome segment 4 as no non-specific amplification was present (lane 3). Good amplification of amplicons with no non-specific background was observed at all three temperatures for genome segment 5 **Figure 3.5C** (lanes 4-6). Thus, 58°C was used as annealing temperature for genome segment 5. The temperature gradient for genome segment 6 showed good amplification of the desired length at all three temperatures **Figure 3.5C**

(lanes 7-9). However, non-specific amplification was observed at 54°C and 58° (lanes 7-8). Thus, 62°C was used as the annealing temperature for genome segment 6 (lane 9).

The temperature gradient for genome segment 7 yielded good amplification of the desired length **Figure 3.5D** (lanes 1-3). However, non-specific amplification was visible at 54°C and 58°C (lanes 1-2). Thus, 62°C was used as annealing temperature for genome segment 7. The temperature gradient of genome segment 9 all showed good amplification of the desired length with no non-specific background **Figure 3.5D** (lanes 4-6). Thus, 58°C was used as annealing temperature for genome segment 9. The temperature gradient of genome segment 10 showed good amplification of the desired length **Figure 3.5D** (lanes 7-9). Non-specific amplification was observed at 54°C and 58°C (lanes 7-8). Thus, 62°C was used as annealing temperature for genome segment 10 as no non-specific amplification was visible (lane 9).

The temperature gradient of pSMART showed good amplification of the desired length with no non-specific background at all three temperatures **Figure 3.5F** (lanes 1-3). Thus, 52°C was used as annealing temperature for pSMART because it was the highest temperature of the temperature gradient.

After the optimal annealing temperatures were determined, a second round of PCRs were conducted with those annealing temperatures **Figure 3.6**. The amplicons were inspected with agarose gel electrophoresis and afterwards purified as described in **Section 3.2.7**. and the concentration of each was determined on a Nanodrop spectrophotometer **Table 3.2**.

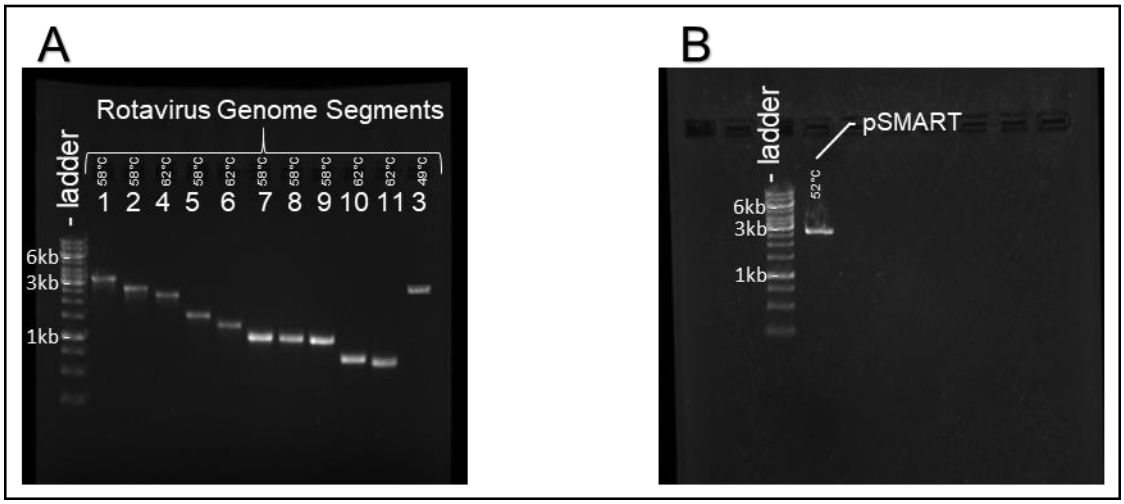

Figure 3.6: Purified PCR amplicons of all rotavirus genome segments and pSMART. (A) Amplicons of eleven genome segments of rotavirus generated with the temperatures as indicated above. (B) pSMART amplicon generated at 52°C.

Table 3.2: Concentrations and absorbance of amplicons of purified rotavirus genome segments and pSMART.

Sample DNA	GS1	GS2	GS3	GS4	GS5	GS6	GS7	GS8	GS9	GS10	GS11	pSMART
Concentration ng/µl	115.5	124.6	73.1	109.2	111.7	121.2	213.0	200.2	230.3	211.4	140.7	209.3
Absorbance 260/280 nm	1.86	1.88	1.88	1.84	1.89	1.9	1.86	1.87	1.87	1.88	1.83	1.87

The amplicons of all the genome segments all show one clear band with no non-specific background **Figure 3.6B**. The purified pSMART is shown in **Figure 3.6B,** and no non-specific background is visible. The concentrations of these amplicons are depicted in **Table 3.3**. The absorbance indicates the level of purity of the DNA. For dsDNA, the ratio of the absorbance at 260/280 nm must be above 1.8. If the is below 1.8, it is indicative of contamination of proteins, and the sample should not be used.

3.3.4. In-Fusion HD cloning

To clone each of the 11 rotavirus genome segments individually into pSMART In-Fusion HD cloning was implemented. This method of cloning obviates the need for restriction enzyme digestion and can clone any insert DNA into any vector seamlessly provided there is 15 complementary base pair overlaps on both ends of the of inserts and vector. The In-Fusion protocol was followed as described in **Section 3.2.8**. According to the user manual of the In-Fusion cloning kit, the best cloning efficiency is achieved by adding 50-200ng of both insert and vector DNA. However, it was found that if less than 100ng of DNA was used, the In-Fusion cloning did not work. Therefore, an adjustment to the protocol was made to use 200ng of both the insert and vector DNA. The In-Fusion reaction mixture was transfected into Zymo 5α cells. Plasmid extractions were performed on all the colonies that were obtained which varied between only two colonies for genome segment 10 and a maximum of 15 colonies for genome segment 11. To determine if the inserts and vector annealed correctly, restriction enzyme analyses were performed.

The undigested plasmid DNA extracted from the bacterial colonies were loaded onto an agarose gel to compare their migration relative to each other and to select colonies to screen with restriction enzyme analyses. The restriction enzyme analyses entailed the linearization of the DNA with an enzyme that would cut in the pSMART region of the newly formed plasmid to determine the length, and a double digestion to determine the identity of the plasmid. In the cases that double cut enzymes were unavailable, a second linearization was conducted with an enzyme that would only cut in the insert region of the plasmids, thus confirming the presence of both the pSMART and the inserts DNA.

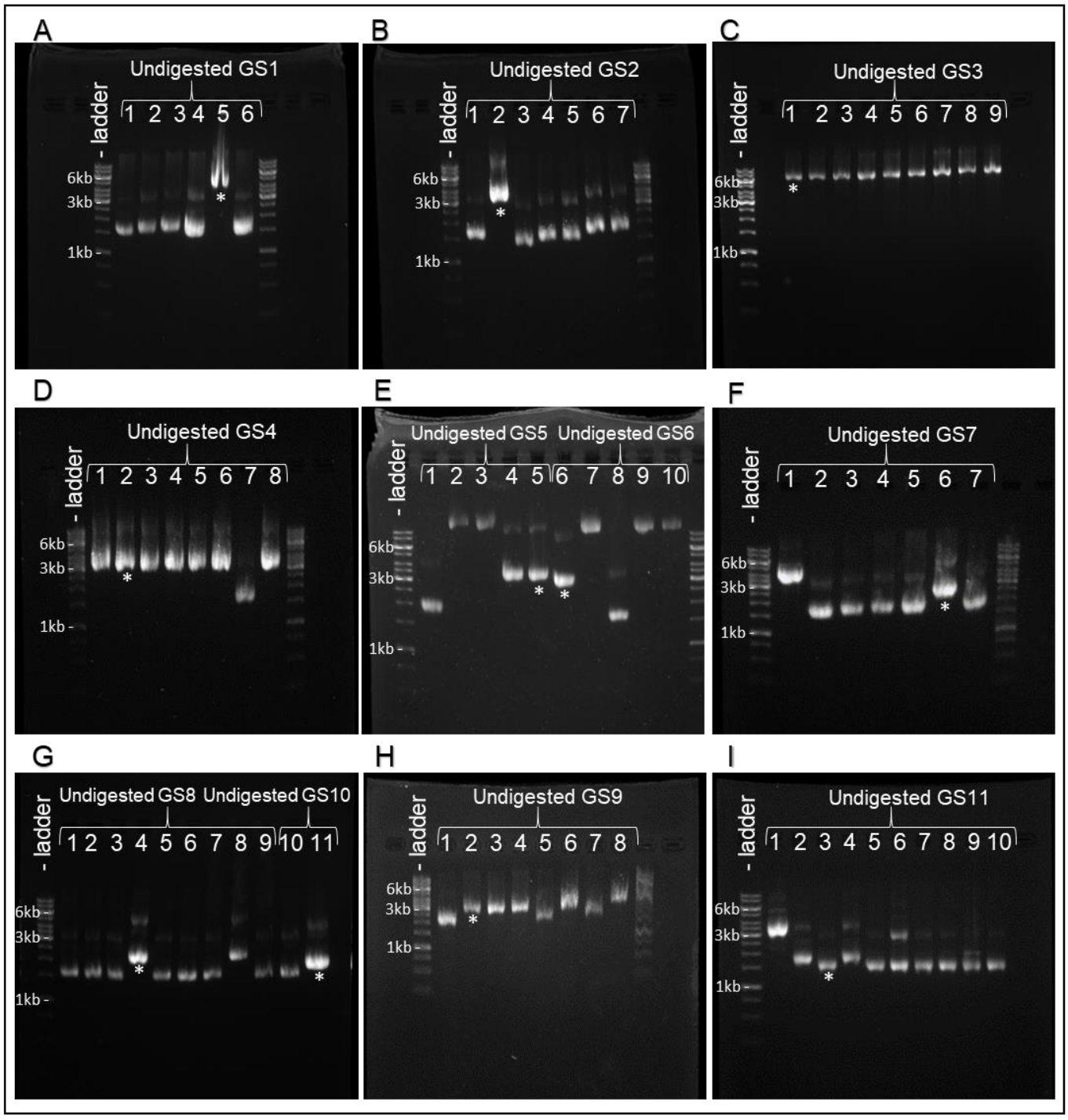

Figure 3.7: Screening of undigested SA11 transcription plasmids extracted from bacteria after transfection of the In-Fusion cloning reactions. The panels A-I depicts the undigested plasmid DNA extracted from different bacterial colonies of each of the genome segments as indicated in the panels. The lanes marked with a "*" was plasmid DNA selected for screening with restriction enzymes.

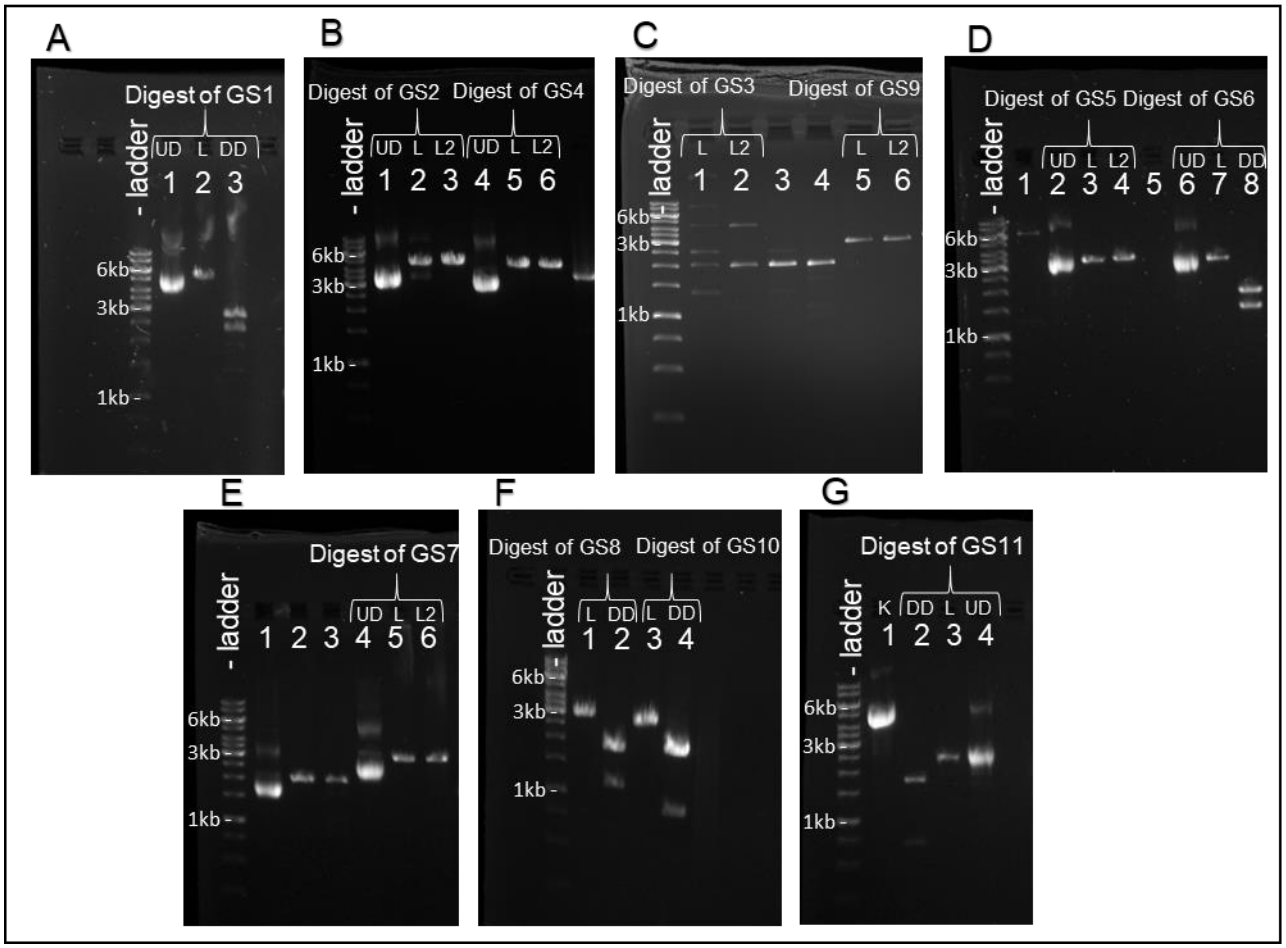

Figure 3.8: Restriction enzyme analyses of SA11 transcription plasmids from In-Fusion cloning of the 11 genome segments. (A) The undigested pSMART-GS1 DNA (lane 1) was linearsed with ApaI (lane 2) and double digested with BamHI (lane 3). (B) The undigested pSMART-GS2 and pSMART-GS4 DNA (lanes 1, 4). pSMART-GS2 was linearised with ApaI (lane 2) and NcoI (lane3). pSMART-GS4 was linearised with ApaI (lane 5) and XbaI (lane 6). (C) pSMART-GS3 was linearised with ApaI (lane 1) and BamHI (lane 2). pSMART-GS9 was linearised with ApaI (lane 5) and BamHI (lane 6). (D) The undigested pSMART-GS5 and pSMART-GS6 (lanes 2, 6). pSMART-GS5 was linearised with ApaI (lane 3) and HindIII (lane 4). pSMART-GS6 was linearised with ApaI (lane 7) and double digested with EcoRV (lane 8). (E) The undigested pSMART-GS7 (lane 4). pSMART-GS7 was linearised with ApaI (lane 5) and BamHI (lane 6). (F) Both pSMART-GS8 and pSMART-GS10 was linearised with ApaI (lanes 1, 3) and double digested with EcoRV (lane 2, 4). (G) The undigested pSMART-GS11 and positive control (lanes 1, 2). pSMART-GS11 was linearised with SacI (lane 3) and double digested with EcoRV (lane 4).

The undigested pSMART-GS1 is depicted in **Figure 3.7A** (lanes 1-6). The efficiency of the transformation was very low because there were only six colonies. The plasmid in lane 5 was selected for restriction enzyme analysis. I am not sure what caused the smear in the in lane 5. The restriction enzyme analysis of pSMART-GS1 is depicted in **Figure 3.8A**. The undigested pSMART-GS1 (lane 1) was linearised with ApaI and yielded one fragment of approximately 5000bp (lane 2). pSMART-GS1 was also double digested with BamHI which yielded two fragments of approximately 2700bp and 2400bp (lane 3). These results were as expected and thus the cloning of genome segment 1 was confirmed.

The undigested pSMART-GS2 and pSMART-GS4 are depicted in **Figure 3.7B** (lanes 1-7) and **Figure 3.7D** (lanes 1-8). The transformation of pSMART-GS2 and pSMART-GS4 yielded 7 and 8 colonies, respectively. The plasmid in lane 2 was selected for restriction enzyme analysis for pSMART-GS2, while the plasmid in lane 2 was selected for pSMART-GS4. The restriction enzyme analysis of pSMART-GS2 and pSMART-GS4 are depicted in **Figure 3.8B**. In both instances, there were no double digest enzymes available, so both genome segments were linearised twice. Once with an enzyme that would cut in the pSMART region and once with an enzyme that would cut in the insert region to confirm the presence of both. The undigested pSMART-GS2 (lane 1) was linearised with ApaI (lane 2), and NcoI (lane 3) and both yielded a single fragment of approximately 4500bp. The undigested pSMART-GS3 (lane 4) was linearised with ApaI (lane 5), and XbaI (lane 6) and both yielded a single fragment of approximately 4000bp. These results were as expected and thus the cloning of genome segment 2 and genome segment 4 were confirmed.

The undigested pSMART-GS5 and pSMART-GS6 are depicted in **Figure 3.7E** (lanes 1-10). The transformation of pSMART-GS5 and pSMART-GS6 both yielded 5 colonies each. The plasmid in lane 5 was selected for restriction enzyme analysis for pSMART-GS5, while the plasmid in lane 6 was selected for pSMART-GS6. The restriction enzyme analysis of pSMART-GS5 and pSMART-GS6 are depicted in **Figure 3.8D**. The undigested pSMART-GS5 (lane 2) was linearised with ApaI (lane 3), and HindIII (lane 4), and both yielded a single fragment of approximately 3500bp. The undigested pSMART-GS6 (lane 6) was linearised with ApaI and yielded one fragment of approximately 3300bp (lane 7). pSMART-GS6 was also double digested with EcoRV which yielded two fragments of approximately 1900bp and 1400bp (lane 8). These

results were as expected and thus the cloning of genome segment 5 and genome segment 6 were confirmed.

The undigested pSMART-GS7 is depicted in **Figure 3.7F** (lanes 1-7). The transformation of pSMART-GS7 yielded 7 colonies. The plasmid in lane 6 was selected for restriction enzyme analysis. The restriction enzyme analysis of pSMART-GS7 is depicted in **Figure 3.8E.** The undigested pSMART-GS7 (lane 4) was linearised with ApaI (lane 5), and BamHI (lane 6) and both yielded a single fragment of approximately 3000bp. These results were as expected and thus the cloning of genome segment 7 was confirmed.

The undigested pSMART-GS8 and pSMART-GS10 are depicted in **Figure 3.7G** (lanes 1-11). The transformation of pSMART-GS8 and pSMART-GS10 yielded 9 and 2 colonies respectively. The plasmid in lane 4 was selected for restriction enzyme analysis for pSMART-GS8 while the plasmid in lane 11 was selected for pSMART-GS10. The restriction enzyme analyses of pSMART-GS8 and pSMART-GS10 are depicted in **Figure 3.8F**. pSMART-GS8 was linearised with ApaI and yielded one fragment of approximately 2900bp (lane 1). pSMART-GS8 was also double digested with EcoRV which yielded two fragments of approximately 1800bp and 1100bp (lane 2). pSMART-GS10 was linearised with ApaI and yielded one fragment of approximately 2600bp (lane 3). pSMART-GS10 was also double digested with EcoRV which yielded two fragments of approximately 1800bp and 800bp (lane 4). The bad resolution was most probably caused by the well comb that was not sufficiently cleaned before use, resulting in the low resolution seen in **Figure 3.8F**. These results were as expected and thus the cloning of genome segment 8 and genome segment 10 was confirmed.

The undigested pSMART-GS11 is depicted in **Figure 3.7I** (lanes 1-10). The transformation of pSMART-GS11 yielded 10 colonies. The transformation of the positive control In-Fusion reaction resulted in a great number of colonies that could not be counted, and DNA was extracted from 1 colony and can be seen in **Figure 3.8G** (lane 1). Due to the cost and limited amount of the In-Fusion reaction enzyme, a positive control was only performed the first time the enzyme was used. The plasmid in lane 3 was selected for restriction enzyme analysis. The restriction enzyme analysis of pSMART-GS11 is depicted in **Figure 3.8G.** The undigested pSMART-GS11 (lane

4) was linearised with SacI and yielded one fragment of approximately 2500bp (lane 3). pSMART-GS11 was also double digested with EcoRV which yielded two fragments of approximately 1800bp and 700bp (lane 4). These results were as expected and thus the cloning of genome segment 7 was confirmed.

The In-Fusion cloning of genome segments 3 and 9 were especially challenging. After multiple attempts, no colonies were obtained after transformation into the Zymo5α cells. In a last effort to successfully clone segment 3 and segment 9, the In-Fusion reactions were transformed in Epicentre's CopyCutter™ EPI400™ Chemically Competent *E. coli* cells that are designed to help with the transformation of unstable DNA sequences. The protocol for transformations with these cells is described in **Section 3.2.1**.

The undigested pSMART-GS3 from transformed CopyCutter cells is depicted in **Figures 3.7C** (lanes 1-9). The undigested pSMART-GS3 seemed to be the same size compared to each other, but it also seemed that they were much larger than any other of the newly synthesised 10 rotavirus transcription plasmids. The plasmid in lane 1 was selected for restriction enzyme analysis. The restriction enzyme analysis of pSMART-GS3 can be seen in **Figure 3.8C**. pSMART-GS3 was linearised with ApaI and yielded 6 bands with a total length that is well over 20 000bp (lane 1). pSMART-GS3 was also linearised with BamHI which yielded 2 fragments of approximately 4500bp and 2000bp (lane 2). This indicated that genome segment 3 was not successfully cloned. These results were very confusing, and I have no explanation for these results. After the failed attempts of cloning, it was decided to create exact 5' and 3' terminals for genome segment 3 with PCR and use the amplicons to create (+)ssRNAs through *in vitro* transcription.

The undigested pSMART-GS9 from transformed CopyCutter cells is depicted in **Figure 3.7H** (lanes 1-8). The transformation of pSMART-GS9 yielded 8 colonies. The plasmid in lane 2 was selected for restriction enzyme analysis. The restriction enzyme analysis of pSMART-GS9 is depicted in **Figure 3.8C.** pSMART-GS9 was linearised with ApaI (lane 5), and BamHI (lane 6) and both yielded a single fragment of approximately 3000bp. These results were as expected and thus the cloning of genome segment 9 was confirmed.

The number of colonies that were present after the transformation of each genome segment was very low, and the number of these colonies that had the desired DNA was even lower. I do not have an explanation for this.

After the In-Fusion of individual genome segments into pSMART was confirmed the samples' concentration was determined on a Nanodrop spectrophotometer and is shown in **Table 3.3**. The concentration of the transcription plasmids varied from approximately 100ng/µl to 500ng/µl. The ratio of absorbance at 260/280 nm of all the plasmids was above 1.8. This indicated that the samples were not contaminated with proteins and they could be used for *in vitro* transcription.

Table 3.3: Concentrations and absorbance of the new rotavirus transcription plasmids

Sample DNA	GS1	GS2	GS4	GS5	GS6	GS7	GS8	GS9	GS10	GS11
Concentration ng/µl	453.0	381.7	538.6	318.8	243.5	332.1	219.0	104.2	201.8	123.2
Absorbance 260/280 nm	1.85	1.85	1.86	1.85	1.86	1.85	1.81	1.86	1.82	1.84

3.3.5. Sanger and Next-generation sequencing of 10 transcription plasmids

The goal of the Sanger sequencing was to determine if the design flaw at the 5' terminal end of all the genome segments was corrected with the In-Fusion cloning. The Sanger sequencing was done at the CAF in Stellenbosch. The 5' terminal ends for genome segments 1, 2 and 4-11 can be seen in **Figure 3.9**. The three extra guanines that were present after the T7 promoter region have been successfully removed with the In-Fusion cloning for all the rotavirus genome segments. After the In-Fusion cloning, all the genome segments should have started on a 5'-GG… after the T7 promoter sequence at the 5' terminal end. However, for genome segment 11 only one guanine was present 5'-G **Figure 3.9**. The reason for this error was found to be that the sequence of SA11 rotavirus genome segment 11 (GenBank Accension nr. JN827255) was incorrectly uploaded to GenBank. The sequence left out a guanine at the 5' terminal end. This caused us to design primers that removed one more guanine at the 5' terminal than should have been removed.

The 3' terminal ends for genome segments1, 2 and 4-11 can be seen in **Figure 3.10**. The results showed that the 3' terminal ends all annealed as expected and that no mismatches of sequences took place. This ensured that the (+)ssRNAs that would be synthesised from these plasmids would have exact 5' and 3' terminal ends.

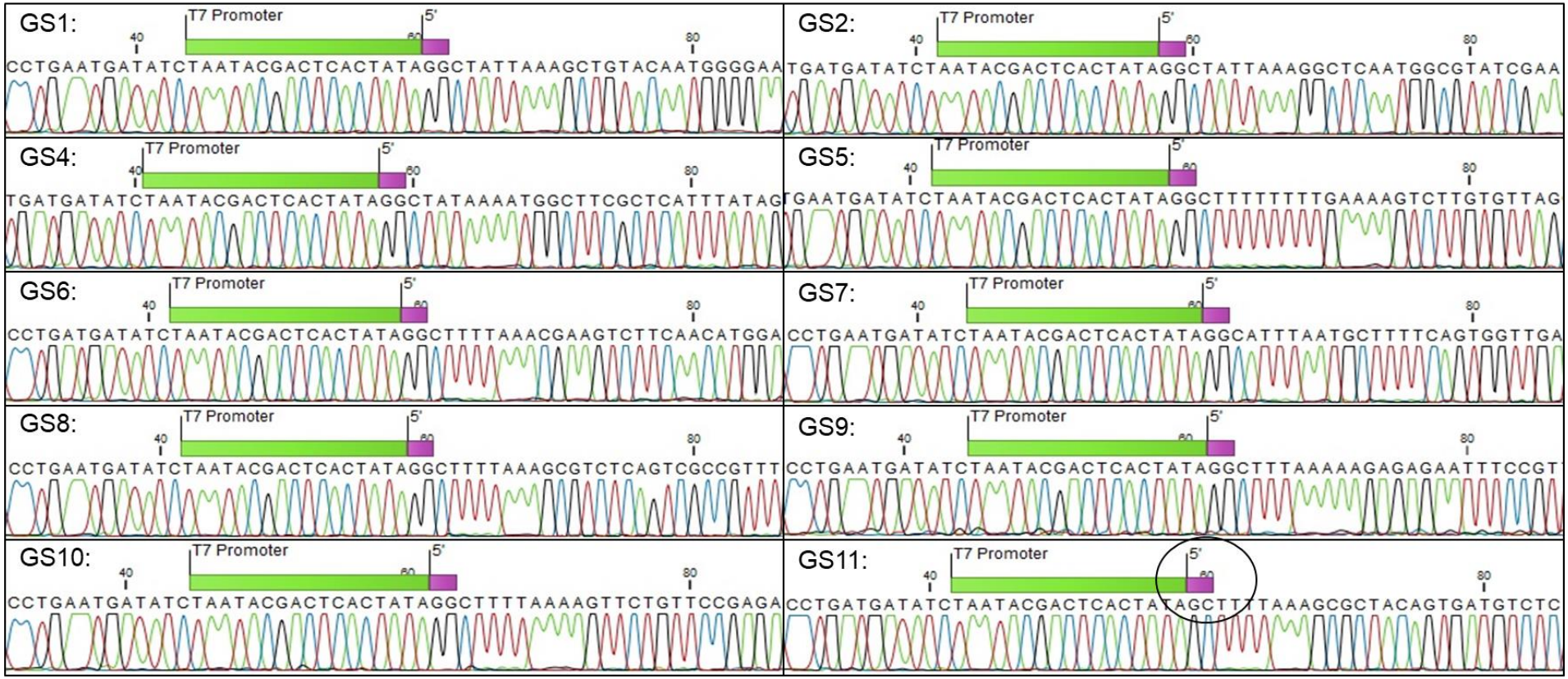

Figure 3.9: Sanger sequencing data of the 5' terminal ends for pSMART-GS1/2/4/5/6/7/8/9/10/11. The figure depicts the Sanger sequencing data of the 5' terminal ends of all 11 rotavirus genome segments with the sequences indicated in green being the T7 promotor region and the sequences in purple being the double guanine at the start of every genome segment. The only exception is genome segment 11 that had only one guanine residue at the 5' terminal end.

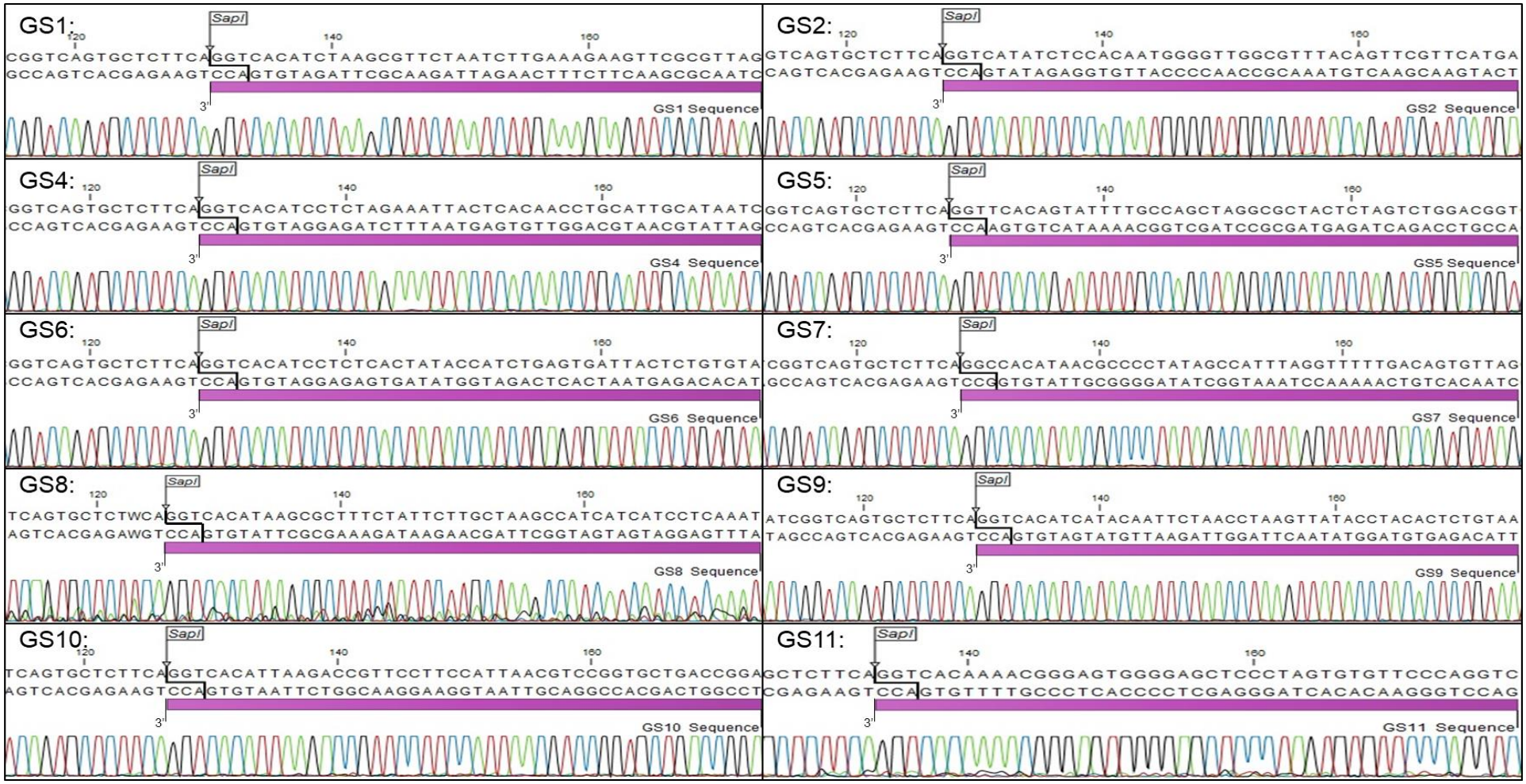

Figure 3.10: Sanger sequencing data of the 3' terminal ends for pSMART-GS1/2/4/5/6/7/8/9/10/11. The figure depicts the Sanger sequencing data of the 3' terminal ends of all 11 rotavirus genome segments and is indicated in purple. The SapI restriction enzyme site is also indicated at each end.

The goal of the NGS was to determine if any nucleotide changes in the sequences occurred when all 11 genome segments were cloned into pSMART with In-Fusion cloning. The samples pSMART-GS1/2/4/5/6/7/8/9/10/11 were sequenced at the NICD and NWU. Only the data from the sequencing performed at the NWU is shown. The data of all the sample showed good coverage that varied from approximately 11 000 reads for genome segment 11 to more than 600 000 reads for genome segment 1 **Figures 3.11-3.21**. The data also showed that no nucleotide change occurred for samples pSMART-GS1/2/4/5/6/7/8/9/10 and that the 5' sequences of each of these genome segment started with 5'-GG… and the 3' sequences ended with …CC-3', ensuring exact 5' and 3' terminal ends. The data of genome segment 11 depicted good coverage of the sequence **Figure 3.21A**. However, it also showed that a nucleotide replacement took place where a thymine was replaced with a cytosine on position 289 **Figure 3.21C**. This change in nucleotide sequence would lead to an amino acid change from a Cysteine to an Arginine. Due to time limitations, this error could not be fixed, and the pSMART-GS11 was used to synthesise (+)ssRNA transcripts and was used in the transfection of BHK-T7 cells (chapter 4).

The data for genome segment 11 also showed that 5' terminal end started with a 5'-GG… sequence **Figure 3.21B**. This contradicted the Sanger sequencing data which showed only one guanine at the 5' terminal. After a lot of deliberation with Prof. Albie van Dijk about this discrepancy between the two data sets, we could not ascertain the reason for the differences in data.

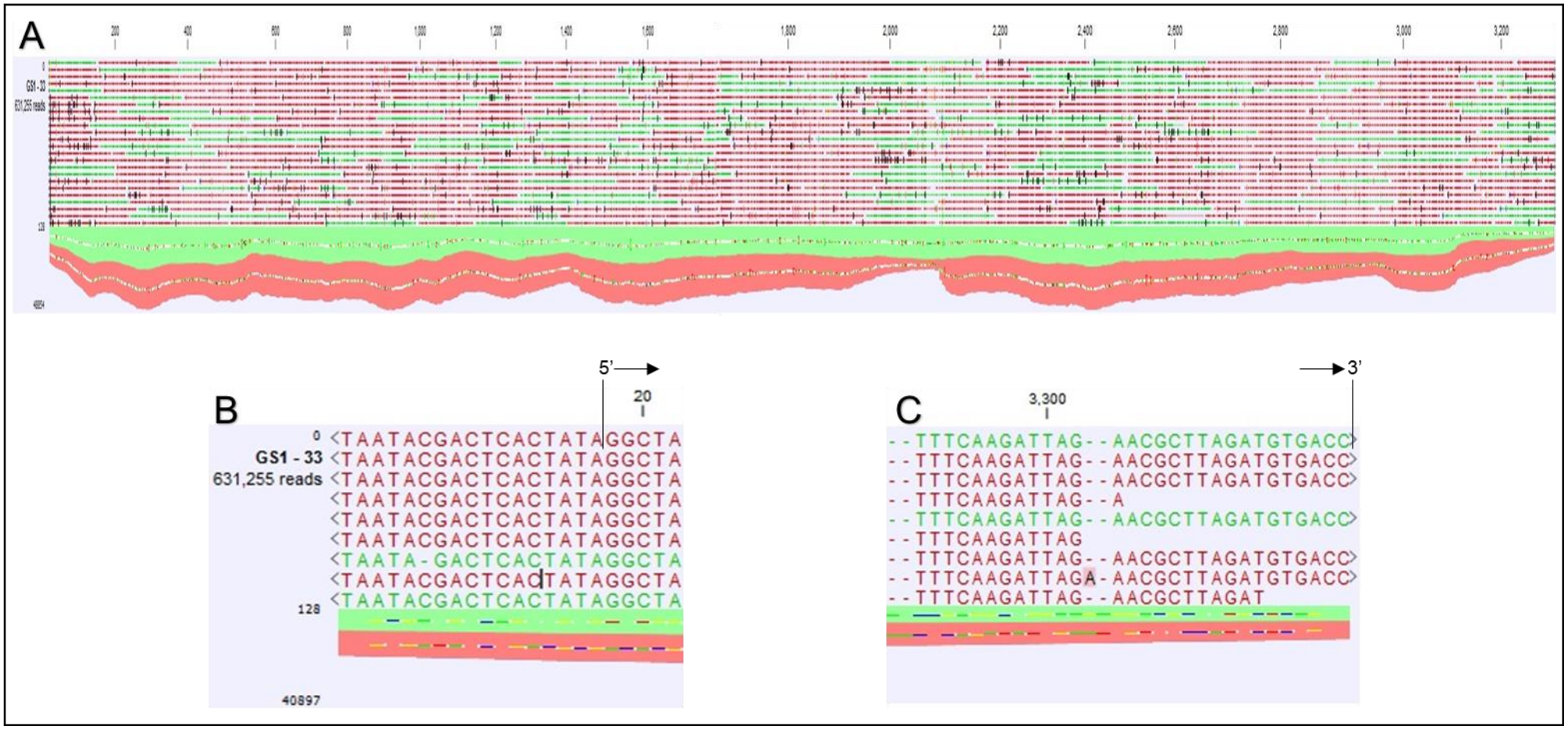

Figure 3.11: Ion-Torrent S5 sequencing data for pSMART-GS1. (A) The next-generation sequencing coverage of pSMART-GS1. Good coverage was shown throughout the sequence, and no nucleotide changes were observed. (B) The corrected 5' terminal end of pSMART-GS1. The sequence after the T7 promoter beginning with a double guanine. (C) The 3' terminal end of pSMART-GS1.

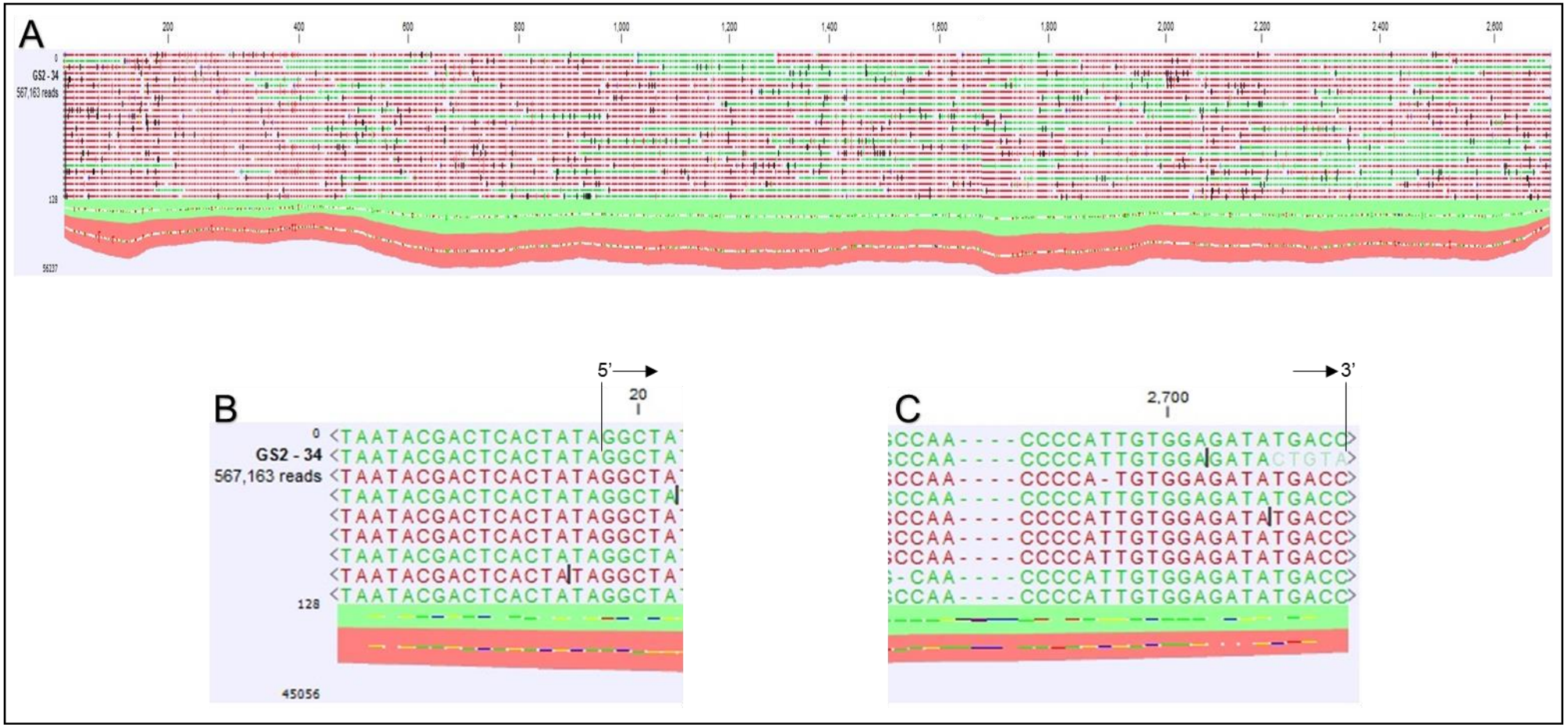

Figure 3.12: Ion-Torrent S5 sequencing data for pSMART-GS2. (A) The next-generation sequencing coverage of pSMART-GS2. Good coverage was shown throughout the sequence, and no nucleotide changes were observed. (B) The corrected 5' terminal end of pSMART-GS2. The sequence after the T7 promoter beginning with a double guanine. (C) The 3' terminal end of pSMART-GS2.

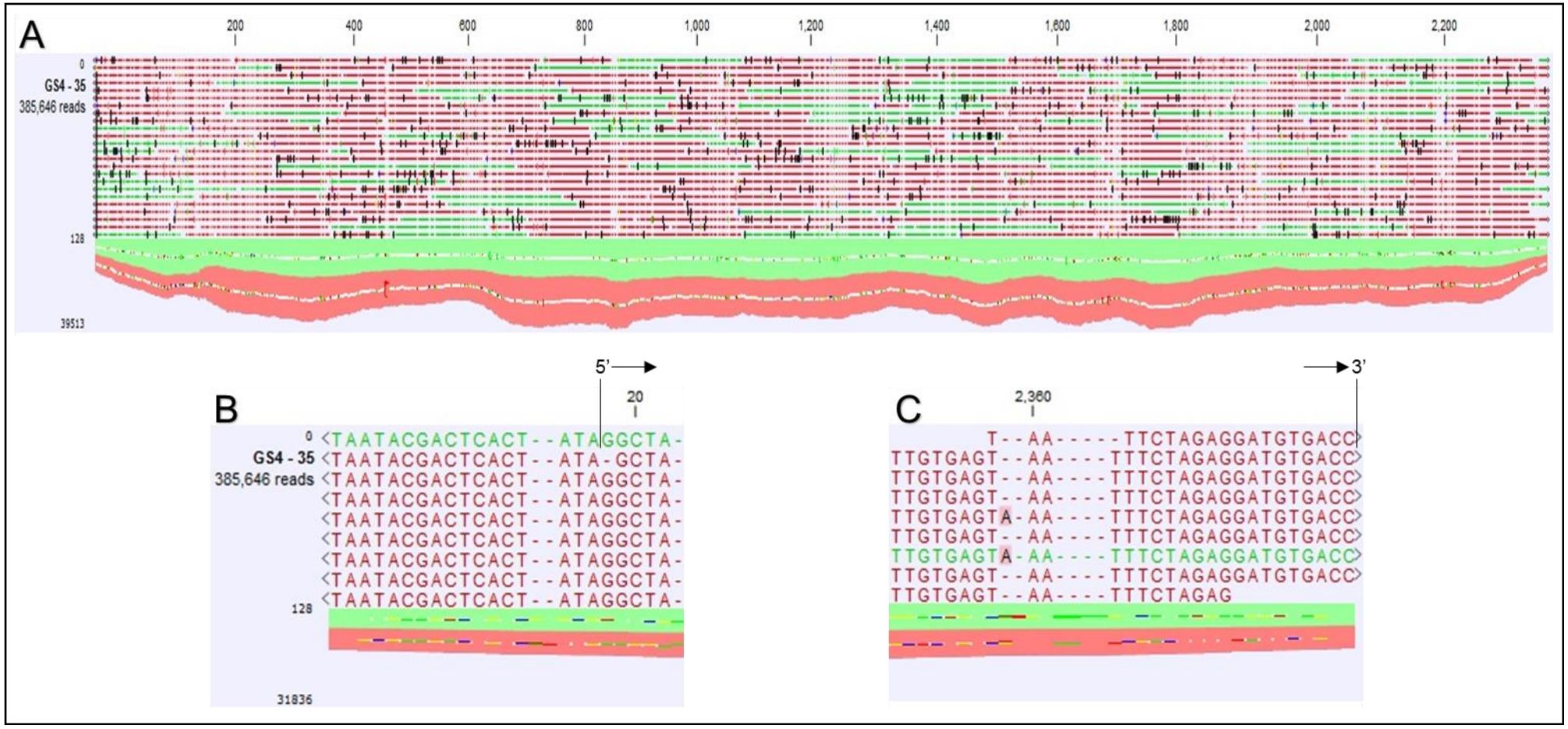

Figure 3.13: Ion-Torrent S5 sequencing data for pSMART-GS4. (A) The next-generation sequencing coverage of pSMART-GS4. Good coverage was shown throughout the sequence, and no nucleotide changes were observed. (B) The corrected 5' terminal end of pSMART-GS4. The sequence after the T7 promoter beginning with a double guanine. (C) The 3' terminal end of pSMART-GS4.

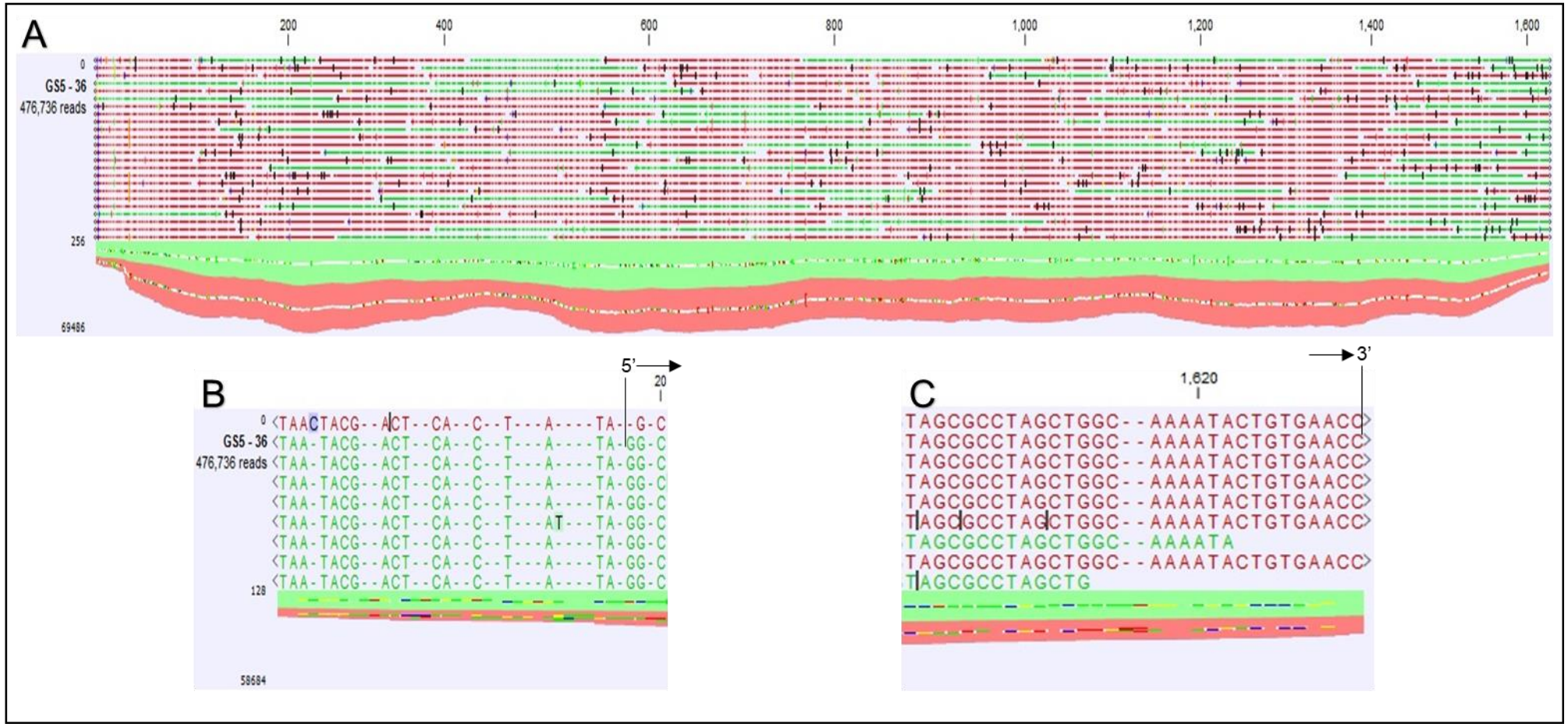

Figure 3.14: Ion-Torrent S5 sequencing data for pSMART-GS5. (A) The next-generation sequencing coverage of pSMART-GS5. Good coverage was shown throughout the sequence, and no nucleotide changes were observed. (B) The corrected 5' terminal end of pSMART-GS5. The sequence after the T7 promoter beginning with a double guanine. (C) The 3' terminal end of pSMART-GS5.

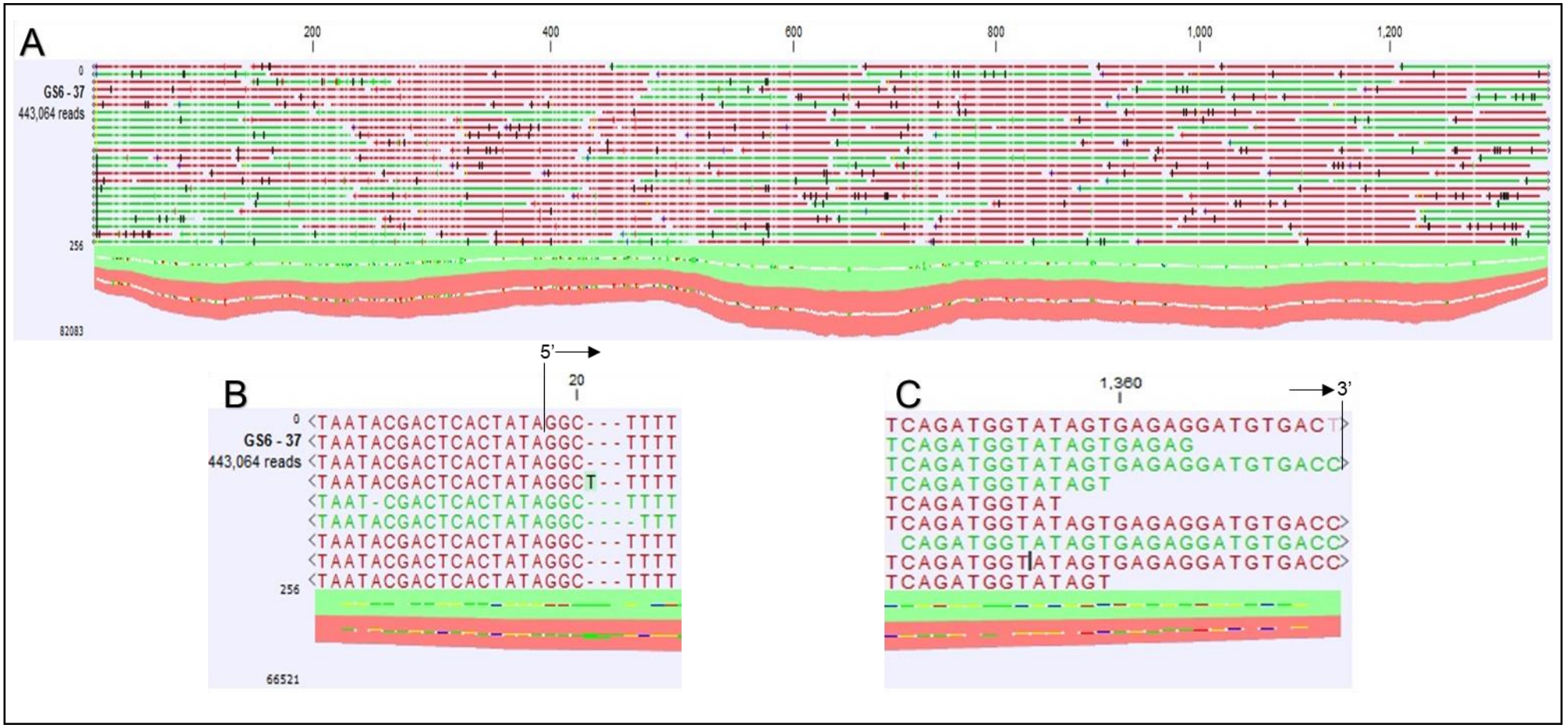

Figure 3.15: Ion-Torrent S5 sequencing data for pSMART-GS6. (A) The next-generation sequencing coverage of pSMART-GS6. Good coverage was shown throughout the sequence, and no nucleotide changes were observed. (B) The corrected 5' terminal end of pSMART-GS6. The sequence after the T7 promoter beginning with a double guanine. (C) The 3' terminal end of pSMART-GS6.

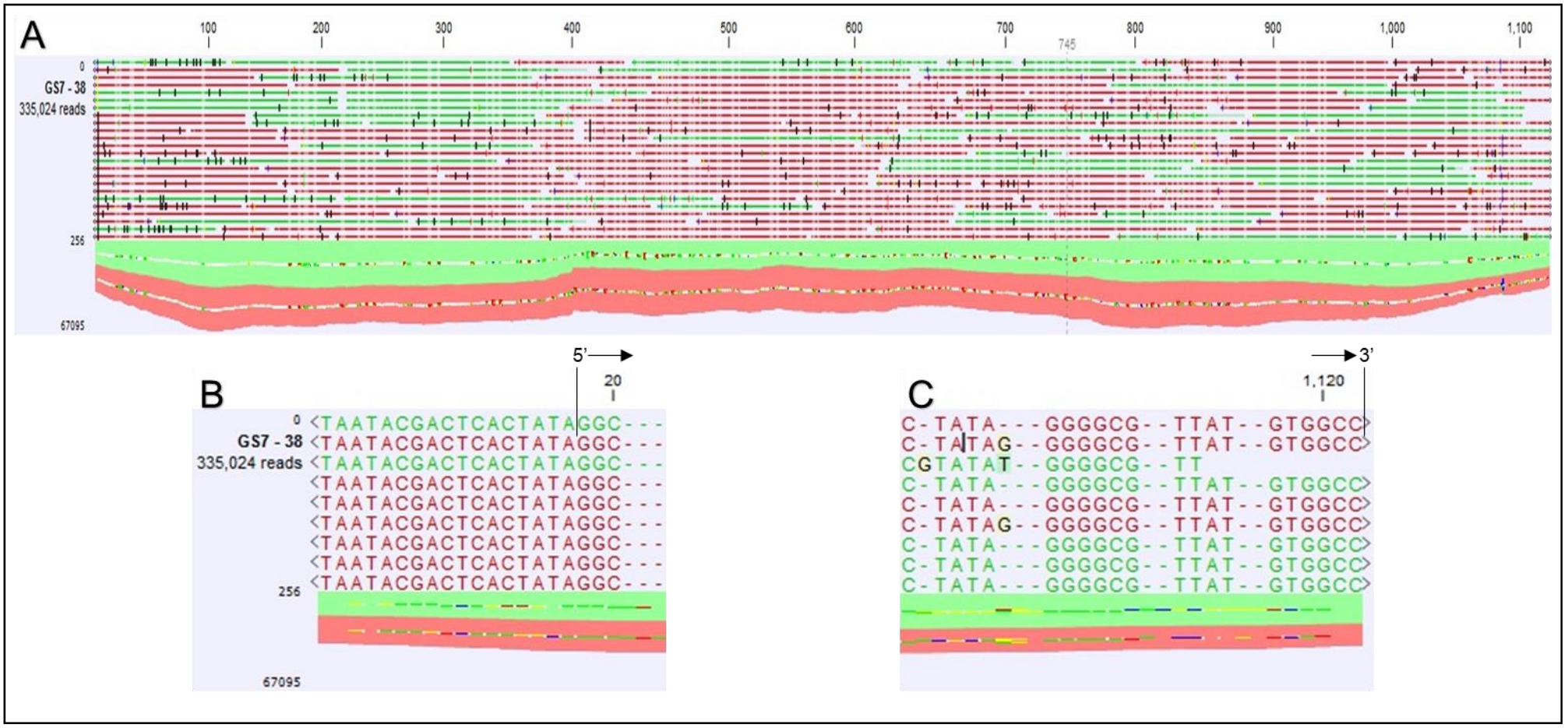

Figure 3.16: Ion-Torrent S5 sequencing data for pSMART-GS7. (A) The next-generation sequencing coverage of pSMART-GS7. Good coverage was shown throughout the sequence, and no nucleotide changes were observed. (B) The corrected 5' terminal end of pSMART-GS7. The sequence after the T7 promoter beginning with a double guanine. (C) The 3' terminal end of pSMART-GS7.

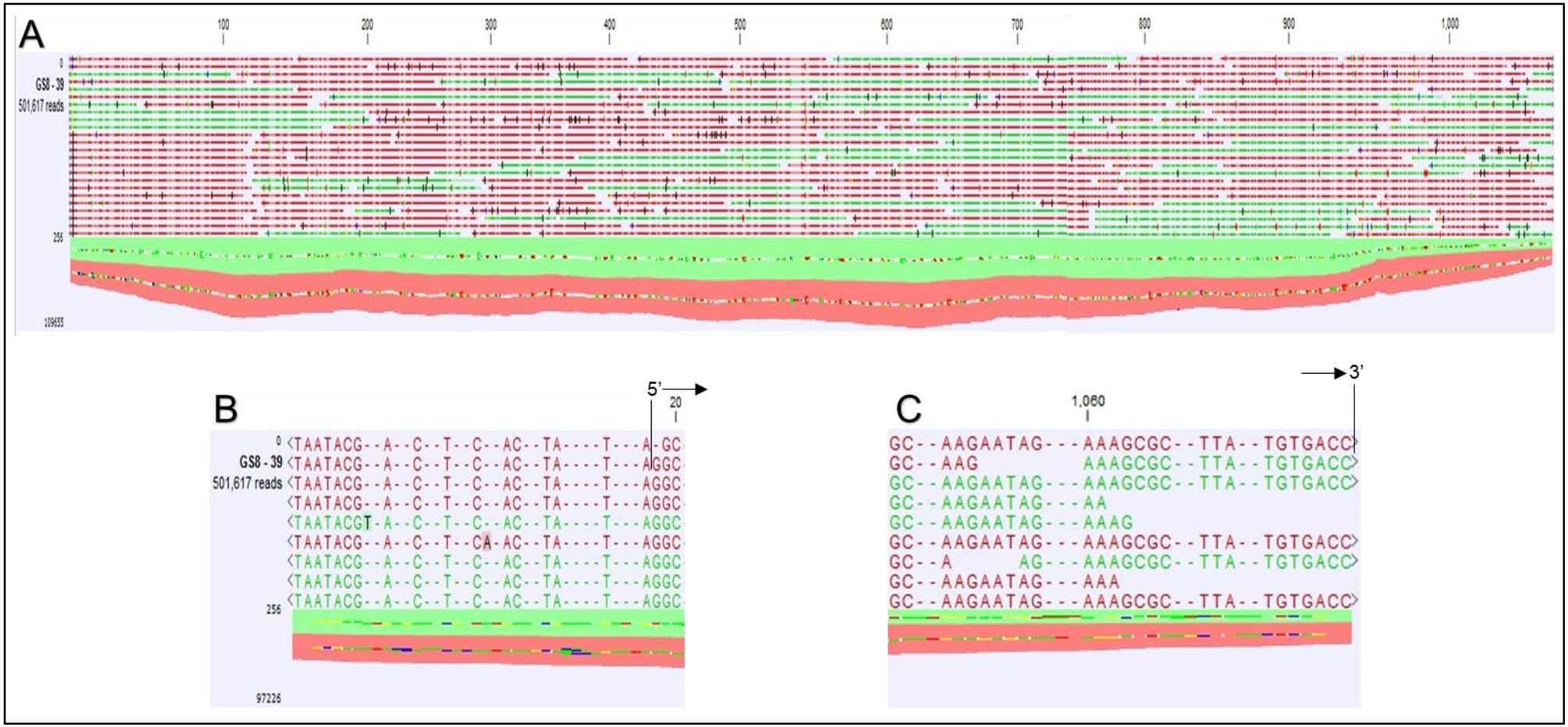

Figure 3.17: Ion-Torrent S5 sequencing data for pSMART-GS8. (A) The next-generation sequencing coverage of pSMART-GS8. Good coverage was shown throughout the sequence, and no nucleotide changes were observed. (B) The corrected 5' terminal end of pSMART-GS8. The sequence after the T7 promoter beginning with a double guanine. (C) The 3' terminal end of pSMART-GS8.

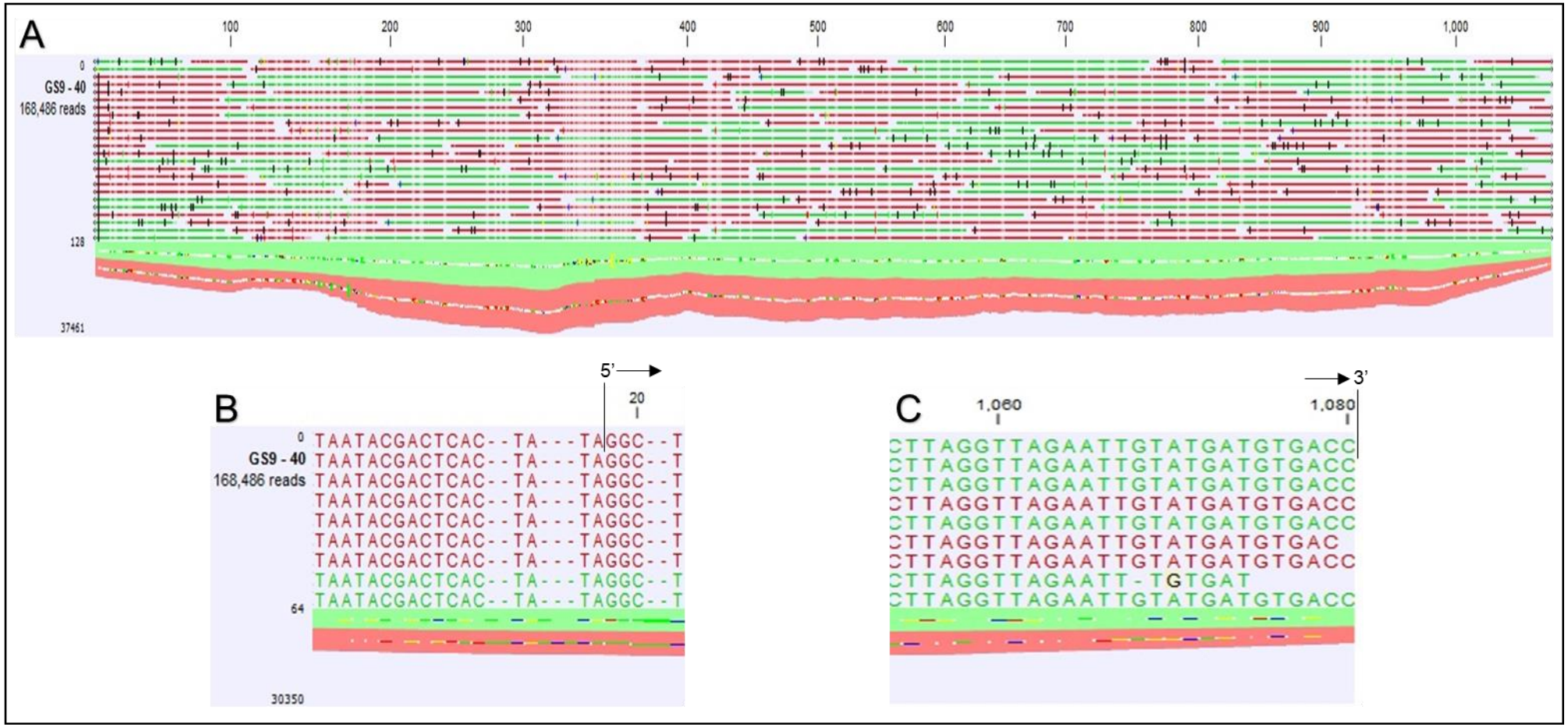

Figure 3.18: Ion-Torrent S5 sequencing data for pSMART-GS9. (A) The next-generation sequencing coverage of pSMART-GS9. Good coverage was shown throughout the sequence, and no nucleotide changes were observed. (B) The corrected 5' terminal end of pSMART-GS9. The sequence after the T7 promoter beginning with a double guanine. (C) The 3' terminal end of pSMART-GS9.

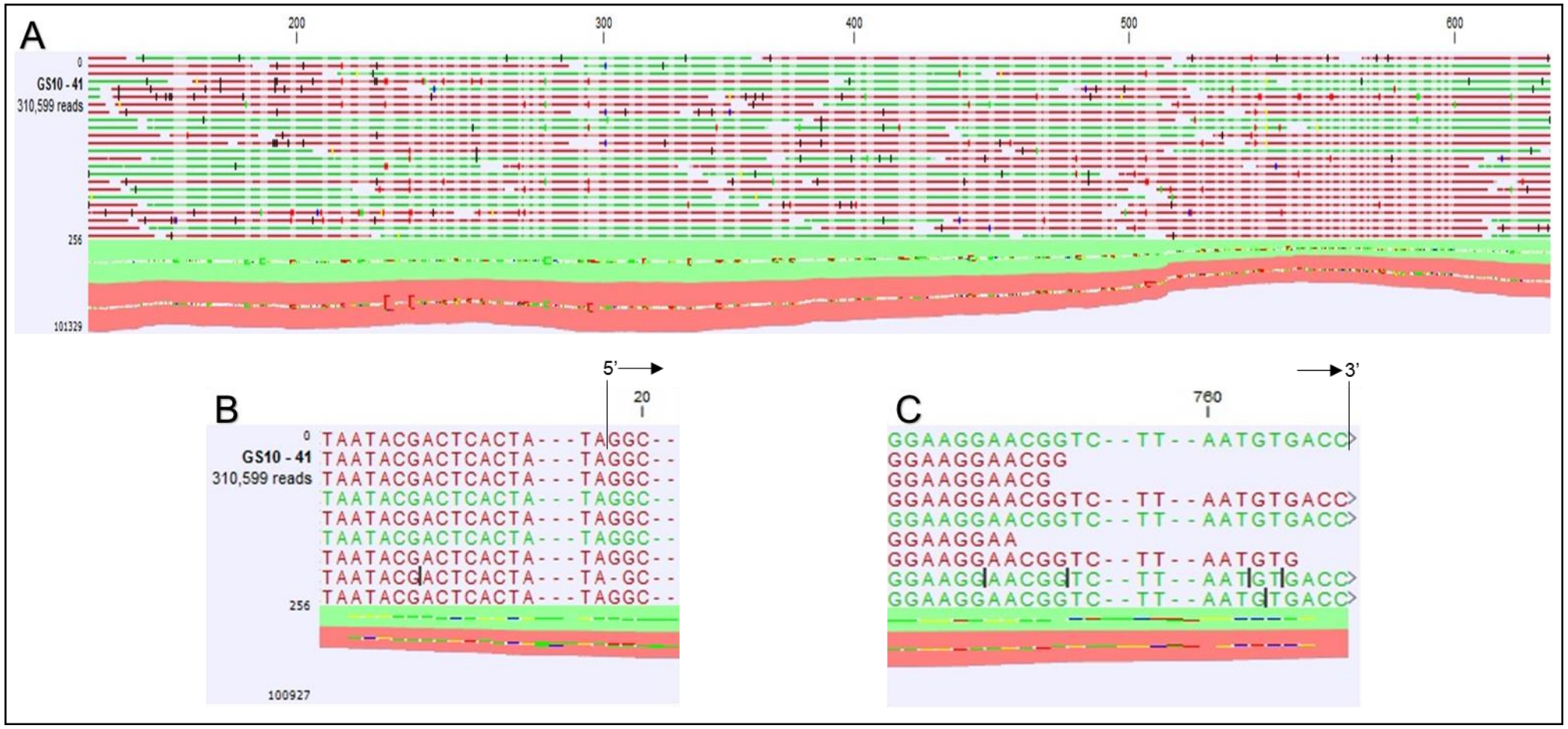

Figure 3.19: Ion-Torrent S5 sequencing data for pSMART-GS10. (A) The next-generation sequencing coverage of pSMART-GS10. Good coverage was shown throughout the sequence, and no nucleotide changes were observed. (B) The corrected 5' terminal end of pSMART-GS10. The sequence after the T7 promoter beginning with a double guanine. (C) The 3' terminal end of pSMART-GS10.

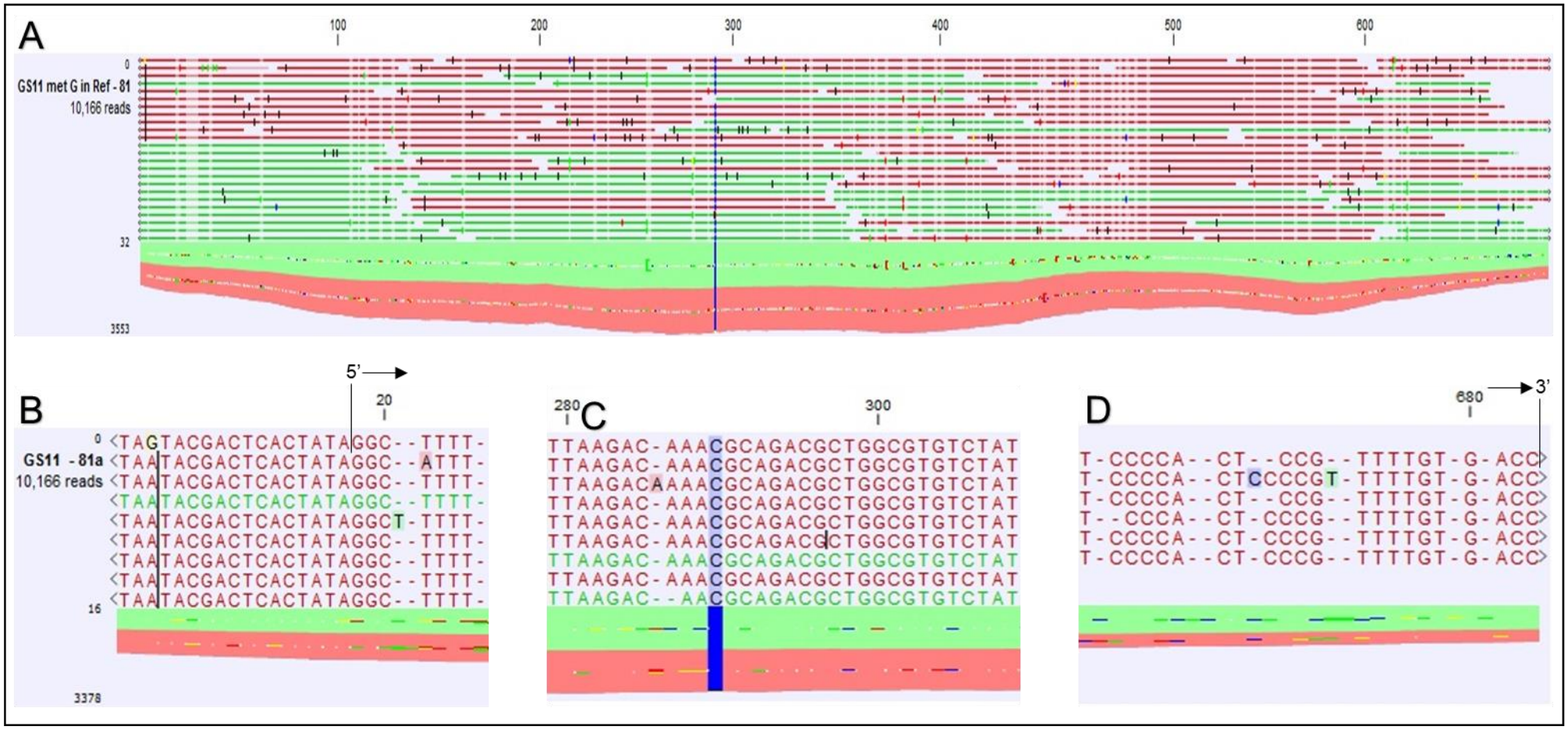

Figure 3.20: Ion-Torrent S5 sequencing data for pSMART-GS11. (A) The next-generation sequencing coverage of pSMART-GS11. Good coverage was shown throughout the sequence, but a nucleotide change was observed and highlighted blue. (B) The corrected 5' terminal end of pSMART-GS11. The sequence after the T7 promoter beginning with a double guanine. (C) The nucleotide change at position 289 changed a thymine to a cytosine (D) The 3' terminal end of pSMART-GS11.

3.3.6 *In vitro* transcription of (+)ssRNAs

The goal of this experiment was to synthesise (+)ssRNAs from the newly created transcription plasmids through *in vitro* transcription. This was done by first linearising the ten transcription plasmids with the non-palindromic SapI restriction enzyme. The T7 promoter, which was placed upstream of the individual insert sequences initiates transcription at the first guanine and ensures an exact 5' terminal. The SapI restriction site would ensure an exact 3' terminal end. 3µg of each of the ten rotavirus plasmids (segments 1,2, and 4-11) was linearised overnight with SapI as described in **Section 3.2.10.** The digestions were loaded on an agarose gel to see if complete digestion was achieved. After this confirmation, the DNA was purified, and the *in vitro* transcription was performed as described in **Section 3.2.9**. An amplicon for genome segment 3 was prepared with exact terminal ends by PCR with specifically designed primers. The results are shown in **Figure 3.21** and **Figure 3.22.**

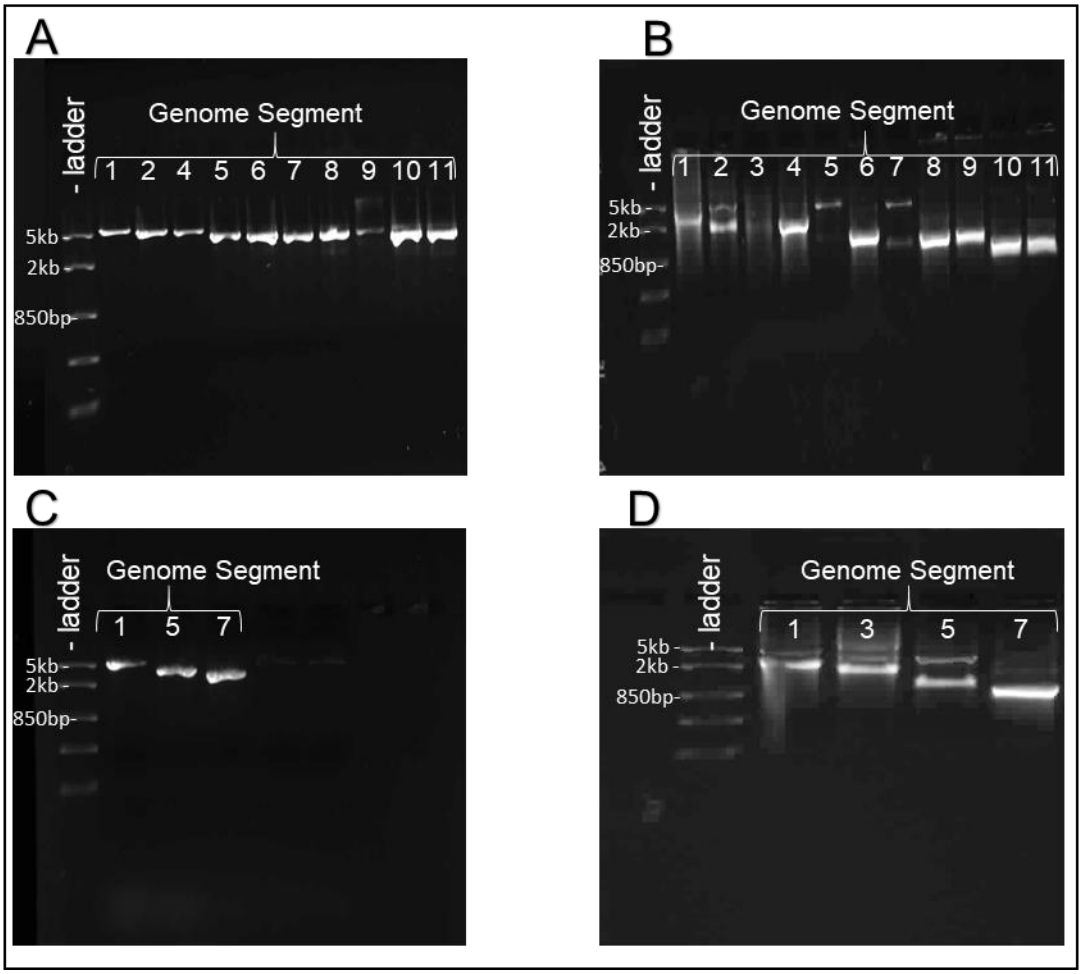

Figure 3.21: Linearised rotavirus transcription plasmids and runoff *in vitro* (+)ssRNAs transcripts. (A) Linearised rotavirus SA11transcription plasmids (lanes 1-11). (B) Unpurified *in vitro*-transcribed (+)ssRNAs of transcription plasmids in A. (C) Second round of linearisation of pSMART-GS1/5/7. (D) Unpurified (+)ssRNAs of pSMART-GS1/3/5/7.

Linearisation of ten of the rotavirus transcription plasmids with SapI was successful, although the yield of pSMART-GS9 was lower than the rest of the transcription plasmids **Figure 3.21A**. The amount was still sufficient to be used for *in vitro* transcription. The size of the linearised fragments, however, was bigger than the expected size of 2500-5000bp. This might be due to the gel being run for only 15 minutes, and thus the separation of different length fragments was not satisfactory. The goal of the gel was not to determine the size of the fragments only to see if complete digestion took place. As mentioned previously segment 3 was linearised through PCR.

The run-off transcripts synthesised through *in vitro* transcription of genome segments 2, 4, 6, 8, 9,10 and 11 were all the expected sized **Figure 3.21B**. The transcripts of genome segment 2, 5 and 7 had two bands (lanes 2, 5 and 7). One band was the

expected size and the second band was bigger than expected. The second, bigger bands were most probably DNA template that was still present in the samples. Why these template DNA was not visible in all the other genome segments, I do not know. The transcripts of genome segment 1 and 3 were also not successful. The *in vitro* transcribed transcripts for genome segment 1 yielded a smear **Figure 3.21B** (lane 1). There are a couple of reasons a gel can smear such as that the gel was improperly prepared with old buffer or the overloading of wells with the sample or contamination of the sample. Because no other samples showed this kind of smearing the overloading of wells and the improper preparation of gel were ruled out, and the most likely reason for the smear was that the sample was contaminated with DNase that would have degraded the DNA template and thus had to be redone. For genome segment 3 no clear transcript of the expected size was visible on the gel (lane 3). This was indicative that no (+)ssRNA was synthesised. This was attributed to the fact that the PCR amplicon was not purified before *in vitro* transcription although the protocol of the MegaScript kit stated that the purification of PCR samples prior to use was not necessary. The PCR of segment 3 was redone, and the sample was purified before use as described in **Section 3.2.7** (results not shown). The *in vitro* transcription of genome segments 5 and 7 yielded two bands (lanes 5, 7). As mentioned above, the bands of larger size is the DNA template used in the *in vitro* transcription, and less clear bands below were the newly synthesised (+)ssRNAs. The yield for the (+)ssRNAs was not sufficient, and the *in vitro* transcription of these two genome segments had to be redone. The most likely reason for the low yield was that not enough of the enzyme mixture was added due to a pipetting error and this affected the synthesis of (+)ssRNAs of these genome segments.

When the linearisation of the transcription plasmids pSMART-GS1/5/7 was repeated, the samples were completely digested as is evident by the single clear bands, **Figure 3.21C** (lanes 1, 3 and 5). The gel was run for approximately an hour so that the linearised fragments would separate better than in **Figure 3.21A**.

The repeat of the *in vitro* transcription of genome segments 1, 3, 5, and 7 is shown in **Figure 3.21D**. The exact same protocol was followed as the previous run, but special care was given that no contamination of the sample could take place and that no pipetting error was made. Two bands can be observed in all the wells. The top one being the template DNA and the lower one the newly synthesised (+)ssRNAs. The

lower bands were of expected size and the *in vitro* transcription was considered as being successful.

After this, all the RNA samples were treated with TURBO DNase to remove the residual DNA template, and the samples were purified as described in **Section 3.2.9.3**. The samples were again loaded on an agarose gel **Figure 3.22,** and the concentration of the (+)ssRNAs was determined on a Nanodrop spectrophotometer **Table 3.5**.

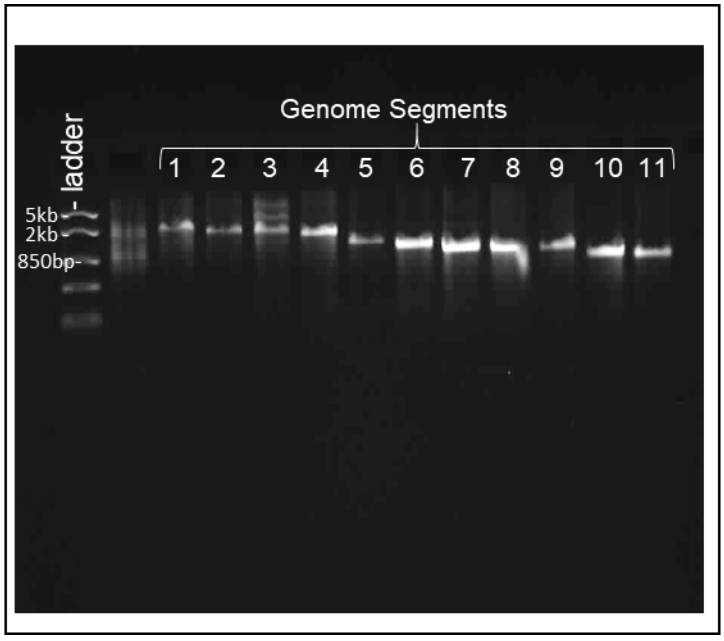

Figure 3.22: *In vitro* transcribed (+)ssRNAs after purification. The newly synthesised (+)ssRNAs after the samples were purified with a MegaClear kit. The number above the individual wells correlates with that specific genome segment number.

A single clear band was observed for 10 of the purified (+)ssRNAs **Figure 3.22**. The transcripts of genome segment 3 had two additional bands above the actual transcript. These bands could be due to secondary structures of the RNA. The occurrence of these secondary structures in gels can be avoided if the specific samples that show secondary structures are heated to approximately 60°C to denature the secondary structures and then loaded onto an agarose gel. This advice was given through personal communication with Prof. Christiaan Potgieter. The concentration and absorbance of each of the *in vitro* transcribed (+)ssRNAs is given in **Table 3.5**.

Table 3.4: Concentration and purity of *in vitro* transcribed (+)ssRNAs to be used in transfections of mammalian cells

Sample DNA	GS1	GS2	GS3	GS4	GS5	GS6	GS7	GS8	GS9	GS10	GS11
Concentration ng/µl	112.3	76.3	167.9	185.3	62.1	287.6	575.9	424.4	106.9	284.1	130.9
Absorbance 260/280 nm	2.26	2.29	2.25	2.23	2.30	2.23	2.35	2.22	2.21	2.24	2.21

The concentrations of the *in vitro*-transcribed (+)ssRNAs varied from approximately 80ng/µl to 580ng/µl. The reason for the difference yield is unclear, but a sufficient amount of (+)ssRNA transcripts of each genome segment was obtained to continue. The absorbance ratio at 260/280 nm of each was higher than the minimum of 2.0, thus indicating the purity of the samples was sufficient to continue.

3.4 Summary and future prospects

The first goal of the work presented in this chapter was to correct the 5' terminal end of the eleven SA11 rotavirus genome segments. The second goal was to use the eleven transcription plasmids to synthesise (+)ssRNAs through *in vitro* transcription. All eleven rotavirus genome segments were individually cloned into pSMART with a T7 promoter region flanking the 5' terminal and the non-palindromic restriction enzyme SapI site on the 3' terminal to ensure exact terminal ends. This was done by utilising the seamless cloning technology of In-Fusion HD. After the successful cloning of the 10 of the 11 viral genome segments into pSMART, all samples were sent for Sanger and next-generation sequencing to determine if the design flaws were corrected and that no other sequence alterations occurred during the cloning process that could affect rescue. Once the sequences were verified the ten rotavirus transcription plasmids were linearised with SapI. Genome segment 3 was linearised and corrected with PCR, and the linearised amplicon was used as a template to synthesise (+)ssRNAs through *in vitro* transcription. These (+)ssRNAs were purified and their concentration measured. These newly synthesised (+)ssRNAs will be used in the transfection of mammalian cells to try and establish a transcript-based reverse genetics system, as described in the next chapter.

Chapter 4: The transfection of *in vitro*-transcribed (+)ssRNAs in mammalian cells

4.1 Introduction

The main objective of this study was to develop a transcript-based reverse genetics system for rotavirus. A transcript-based approach requires the generation of fully infectious virus particles by transfecting mammalian cultured cells with transcriptionally active (+)ssRNAs. Such systems for other viruses belonging to the *Reoviridae* family do exist, for example for bluetongue virus and African horsesickness virus. The BTV transcript-based reverse genetics system was based on a dual transfection principle. In this system, BSR cells were subjected to two transfections. The first transfection was with T7-derived BTV transcripts encoding VP1, VP3, VP4, VP6, NS1 and NS2 viral proteins. The VP1, VP3, VP4, VP6 proteins form the inner core of BTV. After 18 hours of incubation, a second transfection was performed where all ten *in vitro*- derived T7 BTV transcripts were transfected, and viable BTV was rescued (Boyce et al., 2008). The reverse genetics system for African horsesickness virus was also based on a dual transfection system. In this system, 6 expression plasmids encoding VP1, VP3, VP4, VP6, NS1 and NS2 of AHSV serotype 6 (AHSV6) under the control of the CAG promoter were transfected first. After 18 hours of incubation, a full set of AHSV serotype 4 core transcripts were transfected into the cells resulting in virus rescue (Kaname et al., 2013). In both these systems, the first transfection leads to the formation of the replication complex and the second transfection drives the downstream replication processes (Matsuo and Roy, 2009).

The transfection of mammalian cell cultures constitutes the introduction of foreign nucleic acids to the cells which in turn will result in the production of genetically modified cells. The cells were transfected with the transfection reagent Lipofectamine 2000 from Invitrogen. Lipofectamine is a formulation of a cationic liposome which interacts with nucleic acids that need to be transfected into cells and forms a positive charge on its surface, thus allowing contact with the negatively charges cell

membrane. In addition, the lipofectamine's cationic lipid molecules are formed with a neutral co-lipid, and the co-lipid facilitates the fusion of the cell membrane and the liposome allowing entry of transfected DNA/RNA (Dalby et al., 2004).

In this chapter, the transfection of BHK-T7 cells with transcripts derived from 11 rotavirus transcription plasmids, together with 7 SA11 MA104 codon-optimised expression plasmids, FAST plasmid and two VV capping plasmids (D1R and D12L) are described. These plasmids were used in an attempt to better the odds of success for our reverse genetics approach. The MA104 cells were chosen based on the fact that rotavirus propagates well in these cells. However, the MA104 cells are not easily transfected, and it was decided to transfect BHK-T7 cells and after 22 hours co-seed the BHK-T7 cells with MA104. The seven expression plasmids were created for a previous study conducted in our laboratory (Wentzel, 2014). These seven plasmids included VP1, VP2, VP3, VP6 NSP1, NSP2 and NSP5. All of these plasmids were codon-optimised for MA104 cells and was placed downstream of a CMV promoter to synthesise the replication complex scaffold.

4.2 Materials and Methods

4.2.1. Propagation of MA104 and BHK-T7 cells

When propagating the different mammalian cells, all steps were performed in sterile conditions to advert any contamination of cells. Prior to the thawing of the different cell lines, the Dulbecco's Modified Eagle Medium (DMEM), fetal bovine serum (FBS) (from Gibco, Life Technologies) and Anti-Anti (antibiotic/antimycotic) solution (penicillin 10 000 U/ml, 10 mg/ml streptomycin, amphotericin B 25µg/ml) (Sigma-Aldrich), were taken out of storage and placed in a laminar flow hood to heat up to room temperature. The BHK-T7 and MA104 cells were propagated as a monolayer in 25cm^2 Techno Plastic Products (TPP) tissue culture flasks (Sigma-Aldrich). Stocks of these cells were stored in 1ml cryotubes with cryopreservation media in liquid nitrogen.

The BHK-T7 cells were rapidly thawed in a sterile incubator at 37°C and once thawed, they were gently mixed by pipetting as not to damage the cells and then transferred into a sterile 25cm^2 TPP culture flask. 5ml of DMEM containing 5% FBS and 1% Anti-Anti (antibiotic/antimycotic) solution was added(v/v). The addition of the DMEM medium is to dilute the DMSO in the cryopreservation medium which can be toxic to cells. The flasks were incubated in a humidified incubator at 37°C with a constant

supply of 5% CO_2 for 1-2 hours so the cells could attach to the bottom of the flasks. After the incubation, the cells were observed under a microscope to verify the cells have attached to the flasks and once that has been determined the medium was removed and replaced with 5ml of DMEM containing 5% FBS and 1% Anti-Anti (antibiotic/antimycotic) solution. The BHK-T7 cells were then propagated in a humidified incubator at 37°C and 5% CO_2.

The MA104 cells were started-up in the same way as the BHK-T7 cells with the only exception being that the DMEM media used contained 5% FBS and 1% Anti-Anti (antibiotic/antimycotic) solution and 1% non-essential amino acids (NEAA).

4.2.2. Passaging of BHK-T7 and MA104 cells

When the cells reached confluency, the cells were subcultured in a 1:3 ratio. This was done by removing the medium and washing the cells two times with 5ml of phosphate buffered saline (PBS) (Gibco, Life Technologies) to remove the FBS. The last remaining PBS was removed through pipetting. Next, 4ml of 0.05% trypsin-EDTA (Gibco, Life Technologies) was added to the cell monolayer to facilitate the detachment of cells from the culture flasks. The flasks were gently swerved, and after 1 minute, 2.5 ml of the 0.05% trypsin-EDTA was removed, and the flasks were incubated for 3-5 minutes at 37°C in a humidified incubator to aid in the cell detachment. After the incubation period, the respective cells were resuspended in 750µl FBS. Of the 750µl resuspended BHK-T7 cells, 250µl of it was added to three respective 25cm^2 TPP flasks containing 4.75ml DMEM with 1% Anti-Anti (antibiotic/antimycotic) solution and 600µg/ml hygromycin. The hygromycin selects for BHK cells that expresses the T7 polymerase. Of the 750µl resuspended MA104 cells, 250µl of it was added to three respective 25cm^2 TPP flasks containing 4750µl DMEM 1% Anti-Anti (antibiotic/antimycotic) solution and 1% non-essential amino acids (v/v). The cells were then placed back in the humidified incubator at 37°C and 5% CO_2.

4.2.3. Transfection mixture calculations

In an effort to develop a transcript-based reverse genetics system for rotavirus, we combined aspects of various dsRNA reverse genetics systems as recommended by Prof Christiaan Potgieter. The first component in the transfection mixture was the *in vitro*-transcribed (+)ssRNAs. In the development of a transcript-based reverse

genetics system for BTV, BSR cells were transfected with 600ng equimolar amounts of all 10 BTV transcripts (van Gennip et al., 2012). The transfection occurred in 24-well plates which have an area of 2cm^2 per well. Since our transfections occurred in a 10cm^2 flask, we transfected a total of 3µg (+)ssRNAs which contained an equimolar amount of each of the 11 rotavirus (+)ssRNAs. The amount of each genome segment used, as is indicated in **Table 4.1**. The second component in the transfection mixture was the SA11 MA104 codon-optimised expression plasmids VP1, VP2, VP3, VP6, NSP1, NSP2 and NSP5. In this study, we transfected these 7 plasmids in 1.5µg equimolar amounts. This aspect of the transfection was incorporated from a reverse genetics system for African horsesickness virus, where 300ng equimolar amounts of 7 expression plasmids were transfected into 24 well plates (area of 2cm^2) (van de Water et al., 2015). The last component in our transfection mixture was the fusogenic orthoreovirus FAST plasmid and two VV capping enzyme plasmids (D1R and D12L). These 3 components were taken from the rotavirus plasmid-based reverse genetics system (Kanai et al., 2017). In this system 15ng of the FAST plasmid was transfected together with 1.6µg of the VV capping enzyme plasmids (0.8µg of each) and 11 rotavirus genome segment expression plasmids into a 6 well plate (area of 9.61cm^2). Thus, we used the exact same amounts in our transfection mixture. All of these components were added together prior to transfection **Table 4.2**.

Table 4.1. Equimolar amounts of *in vitro*-transcribed (+)ssRNAs

Genome Segment	Amount required (ng)	Working stock concentration (ng/µl)	Volume required (µl)
GS1	531,6	110	4,83
GS2	434,1	74	5,87
GS3	416,6	167	2,49
GS4	380,3	185	2,06
GS5	260,7	61	4,27
GS6	219,6	287	0,78
GS7	179,8	575	0,3
GS8	172,2	421	0,41
GS9	172,5	106,6	1,62
GS10	123,4	279	0,44
GS11	109,3	130,5	0,84
Total :	3000	-	23,91

Table 4.2. The volume of different components used in the transfection mixture

Component	Stock concentration ng/µl	Amount used ng	Volume of component µl
(+)ssRNAs mix	136.5	3000	23.9
Expression plasmids mix	1117.8	1500	1.34
FAST plasmid	15	15	1
D1R plasmid	1335	800	0.6
D12L plasmid	1062	800	0.75
Total	-	6120	27.59

4.2.4. Transfection of mammalian cells

The day before the transfection, the BHK-T7 cells were seeded in two 10cm^2 TPP tubes (Takara Bio) in 3ml DMEM containing 5% FBS and 1% Anti-Anti (antibiotic/antimycotic) solution (penicillin 10 000 U/ml, 10 mg/ml streptomycin, amphotericin B 25µg/ml) but without hygromycin. The day of the transfection the cells were at 70-80% confluency for optimal transfection. Before the transfection, the transfection mixture was compiled as described in **Section 4.2.2**. The BHK-T7 monolayer cells were transfected with 3µg of equimolar amounts of *in vitro*-transcribed (+)ssRNAs together with 1.5µg equimolar amounts of rotavirus expression plasmids (VP1, VP2, VP3, VP6, NSP1, NSP2 and NSP6), 0.8µg of both capping plasmids and 15ng of the fusogenic plasmid. To set up the transfection mixtures, these components were added together to yield a final amount of 6.12µg and was then added to a tube containing 250µl OPTI-MEM® reduced serum medium (Gibco, Life Technologies). The mixture was incubated at room temperature for 5 minutes and then added to a tube containing 18.6µl Lipofectamine® 2000 (Thermo Fisher Scientific) in 250µl of OPTI-MEM® reduced serum medium and incubated for another 5 minutes. For every 1µg of the sample [(+)ssRNAs or plasmids] added, 2.5µl of Lipofectamine® 2000 is required. Before the transfection mixture was added to the BHK-T7 monolayer, 2ml of the media was removed from the 10cm^2 TPP tubes after which the transfection mixture was

added by holding the flasks diagonally and slowly dripping the transfection mixture onto the cells. This was done to ensure that the BHK-T7 cells were subjected to maximum exposure to the transfection mixture. The flask was closed and mixed gently by swirling and afterwards incubated for 22 hours in a humidified incubator at 37°C and 5% CO_2. A positive control was conducted in parallel with the sample transfection where 1µg of a plasmid expressing the T7 green fluorescent protein (pGFP) was added to 250µl OPTI-MEM® reduced serum medium, incubated for 5 minutes and then added to 2.5µl Lipofectamine® 2000 in 250µl OPTI-MEM® reduced serum medium. The rest of the protocol was the same as the described above.

The BHK-T7 cells were selected because they are easily transfected with Lipofectamine, whereas MA104 cells are sensitive to the transfection reagent and can therefore not be easily transfected. However, rotavirus propagates well in MA104 cells, and therefore MA104 cells were chosen to be co-seeded with the transfected BHK-T7 cells. Once the MA104 cells are co-seeded with the BHK-T7 cells, any newly synthesised rotavirus particles that are released by the transfected BHK-T7 cells can then infect the MA104 cells.

Approximately 24 hours after the transfection the transfected BHK-T7 monolayer was trypsinised with 0.05% Trypsin-EDTA (Gibco, Life Technologies) and seeded in a new 25cm^2 flask with MA104 cells at a 1:1 ratio. The passage mixture for the MA104 cells was prepared in a 50ml Falcon tube and consisted of 8.55ml DMEM with 1% Anti-Anti (antibiotic/antimycotic) solution (penicillin 10 000 U/ml, 10 mg/ml streptomycin, amphotericin B 25µg/ml) and 1% non-essential amino acids. The MA104 cells were then passaged as described in **Section 4.2.1.** The trypsinised MA104 cells were resuspended in FBS and then added to the MA104 passage mixture. The passage mixture for the BHK-T7 cells was also prepared in a 50ml Falcon tube and was comprised of 2.85ml DMEM with 1% Anti-Anti (antibiotic/antimycotic) solution (penicillin 10 000 U/ml, 10 mg/ml streptomycin, amphotericin B 25µg/ml) and 1% non-essential amino acids. The BHK-T7 cells' medium was removed, and the cells were washed two times with PBS, and afterwards, all the PBS was removed. Next, the cells were detached from the bottom of the flasks by adding 1ml of 0.05% Trypsin-EDTA and incubating the cells for 5 minutes at 37°C and 5% CO_2. The cells were then resuspended in FBS and added to the BHK-T7 passage mixtures. Next 3ml of the respective passage mixtures were added together in a new 25cm^2 flask and incubated

for 22 hours. Once the BHK-T7 cells co-seeded with MA104 cells reached 100% confluency the medium was replaced without washing with 5ml DMEM containing and 1% Anti-Anti (antibiotic/antimycotic) solution (penicillin 10 000 U/ml, 10 mg/ml streptomycin, amphotericin B 25µg/ml), 1% non-essential amino acids but with no FBS and the cells were then incubated for another 3-7 days or until cytopathic effects (CPE) were observed in the cells. The immunofluorescence monolayer assay (IPMA) was performed to verify virus replication, see **Section 4.2.5.**

4.2.5. Immunofluorescent monolayer assay

The immunofluorescent monolayer assay (IFMA) is a method that is highly specific and allows specific antigens within cultured mammalian cells to be detected. The principle of this method is that primary antibodies, here the antibodies were specific to SA11 rotavirus DLPs, are used to specifically bind to complementary antigens found within cultured cells. Next, secondary goat anti-rabbit antibodies fluorescently labelled with Alexa Fluor bind to the primary antibodies, which can then be visualised under fluorescent light to determine if the targeted antigens are present in the cultured cells. Methanol/Acetone fixation was used, see **Section 4.2.5.1**.

4.2.5.1. Methanol/Acetone fixation

The medium of co-seeded BHK-T7 and MA104 cells were removed and stored at 4°C before the cells were fixed. This was done so that if any fluorescence was detected in the cells, the sample RNA could be extracted, converted to cDNA which can then be sequenced to confirm the that the rotavirus particles were present. The cell monolayer was then fixed with an organic solvent, methanol/acetone in 1:1 (v/v) ratio, and the cells were incubated for 20 minutes at -20ºC. This step removes all lipids of the cell membranes as well as cause the cells to dehydrate which leads to the precipitation of proteins. Next, the methanol/acetone was removed, and a blocking buffer comprised of 1X PBS,1% tryptone and 0.05% Tween-20 solution was added. The blocking buffer prevents unspecific binding of the antibodies. The monolayers were blocked at 37°C for 30 minutes. The blocking buffer was removed, and rabbit anti-SA11 DLP serum diluted 2000 times in a 1X PBS, 1% tryptone and 0.05% Tween-20 solution was added. The rabbit anti-SA11 DLP serum was kindly provided by Prof Christiaan Potgieter from Deltamune, and the cells were incubated at 37°C for 30 minutes. During the incubation, the antibody-antigen complex is formed. After the incubation period, the

cells were carefully washed three times to avoid removing the cells from the bottom of the flask with a 1X PBS solution containing only 0.05% Tween-20. Lastly, the goat anti-rabbit IgG antibodies fluorescently labelled with the secondary antibody Alexa Fluor (ThermoFisher Scientific), was diluted 1:2000 in a 1X PBS solution containing 1% tryptone and 0.05% Tween-20 was added to cells and incubated for 30 minutes at 37°C. The incubation period facilitates the binding of the secondary antibodies to the antibody-antigen complex. After the incubation stage, the cells were observed and photographed using a Nikon Eclipse TE2000-S microscope under fluorescent light.

4.3. Results and Discussion

4.3.1. Transfection of BHK-T7 cells with a set of SA11 CS rotavirus (+)ssRNAs, SA11 expression plasmids and the expression plasmids for FAST and a VV capping enzyme

With the goal to establish a transcript-based reverse genetics system for rotavirus, rotavirus genetic material was introduced into BHK-T7 cells using the transfection reagent Lipofectamine®2000. A positive control transfection was conducted to ensure the transfection reagent Lipofectamine®2000 worked correctly. This was done by transfecting 1µg of pGFP into BHK-T7 cells. The expression of the pGFP control was visible 3 hours after the transfection in BHK-T7 cells **Figure 4.1A**. The expression of the pGFP had increased significantly approximately 22 hours after the transfection **Figure 4.1B**. The transfected BHK-T7 cells were still in good condition after approximately 22 hours of incubation with the transfection mixture **Figure 4.1C**. The positive control indicated that the transfection reagent Lipofectamine® 2000 used, worked properly in mediating the transport of foreign genetic material into the cells.

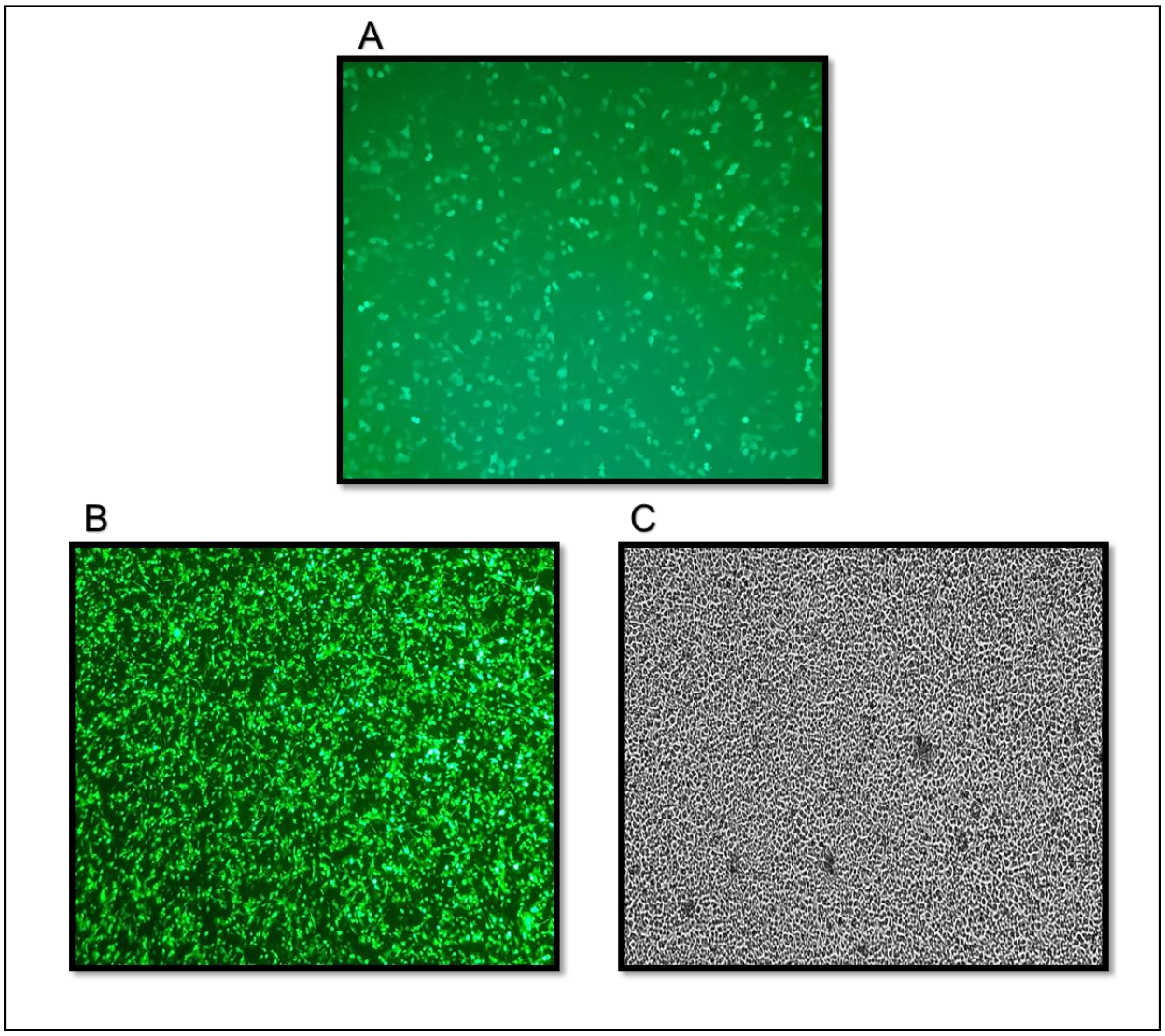

Figure 4.1: Transfection of pGFP into BHK-T7 cells (A) Fluorescence of pGFP expression in BHK-T7 3 hours after transfection. (B) Fluorescence of pGFP expression in BHK-T7 cells 22 hours after transfection. (C) Inverted microscope visualisasion of BHK-T7 cells 22 hours after transfection of the pGFP positive control.

The transfection mixture consisted of eleven *in vitro*-transcribed rotavirus run-off transcripts or (+)ssRNAs together with seven rotavirus expression plasmids for VP1, VP2, VP3, VP6, NSP1, NSP2 and NSP5 to express the replication complex, the fusogenic orthoreovirus (FAST) plasmid and two VV capping plasmids D1R and D12L. The transfection was conducted with BHK-T7 cells as they are easily transfected. After 24 hours of incubation in a humidified incubator at 37°C and 5% CO_2 the BHK-T7 cells were passaged and co-seeded with MA104 cells. These cells were incubated for 3-7 days at 37°C and 5% CO_2 and closely observed for any signs of CPE. After the incubation period, an IFMA was conducted on the cells to determine if rotavirus protein

VP6 was expressed in the cells. The results of this transfection can be observed in **Figure 4.2** and **Figure 4.3**.

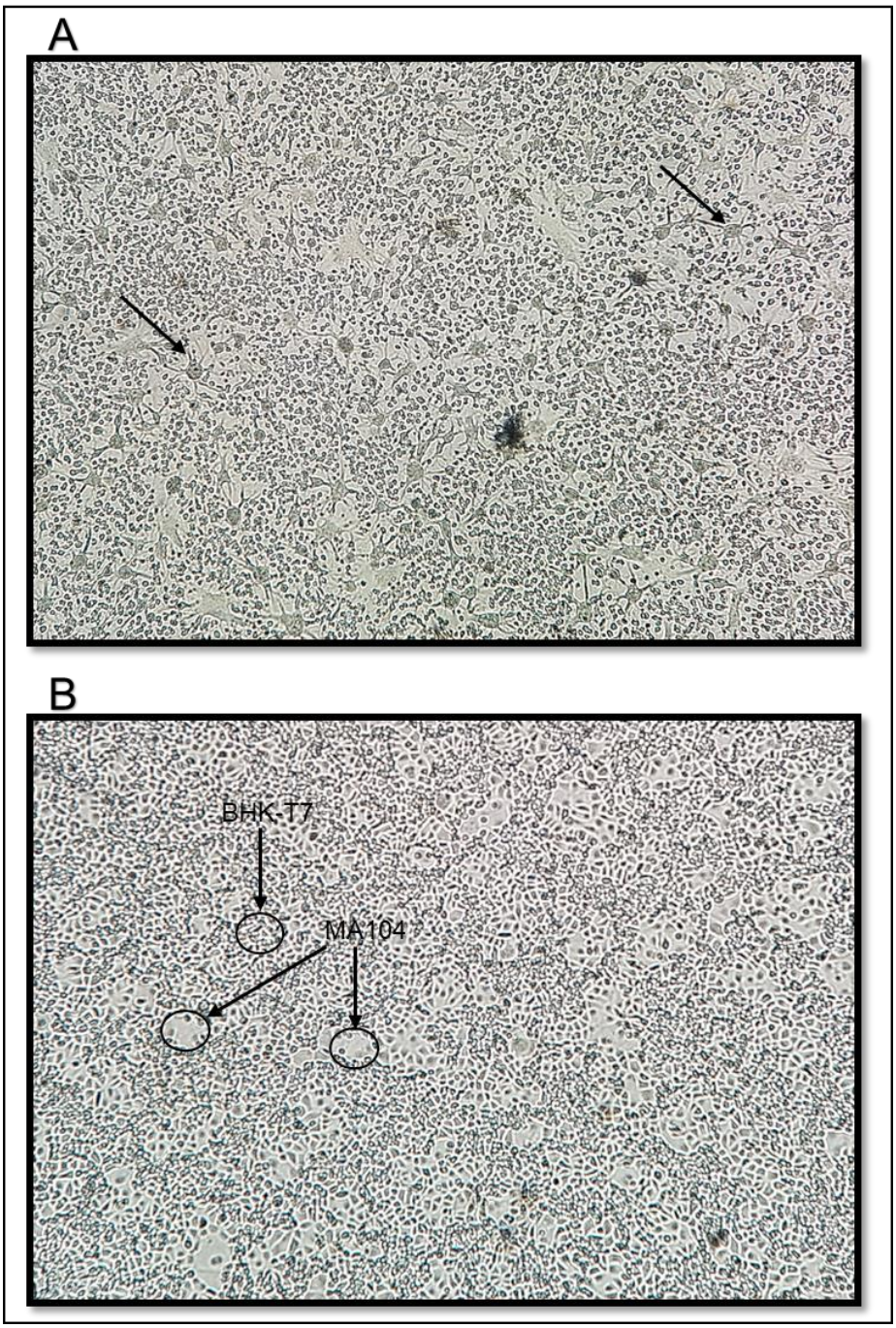

Figure 4.2: BHK-T7 and Co-seeded BHK-T7 and MA104 cells after transfection.
(A) BHK-T7 cells 22 hours after transfection with transfection mixture. The arrows indicate the dendrite-like fused cells caused by the addition of too much FAST plasmid. (B) Co-seeded BHK-T7 and MA104 cells approximately 72 hours after transfection. The BHK-T7 cells are smaller and more discernable and MA104 cells bigger and more transparent as indicated.

At 22 hours post-transfection, the BHK-T7 cells, that were transfected with the seven-rotavirus expression plasmids, the three plasmids from Kanai et al. and the eleven *in vitro*-transcribed rotavirus (+)ssRNAs, showed that some of the cells were fused together and had a dendrite-like structure **Figure 4.2A**. This was most likely caused by the addition of too much of the FAST plasmid due to a pipetting error. When these BHK-T7 cells were co-seeded with the MA104, these dendrite-like fused cells did not reattach to the bottom of the flask and were subsequently removed when the medium was changed. The co-seeded BHK-T7 and MA104 cells of approximately 72 hours post-transfection can be seen in **Figure 4.2B**. At this stage no CPE was observed and the medium of the cells was changed with DMEM containing 1% Anti-Anti (antibiotic/antimycotic) solution (penicillin 10 000 U/ml, 10 mg/ml streptomycin, amphotericin B 25µg/ml), 1% non-essential amino acids and no FBS and the cells were incubated for another 4 days at 37° in 5% CO_2. After the additional incubation period, no CPE was observed in the cells, and an IFMA was conducted as described in **Section 4.2.5**.

4.3.2. Immunofluorescence monolayer assay of co-seeded transfected BHK-T7 and MA104 cells

The purpose of the IFMA was to ascertain if any rotavirus VP6 were present in the co-seeded BHK-T7 and MA104 cells. After the methanol/acetone fixing and blocking of the BHK-T7 and MA104 cells, rabbit anti-SA11 DLP serum was added. This serum probably contained mostly VP6 antibodies seeing as VP6 is very antigenic. After the IFMA the cells were observed and photographed with a Nikon Eclipse TE2000-S microscope to evaluate rotavirus rescue.

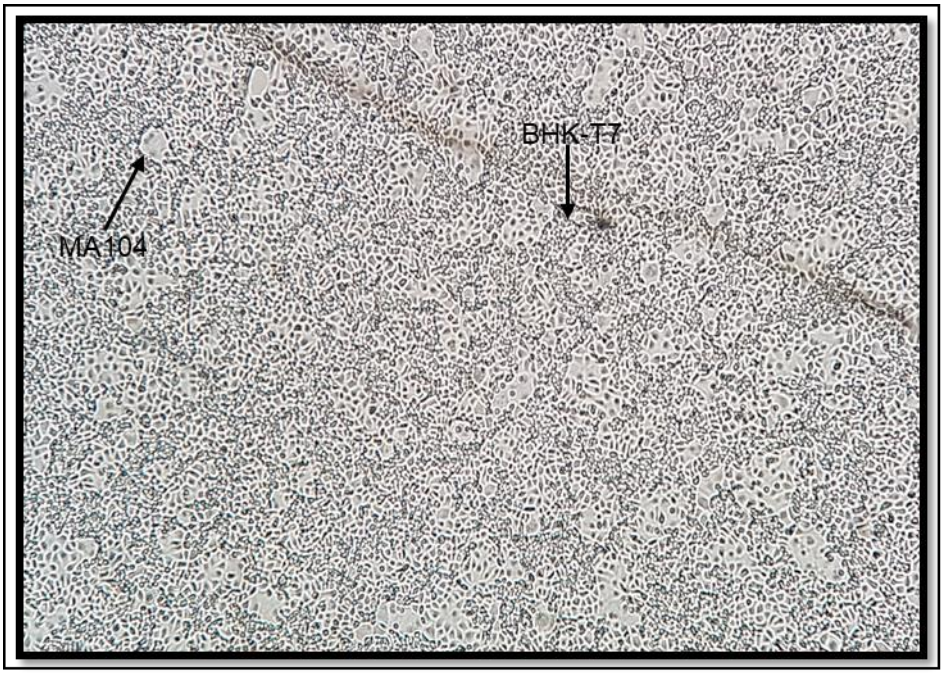

Figure 4.3: Co-seeded BHK-T7 and MA104 cells 7 days post-transfection. The BHK-T7 and MA104 cells 7 days after transfection was done before the IFMA was conducted.

seven days after transfection the BHK-T7 and MA104 cells had no clear signs of CPE such as detachment from flasks, cell shrinkage or cell death **Figure 4.3**. The cells were then used in an IFMA, and no fluorescence was observed, thus indicating that no rotavirus VP6 were present in the cells.

After failing to detect rotavirus rescue, extensive troubleshooting was done. The most prevalent reason for this was attributed to the nucleotide change in genome segment 11. As mentioned in **chapter 3**, the Ion-Torrent S5 sequencing revealed an amino acid change at position 289 of genome segment 11. The change in nucleotide sequence would lead to an amino acid change from a cysteine to an arginine. This change could have altered the function of NSP5/NSP6 and subsequently led to no virus being rescued. Another possible reason for the failed attempt might be the use of too much of the FAST plasmid. As described earlier, the overuse of the FAST plasmid caused some of the BHK-T7 cells to fuse together and look like a dendrite cell. When the FAST expression plasmid was used in a too high concentration in an attempt to increase the efficiency of the MRV rescue system no virus was rescued (Kanai et al., 2017).

4.4. Summary

In this chapter results of experiments were reported of BHK-T7 cells transfected with a combination of run-off T7 (+)ssRNAs derived from the rotavirus transcription plasmids mentioned in **chapter 3**, the seven rotavirus expression plasmids (VP1, VP2, VP3, VP6, NSP1, NSP2 and NSP5) and three plasmids (FAST, D1R and D12L) which were part of the plasmid-based reverse genetic system for rotavirus (Kanai et al., 2017). The function of the seven SA11 rotavirus expression plasmids was to encode the replication complex and viroplasms to help in the synthesis of rotavirus particles. The FAST plasmid has shown to aid in virus replication, while the D1R and D12L VV-capping enzyme increase the translation efficiency (Kanai et al., 2017). These transfected BHK-T7 cells were then co-seeded with MA104 cells and incubated for 6 days after which an IFMA was conducted to evaluate the rescue of any rotavirus. In this chapter, we attempted to combine aspects of the methods used in other studies to rescue rotavirus in a transcript-based reverse genetics system. Unfortunately, no SA11 rotavirus was rescued.

The reasons that this transcript-based reverse genetics system did not work is difficult to point out because of the lack of crucial knowledge in the replication cycle of rotavirus, as well as the packaging of viral proteins. One reason for the failed attempt may be due to nucleotide change that would invoke an amino acid change that could have altered the functions of NSP5/NSP6 encoded by genome segment 11. Another possible reason was the overuse of the FAST plasmid. The overuse of this plasmid in an MRV rescue system caused no virus to be rescued. To develop a successful transcript-based reverse genetics system in the future more information of the replication cycle is essential. Future prospects for this specific study would be to correct the sequence error found in genome segment 11. This could be done by PCR where a new forward primer can be designed to insert an extra guanine at the 5' terminal end of the sequence. Next the In-Fusion of genome segment 11 can be redone and DNA of the In-Fusion product be sequenced to ensure that no nucleotide changes occurred in the sequence. Once that is completed the new genome segment 11 transcription plasmid can be used in *in vitro* transcription to create (+)ssRNA that would be used in another round of transfections to see if that was the cause for this failed attempt. Secondly, the transfection can be done in equimicrogram instead of equimolar amounts as was done in Kanai et al (2017). Lastly, together with the

correction of genome segment 11, the transfection can be done with the no more than 15ng of the FAST plasmid.

Chapter 5: Closing remarks and future prospects

Rotavirus, the single most important cause of gastroenteritis that leads to the death of approximately half a million infants and young children a year, is a significant threat to communities in rural areas and developing countries (Madhi et al., 2010). The two rotavirus vaccines Rotarix™ and Rotateq® show lower degrees of protection in different regions such as Malawi where the rate of protection is lower than 50% compared to countries in North America and Europe that have higher than 95% protection (Clarke and Desselberger, 2015). Thus, the need to develop regional, strain-specific vaccines are imperative to battle the burden of disease. Reverse genetics systems of various viruses have led to valuable insights regarding the replication cycle and underlying mechanisms for pathogenesis. Transcript-based reverse genetics systems have been described for several other dsRNA viruses such as BTV and AHSV (Boyce et al., 2008) (Kobayashi et al., 2010) (Kaname et al., 2013). The extrapolation of those systems into a transcript-based reverse genetics system for rotavirus has proven difficult, and no such system currently exists. It was not until early 2017 when a plasmid-based reverse genetics system for rotavirus was described (Kanai et al., 2017). No transcript-based reverse genetics system for rotavirus has been described as of yet.

In this study, the specific aims were to first correct a design error on a set of SA11 multi-genome segment expression plasmids using the seamless In-Fusion HD cloning method and clone each genome segment into pSMART. Secondly to utilise all eleven corrected SA11 transcription plasmids to synthesise (+)ssRNAs through *in vitro* transcription. Finally, to verify the expression of rotavirus SA11 proteins in tissue culture after the synthesised (+)ssRNAs were transfected.

To correct the rotavirus SA11 multiple genome segment plasmids a state-of-the-art cloning method was utilised to remove the three extra guanine nucleotides from the 5' terminal end of the eleven rotavirus genome segments. This was achieved by conducting PCRs of all eleven rotavirus SA11 genome segments and the vector of choice, pSMART, with specifically designed primers that generated 15bp overlaps on

both the 5’ and 3’ terminal ends. Both purified vector and insert was incubated with the In-Fusion enzyme, which has a unique proofreading activity and facilitates the complementary base pairs on either ends to anneal through base-pairing.

After the synthesis of the transcription plasmids, these plasmids were first sent for Sanger sequencing to verify that the 5’ and 3’ terminal annealed correctly during the In-Fusion cloning and that the design flaw was subsequently removed from the 5’ terminal ends of all eleven plasmids. The plasmids then underwent next-generation sequencing and the National Institute for Communal Diseases (NICD) and NWU to determine if any other alteration in nucleotide sequence occurred. The NGS confirmed that pSMART-GS1/2/4/5/6/7/8/9/10 all had no alterations in the nucleotide sequence. However, a nucleotide change from a thymine to a cytosine was observed in the sequence of pSMART-GS11. This would lead to an amino acid change from cysteine to an arginine when the sequence is translated. Due to time limitations, we did not have time to redo pSMART-GS11, and this plasmid together with the other transcription plasmids was then used to synthesis (+)ssRNAs through *in* vitro transcription from all eleven rotavirus genome segments.

The *in vitro*-transcribed (+)ssRNAs were then used to transfect BHK-T7 cells along with seven rotavirus expression plasmids form a previous study, that encode the replication complex, and the fusogenic orthoreovirus FAST plasmid and two vaccinia virus capping enzyme plasmids D1R and D12L (Kanai et al., 2017) (Wentzel, 2014). After the transfection with these components, the BHK-T7 cells were co-seeded with MA104 cells in an attempt to infect the MA104 cells with any rotavirus that was synthesised in the BHK-T7 cells. To validate rescue of rotavirus in the MA104 cells, the cells were subjected to an immunofluorescence monolayer assay (IFMA). Unfortunately, no rotavirus rescue was detected.

Several reasons for the failure to rescue rotavirus were considered. First, the nucleotide change in the sequence of genome segment 11 would lead to an amino acid change which could alter the functions of NSP5/6 and subsequently lead to no virus rescue. Second, the BHK-T7 cells were transfected with too much of the FAST plasmid. This pipetting error caused clusters of BHK-T7 cells to fuse together and looked like dendritic cells. The coexpression of FAST increased the amount of virus

rescue in an MRV reverse genetic system. However, no virus was rescued if this plasmid was overused (Kanai et al., 2017).

Several aspects can be considered to continue the work conducted in this study. One has to be to redo the In-Fusion of genome segment 11 and ensure that no nucleotide changes occur again. Next to synthesise new (+)ssRNAs for genome segment 11 and redoing the transfection. In addition to this, special care should be given when adding the FAST plasmid so that the fusion of BHK-T7 cells can be avoided. Furthermore, in an effort to circumvent the innate immune response, specifically the RIG-I pathway, the transfection can be done in RIG-I deficient BSR-T7 cells and afterwards be co-seeded with MA104/SV5-V/NPro cells which are also RIG-I deficient. Lastly, the transfection can be done as the transcript-based reverse genetics system for BTV, where the two transfections take place (Boyce et al., 2008). The first transfection would be only with the expression plasmids that encode the replication complex and viroplasm of rotavirus. The second transfection, 18 hours after the first transfection, would be the 11 (+)ssRNAs, two VV capping enzyme plasmids and the FAST plasmid. This dual transfection system might improve the odds of success.

Several key aspects of the replication cycle of rotavirus are not completely understood, and this hinders the process of establishing an effective transcript-based reverse genetics system for this virus. The keys aspects in question are the mechanisms of how the transcripts are transported into the viroplasms along with the selective packaging signals that package ssRNAs into viral cores and several other issues mentioned by Desselberger (2014). Discovering the answers to these questions might help with establishing a comprehensive transcript-based reverse genetics system for rotavirus. Perhaps by utilising the newly developed plasmid-based reverse genetics system developed by Kanai and co-workers (2017) a lot of insight into the replication cycle can be gained and that knowledge can be used to create a comprehensive rotavirus transcript-based reverse genetics system in the future.

References

ADAMS, W. R. & KRAFT, L. M. 1963. Epizootic diarrhea of infant mice: indentification of the etiologic agent. *Science,* 141**,** 359-60.

ANGEL, J., FRANCO, M. A. & GREENBERG, H. B. 2012. Rotavirus immune responses and correlates of protection. *Curr Opin Virol,* 2**,** 419-25.

ARNOLD, M. M., BARRO, M. & PATTON, J. T. 2013a. Rotavirus NSP1 mediates degradation of interferon regulatory factors through targeting of the dimerization domain. *J Virol,* 87**,** 9813-21.

ARNOLD, M. M. & PATTON, J. T. 2011. Diversity of interferon antagonist activities mediated by NSP1 proteins of different rotavirus strains. *J Virol,* 85**,** 1970-9.

ARNOLD, M. M., SEN, A., GREENBERG, H. B. & PATTON, J. T. 2013b. The battle between rotavirus and its host for control of the interferon signaling pathway. *PLoS Pathog,* 9**,** e1003064.

AYALA-BRETON, C., ARIAS, M., ESPINOSA, R., ROMERO, P., ARIAS, C. F. & LOPEZ, S. 2009. Analysis of the kinetics of transcription and replication of the rotavirus genome by RNA interference. *J Virol,* 83**,** 8819-31.

BARRO, M. & PATTON, J. T. 2005. Rotavirus nonstructural protein 1 subverts innate immune response by inducing degradation of IFN regulatory factor 3. *Proc Natl Acad Sci U S A,* 102**,** 4114-9.

BARRO, M. & PATTON, J. T. 2007. Rotavirus NSP1 inhibits expression of type I interferon by antagonizing the function of interferon regulatory factors IRF3, IRF5, and IRF7. *J Virol,* 81**,** 4473-81.

BERNSTEIN, D. I., SACK, D. A., ROTHSTEIN, E., REISINGER, K., SMITH, V. E., O'SULLIVAN, D., SPRIGGS, D. R. & WARD, R. L. 1999. Efficacy of live, attenuated, human rotavirus vaccine 89-12 in infants: a randomised placebo-controlled trial. *Lancet,* 354**,** 287-90.

BHOWMICK, R., HALDER, U. C., CHATTOPADHYAY, S., NAYAK, M. K. & CHAWLA-SARKAR, M. 2013. Rotavirus-encoded nonstructural protein 1 modulates cellular apoptotic machinery by targeting tumor suppressor protein p53. *J Virol,* 87**,** 6840-50.

BISHOP, R. F., DAVIDSON, G. P., HOLMES, I. H. & RUCK, B. J. 1973. Virus particles in epithelial cells of duodenal mucosa from children with acute non-bacterial gastroenteritis. *Lancet,* 2**,** 1281-3.

BOYCE, M., CELMA, C. C. & ROY, P. 2008. Development of reverse genetics systems for bluetongue virus: recovery of infectious virus from synthetic RNA transcripts. *J Virol,* 82**,** 8339-48.

BURNS, J. W., SIADAT-PAJOUH, M., KRISHNANEY, A. A. & GREENBERG, H. B. 1996. Protective effect of rotavirus VP6-specific IgA monoclonal antibodies that lack neutralizing activity. *Science,* 272**,** 104-7.

CHARPILIENNE, A., LEPAULT, J., REY, F. & COHEN, J. 2002. Identification of rotavirus VP6 residues located at the interface with VP2 that are essential for capsid assembly and transcriptase activity. *J Virol,* 76**,** 7822-31.

CHIBA, S., YOKOYAMA, T., NAKATA, S., MORITA, Y., URASAWA, T., TANIGUCHI, K., URASAWA, S. & NAKAO, T. 1986. Protective effect of naturally acquired homotypic and heterotypic rotavirus antibodies. *Lancet,* 2**,** 417-21.

CIARLET, M. & ESTES, M. K. 1999. Human and most animal rotavirus strains do not require the presence of sialic acid on the cell surface for efficient infectivity. *J Gen Virol,* 80 (Pt 4)**,** 943-8.

CLARKE, E. & DESSELBERGER, U. 2015. Correlates of protection against human rotavirus disease and the factors influencing protection in low-income settings. *Mucosal Immunol,* 8**,** 1-17.

COULSON, B. S., LONDRIGAN, S. L. & LEE, D. J. 1997. Rotavirus contains integrin ligand sequences and a disintegrin-like domain that are implicated in virus entry into cells. *Proc Natl Acad Sci U S A,* 94**,** 5389-94.

CRAWFORD, S. E., MUKHERJEE, S. K., ESTES, M. K., LAWTON, J. A., SHAW, A. L., RAMIG, R. F. & PRASAD, B. V. 2001. Trypsin cleavage stabilizes the rotavirus VP4 spike. *J Virol,* 75**,** 6052-61.

CRAWFORD, S. E., RAMANI, S., TATE, J. E., PARASHAR, U. D., SVENSSON, L., HAGBOM, M., FRANCO, M. A., GREENBERG, H. B., O'RYAN, M., KANG, G., DESSELBERGER, U. & ESTES, M. K. 2017. Rotavirus infection. *Nat Rev Dis Primers,* 3**,** 17083.

CRIGLAR, J., GREENBERG, H. B., ESTES, M. K. & RAMIG, R. F. 2011. Reconciliation of rotavirus temperature-sensitive mutant collections and assignment of reassortment groups D, J, and K to genome segments. *J Virol,* 85**,** 5048-60.

CRIGLAR, J. M., HU, L., CRAWFORD, S. E., HYSER, J. M., BROUGHMAN, J. R., PRASAD, B. V. & ESTES, M. K. 2014. A novel form of rotavirus NSP2 and phosphorylation-dependent NSP2-NSP5 interactions are associated with viroplasm assembly. *J Virol,* 88**,** 786-98.

DALBY, B., CATES, S., HARRIS, A., OHKI, E. C., TILKINS, M. L., PRICE, P. J. & CICCARONE, V. C. 2004. Advanced transfection with Lipofectamine 2000 reagent: primary neurons, siRNA, and high-throughput applications. *Methods,* 33**,** 95-103.

DESSELBERGER, U. 2014. Rotaviruses. *Virus Res,* 190**,** 75-96.

DESSELBERGER, U. & HUPPERTZ, H. I. 2011. Immune responses to rotavirus infection and vaccination and associated correlates of protection. *J Infect Dis,* 203**,** 188-95.

DONNELLY, R. P. & KOTENKO, S. V. 2010. Interferon-lambda: a new addition to an old family. *J Interferon Cytokine Res,* 30**,** 555-64.

DORMITZER, P. R., SUN, Z. Y., BLIXT, O., PAULSON, J. C., WAGNER, G. & HARRISON, S. C. 2002a. Specificity and affinity of sialic acid binding by the rhesus rotavirus VP8* core. *J Virol,* 76**,** 10512-7.

DORMITZER, P. R., SUN, Z. Y., WAGNER, G. & HARRISON, S. C. 2002b. The rhesus rotavirus VP4 sialic acid binding domain has a galectin fold with a novel carbohydrate binding site. *Embo j,* 21**,** 885-97.

EDINGER, A. L. & THOMPSON, C. B. 2004. Death by design: apoptosis, necrosis and autophagy. *Curr Opin Cell Biol,* 16**,** 663-9.

ESTES, M. K. & GREENBERG, H. B. 2013. Rotavirus. *In:* FIELDS, B. N., KNIPE, D. M. & HOWLEY, P. M. (eds.) *Fields Virology.* 6th ed. ed.: Philadelphia : Wolters Kluwer Health/Lippincott Williams & Wilkins, c2013.

FABBRETTI, E., AFRIKANOVA, I., VASCOTTO, F. & BURRONE, O. R. 1999. Two non-structural rotavirus proteins, NSP2 and NSP5, form viroplasm-like structures in vivo. *J Gen Virol,* 80 (Pt 2)**,** 333-9.

FIORE, L., GREENBERG, H. B. & MACKOW, E. R. 1991. The VP8 fragment of VP4 is the rhesus rotavirus hemagglutinin. *Virology,* 181**,** 553-63.

FLEWETT, T. H., BRYDEN, A. S., DAVIES, H., WOODE, G. N., BRIDGER, J. C. & DERRICK, J. M. 1974. Relation between viruses from acute gastroenteritis of children and newborn calves. *Lancet,* 2**,** 61-3.

FRANCO, M. A., ANGEL, J. & GREENBERG, H. B. 2006. Immunity and correlates of protection for rotavirus vaccines. *Vaccine,* 24**,** 2718-31.

GALLEGOS, C. O. & PATTON, J. T. 1989. Characterization of rotavirus replication intermediates: a model for the assembly of single-shelled particles. *Virology,* 172**,** 616-27.

GARDET, A., BRETON, M., FONTANGES, P., TRUGNAN, G. & CHWETZOFF, S. 2006. Rotavirus spike protein VP4 binds to and remodels actin bundles of the epithelial brush border into actin bodies. *J Virol,* 80**,** 3947-56.

GLASS, R. I., PARASHAR, U., PATEL, M., GENTSCH, J. & JIANG, B. 2014. Rotavirus vaccines: successes and challenges. *J Infect,* 68 Suppl 1**,** S9-18.

GRAFF, J. W., EWEN, J., ETTAYEBI, K. & HARDY, M. E. 2007. Zinc-binding domain of rotavirus NSP1 is required for proteasome-dependent degradation of IRF3 and autoregulatory NSP1 stability. *J Gen Virol,* 88**,** 613-20.

GUERRERO, C. A., BOUYSSOUNADE, D., ZARATE, S., ISA, P., LOPEZ, T., ESPINOSA, R., ROMERO, P., MENDEZ, E., LOPEZ, S. & ARIAS, C. F. 2002. Heat shock cognate protein 70 is involved in rotavirus cell entry. *J Virol,* 76**,** 4096-102.

HEATON, P. M., GOVEIA, M. G., MILLER, J. M., OFFIT, P. & CLARK, H. F. 2005. Development of a pentavalent rotavirus vaccine against prevalent serotypes of rotavirus gastroenteritis. *J Infect Dis,* 192 Suppl 1**,** S17-21.

HEIMAN, E. M., MCDONALD, S. M., BARRO, M., TARAPOREWALA, Z. F., BAR-MAGEN, T. & PATTON, J. T. 2008. Group A human rotavirus genomics: evidence that gene constellations are influenced by viral protein interactions. *J Virol,* 82**,** 11106-16.

HONDA, K. & TANIGUCHI, T. 2006. IRFs: master regulators of signalling by Toll-like receptors and cytosolic pattern-recognition receptors. *Nat Rev Immunol,* 6**,** 644-58.

JAIMES, M. C., ROJAS, O. L., GONZALEZ, A. M., CAJIAO, I., CHARPILIENNE, A., POTHIER, P., KOHLI, E., GREENBERG, H. B., FRANCO, M. A. & ANGEL, J. 2002. Frequencies of virus-specific CD4(+) and CD8(+) T lymphocytes secreting gamma interferon after acute natural rotavirus infection in children and adults. *J Virol,* 76**,** 4741-9.

JIANG, X., JAYARAM, H., KUMAR, M., LUDTKE, S. J., ESTES, M. K. & PRASAD, B. V. 2006. Cryoelectron microscopy structures of rotavirus NSP2-NSP5 and NSP2-RNA complexes: implications for genome replication. *J Virol,* 80**,** 10829-35.

KANAI, Y., KOMOTO, S., KAWAGISHI, T., NOUDA, R., NAGASAWA, N., ONISHI, M., MATSUURA, Y., TANIGUCHI, K. & KOBAYASHI, T. 2017. Entirely plasmid-based reverse genetics system for rotaviruses. *Proc Natl Acad Sci U S A,* 114**,** 2349-2354.

KANAME, Y., CELMA, C. C., KANAI, Y. & ROY, P. 2013. Recovery of African horse sickness virus from synthetic RNA. *J Gen Virol,* 94**,** 2259-65.

KAPIKIAN, A. Z., HOSHINO, Y., CHANOCK, R. M. & PEREZ-SCHAEL, I. 1996. Efficacy of a quadrivalent rhesus rotavirus-based human rotavirus vaccine aimed at preventing severe rotavirus diarrhea in infants and young children. *J Infect Dis,* 174 Suppl 1**,** S65-72.

KAPIKIAN, A. Z., SIMONSEN, L., VESIKARI, T., HOSHINO, Y., MORENS, D. M., CHANOCK, R. M., LA MONTAGNE, J. R. & MURPHY, B. R. 2005. A hexavalent human rotavirus-bovine rotavirus (UK) reassortant vaccine designed for use in developing countries and delivered in a schedule with the potential to eliminate the risk of intussusception. *J Infect Dis,* 192 Suppl 1**,** S22-9.

KOBAYASHI, T., OOMS, L. S., IKIZLER, M., CHAPPELL, J. D. & DERMODY, T. S. 2010. An improved reverse genetics system for mammalian orthoreoviruses. *Virology,* 398**,** 194-200.

KOMOTO, S., SASAKI, J. & TANIGUCHI, K. 2006. Reverse genetics system for introduction of site-specific mutations into the double-stranded RNA genome of infectious rotavirus. *Proc Natl Acad Sci U S A,* 103**,** 4646-51.

LI, W., MANKTELOW, E., VON KIRCHBACH, J. C., GOG, J. R., DESSELBERGER, U. & LEVER, A. M. 2010. Genomic analysis of codon, sequence and structural conservation with selective biochemical-structure mapping reveals highly conserved and dynamic structures in rotavirus RNAs with potential cis-acting functions. *Nucleic Acids Res,* 38**,** 7718-35.

LONG, C. P. & MCDONALD, S. M. 2017. Rotavirus genome replication: Some assembly required. *PLoS Pathog,* 13**,** e1006242.

LOPEZ, T., CAMACHO, M., ZAYAS, M., NAJERA, R., SANCHEZ, R., ARIAS, C. F. & LOPEZ, S. 2005. Silencing the morphogenesis of rotavirus. *J Virol,* 79**,** 184-92.

LUDERT, J. E., MICHELANGELI, F., GIL, F., LIPRANDI, F. & ESPARZA, J. 1987. Penetration and uncoating of rotaviruses in cultured cells. *Intervirology,* 27**,** 95-101.

MADHI, S. A., CUNLIFFE, N. A., STEELE, D., WITTE, D., KIRSTEN, M., LOUW, C., NGWIRA, B., VICTOR, J. C., GILLARD, P. H., CHEUVART, B. B., HAN, H. H. & NEUZIL, K. M. 2010. Effect of human rotavirus vaccine on severe diarrhea in African infants. *N Engl J Med,* 362**,** 289-98.

MADHI, S. A., CUNLIFFE, N. A., STEELE, D., WITTE, D., KIRSTEN, M., LOUW, C., NGWIRA, B., VICTOR, J. C., GILLARD, P. H., CHEUVART, B. B., HAN, H. H. & NEUZIL, K. M. 2016. Effect of human rotavirus vaccine on severe diarrhea in African infants. *Malawi Med J,* 28**,** 108-114.

MAES, P., MATTHIJNSSENS, J., RAHMAN, M. & VAN RANST, M. 2009. RotaC: a web-based tool for the complete genome classification of group A rotaviruses. *BMC Microbiol,* 9**,** 238.

MALHERBE, H. & HARWIN, R. 1963. The cytopathic effects of vervet monkey viruses. *S Afr Med J,* 37**,** 407-11.

MARTIN, D., DUARTE, M., LEPAULT, J. & PONCET, D. 2010. Sequestration of free tubulin molecules by the viral protein NSP2 induces microtubule depolymerization during rotavirus infection. *J Virol,* 84**,** 2522-32.

MATHIEU, M., PETITPAS, I., NAVAZA, J., LEPAULT, J., KOHLI, E., POTHIER, P., PRASAD, B. V., COHEN, J. & REY, F. A. 2001. Atomic structure of the major capsid protein of rotavirus: implications for the architecture of the virion. *Embo j,* 20**,** 1485-97.

MATSUO, E. & ROY, P. 2009. Bluetongue virus VP6 acts early in the replication cycle and can form the basis of chimeric virus formation. *J Virol,* 83**,** 8842-8.

MATTHIJNSSENS, J., CIARLET, M., HEIMAN, E., ARIJS, I., DELBEKE, T., MCDONALD, S. M., PALOMBO, E. A., ITURRIZA-GOMARA, M., MAES, P., PATTON, J. T., RAHMAN, M. & VAN RANST, M. 2008a. Full genome-based classification of rotaviruses reveals a common origin between human Wa-Like and porcine rotavirus strains and human DS-1-like and bovine rotavirus strains. *J Virol,* 82**,** 3204-19.

MATTHIJNSSENS, J., CIARLET, M., MCDONALD, S. M., ATTOUI, H., BANYAI, K., BRISTER, J. R., BUESA, J., ESONA, M. D., ESTES, M. K., GENTSCH, J. R., ITURRIZA-GOMARA, M., JOHNE, R., KIRKWOOD, C. D., MARTELLA, V., MERTENS, P. P., NAKAGOMI, O., PARRENO, V., RAHMAN, M., RUGGERI, F. M., SAIF, L. J., SANTOS, N., STEYER, A., TANIGUCHI, K., PATTON, J. T., DESSELBERGER, U. & VAN RANST, M. 2011. Uniformity of rotavirus strain nomenclature proposed by the Rotavirus Classification Working Group (RCWG). *Arch Virol,* 156**,** 1397-413.

MATTHIJNSSENS, J., CIARLET, M., RAHMAN, M., ATTOUI, H., BANYAI, K., ESTES, M. K., GENTSCH, J. R., ITURRIZA-GOMARA, M., KIRKWOOD, C. D., MARTELLA, V., MERTENS, P. P., NAKAGOMI, O., PATTON, J. T., RUGGERI, F. M., SAIF, L. J., SANTOS, N., STEYER, A., TANIGUCHI, K., DESSELBERGER, U. & VAN RANST, M. 2008b. Recommendations for the classification of group A rotaviruses using all 11 genomic RNA segments. *Arch Virol,* 153**,** 1621-9.

MATTHIJNSSENS, J., HEYLEN, E., ZELLER, M., RAHMAN, M., LEMEY, P. & VAN RANST, M. 2010. Phylodynamic analyses of rotavirus genotypes G9 and G12 underscore their potential for swift global spread. *Mol Biol Evol,* 27**,** 2431-6.

MATTHIJNSSENS, J., OTTO, P. H., CIARLET, M., DESSELBERGER, U., VAN RANST, M. & JOHNE, R. 2012. VP6-sequence-based cutoff values as a criterion for rotavirus species demarcation. *Arch Virol,* 157**,** 1177-82.

MCCLAIN, B., SETTEMBRE, E., TEMPLE, B. R., BELLAMY, A. R. & HARRISON, S. C. 2010. X-ray crystal structure of the rotavirus inner capsid particle at 3.8 A resolution. *J Mol Biol,* 397**,** 587-99.

MCDONALD, S. M. & PATTON, J. T. 2011. Assortment and packaging of the segmented rotavirus genome. *Trends Microbiol,* 19**,** 136-44.

MEBUS, C. A., UNDERDAHL, N. R., RHODES, M. B. & TWIEHAUS, M. J. 1969. Further studies on neonatal calf diarrhea virus. *Proc Annu Meet U S Anim Health Assoc,* 73**,** 97-9.

MLERA, L. 2012. *Preparatory investigations for developing a transcript-based rotavirus reverse genetics system.* Ph.D, North-West University.

MLERA, L., O'NEILL, H. G., JERE, K. C. & VAN DIJK, A. A. 2013. Whole-genome consensus sequence analysis of a South African rotavirus SA11 sample reveals a mixed infection with two close derivatives of the SA11-H96 strain. *Arch Virol,* 158**,** 1021-30.

NEUMANN, G., OZAWA, M. & KAWAOKA, Y. 2012. Reverse genetics of influenza viruses. *Methods Mol Biol,* 865**,** 193-206.

PARASHAR, U. D., BURTON, A., LANATA, C., BOSCHI-PINTO, C., SHIBUYA, K., STEELE, D., BIRMINGHAM, M. & GLASS, R. I. 2009. Global mortality associated with rotavirus disease among children in 2004. *J Infect Dis,* 200 Suppl 1**,** S9-s15.

PATTON, J. T., VASQUEZ-DEL CARPIO, R. & SPENCER, E. 2004. Replication and transcription of the rotavirus genome. *Curr Pharm Des,* 10**,** 3769-77.

PESAVENTO, J. B., CRAWFORD, S. E., ESTES, M. K. & PRASAD, B. V. 2006. Rotavirus proteins: structure and assembly. *Curr Top Microbiol Immunol,* 309**,** 189-219.

PIRON, M., DELAUNAY, T., GROSCLAUDE, J. & PONCET, D. 1999. Identification of the RNA-binding, dimerization, and eIF4GI-binding domains of rotavirus nonstructural protein NSP3. *J Virol,* 73**,** 5411-21.

PIRON, M., VENDE, P., COHEN, J. & PONCET, D. 1998. Rotavirus RNA-binding protein NSP3 interacts with eIF4GI and evicts the poly(A) binding protein from eIF4F. *Embo j,* 17**,** 5811-21.

RUIZ-PALACIOS, G. M., PEREZ-SCHAEL, I., VELAZQUEZ, F. R., ABATE, H., BREUER, T., CLEMENS, S. C., CHEUVART, B., ESPINOZA, F., GILLARD, P., INNIS, B. L., CERVANTES, Y., LINHARES, A. C., LOPEZ, P., MACIAS-PARRA, M., ORTEGA-BARRIA, E., RICHARDSON, V., RIVERA-MEDINA, D. M., RIVERA, L., SALINAS, B., PAVIA-RUZ, N., SALMERON, J., RUTTIMANN, R., TINOCO, J. C., RUBIO, P., NUNEZ, E., GUERRERO, M. L., YARZABAL, J. P., DAMASO, S., TORNIEPORTH, N., SAEZ-LLORENS, X., VERGARA, R. F., VESIKARI, T., BOUCKENOOGHE, A., CLEMENS, R., DE VOS, B. & O'RYAN, M. 2006. Safety and efficacy of an attenuated vaccine against severe rotavirus gastroenteritis. *N Engl J Med,* 354**,** 11-22.

RUIZ, M. C., ABAD, M. J., CHARPILIENNE, A., COHEN, J. & MICHELANGELI, F. 1997. Cell lines susceptible to infection are permeabilized by cleaved and solubilized outer layer proteins of rotavirus. *J Gen Virol,* 78 (Pt 11)**,** 2883-93.

SAMBROOK, J. F. & RUSSELL, D. W. 2001. *Molecular Cloning: A Laboratory Manual*, Cold Spring Harbor Laboratory Press.

SAMUEL, C. E. 2001. Antiviral actions of interferons. *Clin Microbiol Rev,* 14**,** 778-809, table of contents.

SANTOSHAM, M., LETSON, G. W., WOLFF, M., REID, R., GAHAGAN, S., ADAMS, R., CALLAHAN, C., SACK, R. B. & KAPIKIAN, A. Z. 1991. A field study of the safety and efficacy of two candidate rotavirus vaccines in a Native American population. *J Infect Dis,* 163**,** 483-7.

SEN, A., ROTT, L., PHAN, N., MUKHERJEE, G. & GREENBERG, H. B. 2014. Rotavirus NSP1 protein inhibits interferon-mediated STAT1 activation. *J Virol,* 88**,** 41-53.

SETTEMBRE, E. C., CHEN, J. Z., DORMITZER, P. R., GRIGORIEFF, N. & HARRISON, S. C. 2011. Atomic model of an infectious rotavirus particle. *EMBO J,* 30**,** 408-16.

SUBBARAO, K. & KATZ, J. M. 2004. Influenza vaccines generated by reverse genetics. *Curr Top Microbiol Immunol,* 283**,** 313-42.

TANIGUCHI, K. & KOMOTO, S. 2012. Genetics and reverse genetics of rotavirus. *Curr Opin Virol,* 2**,** 399-407.

TAXONOMY, I. C. O. 2017. *Taxonomy* [Online]. Available: https://talk.ictvonline.org/taxonomy/ [Accessed 27 July 2017 2017].

TORTORICI, M. A., SHAPIRO, B. A. & PATTON, J. T. 2006. A base-specific recognition signal in the 5' consensus sequence of rotavirus plus-strand RNAs promotes replication of the double-stranded RNA genome segments. *Rna,* 12**,** 133-46.

TRASK, S. D., BOEHME, K. W., DERMODY, T. S. & PATTON, J. T. 2013. Comparative analysis of Reoviridae reverse genetics methods. *Methods,* 59**,** 199-206.

TRASK, S. D., MCDONALD, S. M. & PATTON, J. T. 2012. Structural insights into the coupling of virion assembly and rotavirus replication. *Nat Rev Microbiol,* 10**,** 165-77.

TRASK, S. D., TARAPOREWALA, Z. F., BOEHME, K. W., DERMODY, T. S. & PATTON, J. T. 2010. Dual selection mechanisms drive efficient single-gene reverse genetics for rotavirus. *Proc Natl Acad Sci U S A,* 107**,** 18652-7.

TROUPIN, C., DEHEE, A., SCHNURIGER, A., VENDE, P., PONCET, D. & GARBARG-CHENON, A. 2010. Rearranged genomic RNA segments offer a new approach to the reverse genetics of rotaviruses. *J Virol,* 84**,** 6711-9.

VAN DE WATER, S. G., VAN GENNIP, R. G., POTGIETER, C. A., WRIGHT, I. M. & VAN RIJN, P. A. 2015. VP2 Exchange and NS3/NS3a Deletion in African Horse Sickness Virus (AHSV) in Development of Disabled Infectious Single Animal Vaccine Candidates for AHSV. *J Virol,* 89**,** 8764-72.

VAN GENNIP, R. G., VAN DE WATER, S. G., POTGIETER, C. A., WRIGHT, I. M., VELDMAN, D. & VAN RIJN, P. A. 2012. Rescue of recent virulent and avirulent field strains of bluetongue virus by reverse genetics. *PLoS One,* 7**,** e30540.

VAN RIJN, P. A., VAN DE WATER, S. G., FEENSTRA, F. & VAN GENNIP, R. G. 2016. Requirements and comparative analysis of reverse genetics for bluetongue virus (BTV) and African horse sickness virus (AHSV). *Virol J,* 13**,** 119.

VELAZQUEZ, F. R. 2009. Protective effects of natural rotavirus infection. *Pediatr Infect Dis J,* 28**,** S54-6.

VENDE, P., PIRON, M., CASTAGNE, N. & PONCET, D. 2000. Efficient translation of rotavirus mRNA requires simultaneous interaction of NSP3 with the eukaryotic translation initiation factor eIF4G and the mRNA 3' end. *J Virol,* 74**,** 7064-71.

VESIKARI, T., MATSON, D. O., DENNEHY, P., VAN DAMME, P., SANTOSHAM, M., RODRIGUEZ, Z., DALLAS, M. J., HEYSE, J. F., GOVEIA, M. G., BLACK, S. B., SHINEFIELD, H. R., CHRISTIE, C. D., YLITALO, S., ITZLER, R. F., COIA, M. L., ONORATO, M. T., ADEYI, B. A., MARSHALL, G. S., GOTHEFORS, L., CAMPENS, D., KARVONEN, A., WATT, J. P., O'BRIEN, K. L., DINUBILE, M. J., CLARK, H. F., BOSLEGO, J. W., OFFIT, P. A. & HEATON, P. M. 2006. Safety and efficacy of a pentavalent human-bovine (WC3) reassortant rotavirus vaccine. *N Engl J Med,* 354**,** 23-33.

VILLENA, J., VIZOSO-PINTO, M. G. & KITAZAWA, H. 2016. Intestinal Innate Antiviral Immunity and Immunobiotics: Beneficial Effects against Rotavirus Infection. *Front Immunol,* 7**,** 563.

WENTZEL, J. F. 2014. *Investigating the Importance of Co-expressedRotavirus Proteins in the Development of a Selection-Free Rotavirus ReverseGenetics System.* PhD, North-West University

ZHU, B., CAI, G., HALL, E. O. & FREEMAN, G. J. 2007. In-fusion assembly: seamless engineering of multidomain fusion proteins, modular vectors, and mutations. *Biotechniques,* 43**,** 354-9.